THE UNIVERSITY
of EDINBURGH

Exosome signalling in the kidney

Wilna Oosthuyzen

Thesis submitted in fulfilment of the requirements for the degree

Doctor of Philosophy

2016

ABSTRACT

Urine contains exosomes originating from the circulation and all cells lining the urinary tract. Exosomes are a route of inter-cellular communication along the nephron potentially able to transfer of protein and/or RNA. It is not known whether this is a regulated process analogous to other cell-to-cell signalling systems. The aims of this study were to develop nanoparticle tracking analysis (NTA) as a technique to quantify exosomes in urine. Secondly, the hormonal regulation of exosome uptake *in vitro* and *in vivo* was investigated. Thirdly, exosome excretion in a central diabetes insipidus (DI) patient and a patient group after radiocontrast exposure was measured to investigate exosome excretion along the kidney in injury.

Using the fluorescent capabilities of NTA, urinary exosomes were quantified in urine samples. NTA was able to detect changes in aquaporin 2 levels *in vitro* and *in vivo*. Storage conditions for human urinary exosomes were also optimised using NTA. A kidney cortical collecting duct cell line (CCDs) was used to model regulation of exosome uptake in vitro. CCDs were stimulated with desmopressin, a vasopressin analogue, and uptake of fluorescently-loaded or microRNA-loaded exosomes was measured. Desmopressin stimulated exosome uptake into collecting duct cells via V2 receptor stimulation. Intra-cellular uptake of exosomes was confirmed by microRNA specific mRNA down-regulation. Mechanistically, exosome uptake in response to desmopressin required cyclic AMP production, was mediated by clathrin-dependent endocytosis and was selective for exosomes from kidney tubular cells. In mice, fluorescently-loaded exosomes were systemically injected before and after administration of the V2 antagonist, tolvaptan, and urinary exosome excretion was measured. Basally, 2.5% of injected exosomes were recovered in urine; tolvaptan treatment resulted in a 5-fold increase. By combining antibodies to nephron segment-specific proteins with NTA we measured human urinary exosome excretion in central diabetes insipidus (DI) and after radiocontrast exposure (n=37). In DI, desmopressin reduced the excretion of exosomes derived from upstream glomerular and proximal tubule cells. In patients exposed to radiocontrast, urinary exosomes from the glomerulus were positively correlated with the tubular injury markers KIM-1 and NGAL.

These findings therefore show that tubular exosome uptake is a specific, hormonally regulated process that is reduced with injury. Physiologically, exosomes are a mechanism of inter-cellular communication; therapeutically, exosomes represent a novel vehicle by which RNA therapy could be targeted for the treatment of kidney disease.

DECLARATION

I, Wilna Oosthuyzen, declare that I have composed the thesis and the thesis is the result of my own work with the following exceptions:

- *Chapter 2* – Nicole Sime performed the rodent studies and measurements;
- *Chapter 6* – Jeroen Koomen performed the patient sample measurements and Adrian Thompson performed the biomarker and creatinine assays;
- All other creatinine assays were performed by the Shared University Research Facilities.

This work has not previously been submitted for any degree or professional qualification.

Wilna Oosthuyzen

2016

ACKNOWLEDGEMENTS

This thesis is dedicated to my family, friends, supervisors and colleagues, who have supported and guided me throughout my studies.

Special thanks must go to:

- The E3.17 laboratory staff and students for their good humour and help,
- My colleagues and friends, Dr Emma Morrison and Gianna Panagakou for all their technical knowledge and support so generously shared,
- My parents for the beliefs they have instilled in me and their constant encouragement,
- My husband for his continued love, support and good sense of humour throughout,
- Professor David Webb, who afforded me the opportunity to undertake this PhD in the first place and supported me throughout,
- Dr Matthew Bailey, my second supervisor, for not only his scientific knowledge but pastoral care and help in obtaining and completing my studies,
- And finally, my supervisor, Dr James Dear, for his optimistic approach and guidance and the opportunities he has continually provided me to develop as a scientist and person, for which I will be forever grateful to him.

Thank you.

TABLE OF CONTENTS

LIST OF TABLES

LIST OF FIGURES

LIST OF ABBREVIATIONS

ΔΔCt	Delta delta cycle threshold
°C	Degrees Celsius
AD	Alzheimer's Disease
Ago2	Argonaute 2
AKI	Acute kidney injury
ANOVA	Analysis of variance
AQP2	Aquaporin 2
AUC	Area under the curve
AVP	Arginine vasopressin
CA9	Carbonic Anhydrase 9
cAMP	Cyclic adenosine monophosphate
CCD	Cortical collecting duct cell line
CCNE1	Cyclin E1
CD24	Cluster of differentiation 24
CDC25A	Cell division cycle 25 A
CI-AKI	Contrast media induced acute kidney injury
CKD	Chronic kidney disease
CLTC	Clathrin heavy chain
CCV	Clathrin coated vesicle
CM	Contrast media
CSF	Cerebrospinal fluid
Ct	Cycle threshold
CU	Cubilin
CVi	Intra-assay coefficient of variation
dDAVP	Desmopressin
DI	Diabetes insipidus
DNA	Deoxyribonucleic acid
EDTA	Ethylenediaminetetraacetic acid
EGFR	Epithelial growth factor receptor
ESCRT	Endosomal Sorting Complex Required for Transport
FCS	Fetal calf serum

FGF	Fibroblast growth factor
g	Gravitational force
gDNA	Genomic DNA
GTP	Guanosine-5'-triphosphate
HepaCAM	Hepatocyte cell adhesion molecule
HIV	Human immunodeficiency virus type-1
HK2	Human proximal tubular cells
HSP	Heat shock protein
HUVEC	Human umbilical vein endothelial cells
i.v	Intravenously
IgG	Immunoglobulin G
ILV	Intraluminal vesicle
IQR	Interquartile range
KIM-1	Kidney injury molecule-1
LAMP-1	Lysosome-associated membrane protein
MFI	Mean fluorescence intensity
miRNA	Micro-RNA
mmol/l	Millimole per litre
mRNA	Messenger RNA
mtDNA	Mitochondrial DNA
MSC	Mesenchymal stem cell
MVE	Multivesicular endosomes
n	Sample size
NaCl	Sodium chloride
NCC	Sodium chloride co-transporter
NGAL	Neutrophil-gelatinase-associated lipocalin
nSMase2	Neutral sphingomyelinase 2
NTA	Nanoparticle tracking analyses
PBS	Phosphate buffered saline
PD	Parkinson’s Disease
PKA	Protein kinase A
PODXL	Podocalyxin-like protein
Qdots	Quantum dots

RCC	Renal clear cell
RG1	Juxtaglomerular cells
RNA	Ribonucleic acid
ROS	Reactive oxygen species
RT	Room temperature
SD	Standard deviation
SDS-page	Sodium dodecyl sulfate polyacrylamide gel electrophoresis
SEM	Standard error of the mean
SUMO	Small ubiquitin-like modifier proteins
TEM	Transmission electron microscopy
TSG101	Tumour susceptibility gene 101
UC	Ultracentrifugation
V2	Vasopressin 2
VEGF-A	Vascular endothelial growth factor A
WT1	Wilms tumor 1

PUBLICATIONS

Publications from work arising from this thesis:

1. **Oosthuyzen W**, Sime NE, Ivy JR, Turtle EJ, Street JM, Pound J, Bath LE, Webb DJ, Gregory CD, Bailey MA, Dear JW. Quantification of human urinary exosomes by nanoparticle tracking analysis. **Journal of Physiology**. 2013 Dec 1;591(Pt 23):5833-42.

2. Liga A, Vliegenthart AD, **Oosthuyzen W**, Dear JW, Kersaudy-Kerhoas M. Exosome isolation: a microfluidic road-map. **Lab on a chip**. 2015 Jun 7;15(11):2388-94.

3. Ivy JR, **Oosthuyzen W**, Peltz TS, Howarth A, Hunter RW, Dhaun N, Al-Dujaili EAS, Webb DJ, Dear JW, Flatman PW, Bailey, MA. Glucocorticoids Induce Nondipping Blood Pressure by Activating the Thiazide-Sensitive Cotransporter. **Hypertension**. Published online before print March 7, 2016, doi: 10.1161/HYPERTENSIONAHA.115.06977

4. **Oosthuyzen W**, Scullion KM, Ivy JR, Morrison EE, Hunter RW, Starkey Lewis PJ, O'Duibhir E, Street JM, Caporali A, Gregory CD, Forbes SJ, Webb DJ, Bailey MA, Dear JW. (2016). Vasopressin Regulates Extracellular Vesicle Uptake by Kidney Collecting Duct Cells. **Journal of American Society of Nephrology** Published online before print March 28, 2016, doi: 10.1681/ASN.2015050568

.

CHAPTER 1

Introduction

Intercellular signalling controls a diverse range of cellular processes and activities in multicellular organisms. In the kidney, understanding intercellular signalling is vital, not only in physiology but also pathological states, particularly the development and progression of kidney disease. The unidirectional flow of urine along the renal tubule provides a natural transport system for cell-to-cell communication. The kidney is therefore the ideal anatomical model to study intercellular signalling mediated by components of urine.

There has been increased interest in the emerging role of extracellular vesicles as mediators of intercellular signalling and communication. Exosomes are a subset of extracellular vesicles, distinguished by their unique biogenesis in the endosomal pathway and identified by their physico-chemical properties. Exosomes are of specific interest in renal function due their ubiquitous nature and recognised function as vehicles of cellular information and function. A major ongoing challenge in the field, however, is to discriminate between exosomes and other extracellular vesicles such as microvesicles and apoptopic bodies (Table 1.1): the literature contains nomenclature that can be ambiguous. For clarity, in this study, "exosomes" are defined as extracellular vesicles sized between 20-100nm. These vesicles are derived from extracellular fluid such as cell culture supernatant or biological fluids such as urine and will not be distinguished based on cellular origin. Further distinguishing properties such as specific surface markers and purification methods will also be used for distinguishing exosomes from other cell-derived vesicles, as per recent international recommendations[1].

Table 1.1 Extracellular vesicles and their characteristics

Vesicles	Origin	Shape	Size	Markers	Sedimentation	Contents
Exosomes	Endosomal pathway	Cup shaped	20-100nm	Tetraspanins (CD63, CD24) TSG101, flotilin, ALIX, HSP70	100 000*g*	Cytoplasmic and membrane proteins, mRNA, miRNA, non-coding proteins, mtDNA and gDNA
Microvesicles	Cell surface; budding of cell membrane	Irregular, electron dense	50-1000nm	Integrins, selectins, Annexin V	10 000*g*	Cytoplasmic and Membrane proteins mRNA, miRNA, non-coding RNAs
Apoptopic bodies	Cell surface; outward blebbing of apoptopic cell membrane	Hetero-genous	500-2000nm	Phosphatidyl-serine, Annexin V, histones	1 200*g* – 10 000*g*	Nuclear fractions, cell organelles

Adapted from Andaloussi *et al*., 2013 and Braicu *et al*., 2015

1.1 Biogenesis of exosomes

Exosomes are small vesicles of endocytic origin which are homogenous in shape and size. *In vitro*, exosomes are released from a number of cell types including epithelial cells[2], endothelial cells[3], and B and T cells[4] amongst others. *In vivo*, exosomes have been identified and well characterised in a number of complex biological fluids including plasma[5], serum[6], saliva[7] and urine[8]. Currently, exosomes can be distinguished from other extracellular vesicles by a set of specific physico-chemical properties and their unique biogenesis within the endosomal pathway. The physico-chemical properties that distinguish exosomes from other extracellular vesicles include: their density when floated on a sucrose gradient (1.13 g/ml – 1.19 g/ml); unique 'cup-shaped' morphology with a distinct limiting lipid bi-layer and size between 20-100nm when viewed under transmission electron microscopy (TEM)[9]; and specific proteins central to their production and formation such as heat shock proteins (HSP) and tetraspannins[10,11].

The first step in the biogenesis of exosomes is the inward invagination of clathrin-coated micro-domains on the plasma membrane. Once these vacuoles enter the cells, the Endosomal Sorting Complex Required for Transport (ESCRT) facilitates the development into late endosomes. Maturation of early endosomes into late endosomes results in changes in contents and increased accessibility and subsequent accumulation of plasma membrane derived vesicles. This leads to an increased number of internal vesicles and total vesicle size. Late endosomes are therefore referred to as multivesicular endosomes (MVEs) (Figure 1.1). Vacuolar endosomes form vesicles by reversed budding into the lumen resulting into a 'right-side out' orientation in relation to the plasma membrane. These accumulated intraluminal vesicles (ILVs) have three fates: targeted to lysosomes for degradation; acting as vesicular intermediates to deliver histocompatibility complexes to the plasma membrane and finally, following fusion of these ILVs with the plasma membrane, these vesicles are released into the extracellular space and are now termed "exosomes"[12]. Secretion of exosomes into the extracellular environment is promoted by the RAB family of small GTPase such as RAB27A and 27B, with different molecules being described in different cells types[13].

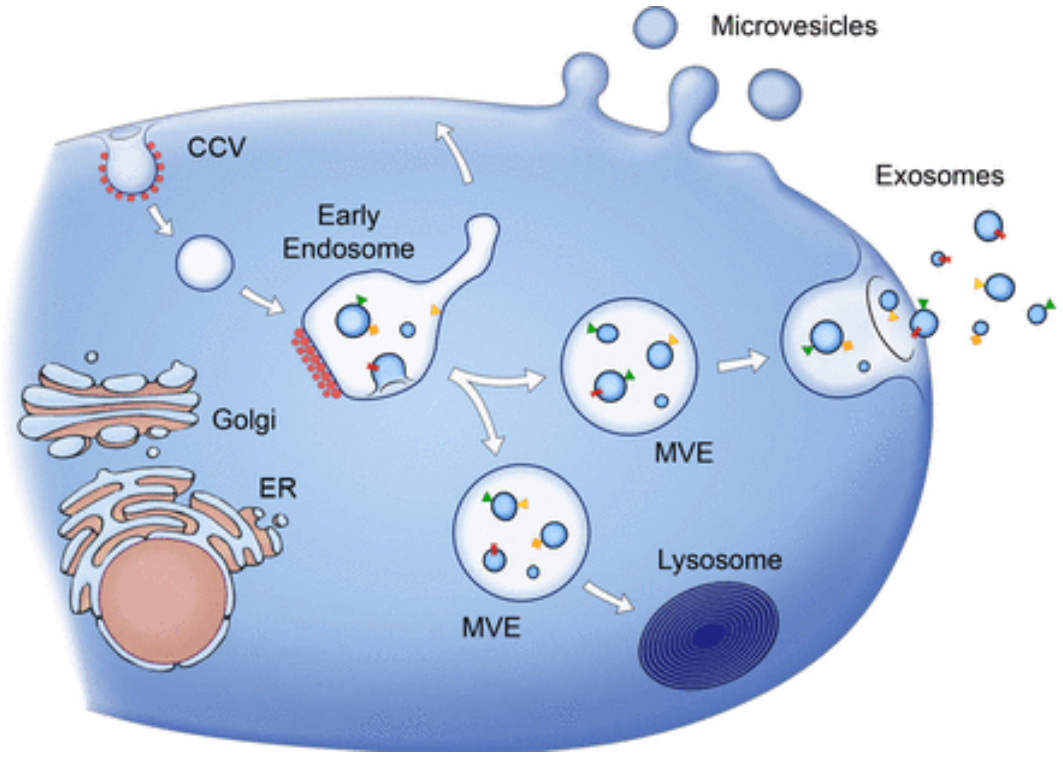

Figure 1.1: Exosome biogenesis within the endosomal pathway

Exosomes are represented by small heterogeneous vesicles that are formed following the inward invagination of clathrin-coated vesicles (CCV) on the plasma membrane. Maturation of early endosomes into late endosomes results in changes in contents and increased accessibility and subsequent accumulation of plasma membrane derived vesicles. Late endosomes are therefore referred to as multivesicular endosomes (MVEs). Exosomes are released by fusion of MVEs with the plasma membrane. Other MVEs fuse with lysosomes. Red spots symbolise clathrin associated with vesicles at the plasma membrane (clathrin-coated vesicles [CCV]). Membrane-associated and transmembrane proteins on vesicles are represented as triangles and rectangles, respectively. Arrows represent proposed directions of protein and lipid transport between organelles and between MVEs and the plasma membrane for exosome secretion. (Adapted from Raposo *et al*., 2013[14]).

1.2 Exosome purification, characterisation and detection methods

There is currently no clear consensus on the most efficient methods for obtaining high yields of pure exosomes from cell culture supernatant and complex biological fluids. The nano-sized scale of an exosome presents a challenge for accurate characterisation and detection but these needs to be addressed in order to harness their potential as biomarkers or therapeutics.

The International Society of Extracellular Vesicles has recently proposed the minimal experimental requirements required to define sub-populations of extracellular vesicles. The requirements state that the vesicles must be purified from extracellular fluid in a cell disruption limiting manner; at least three proteins characteristic of exosomes should be identified in a semi-quantitative manner; and finally, at least two different technologies of detecting and characterising exosomes should be used[1]. Here, purification and detection methods routinely being used will be discussed.

1.2.1 Differential ultracentrifugation

The most widely applied, and basic, method - due to its ease and high capacity - for separating exosomes from cells, apoptotic bodies, and microvesicles is differential ultracentrifugation. Ultracentrifugation has long been seen as the gold standard for the isolation of relatively homogenous size populations of exosomes. Briefly, this method involves slow centrifugation (~2000*g*) of the cell culture supernatant or fluid which will sediment cell debris, followed by pelleting of the exosomal fraction by a high *g*-force ultracentrifugation (~100 000*g*) step. This centrifugation approach, however, will also co-purify other non-exosomal components present in the cell culture supernatant or biological fluid. Sedimentation profiles were shown to be cell line dependent, in terms of both protein yield and purity[15]. In a complex biological fluid, for example urine, pelleting of urinary exosomes by ultracentrifugation showed 40% of exosome proteins remaining in the supernatant post-ultracentrifugation[16]. Ultracentrifugation is also not always applicable to clinical samples due to the large starting volume required and low throughput of this method coupled with variable

user-dependent recovery rates: a recent study showed 100% exosome recovery in a complex biological fluid such as plasma could not be achieved despite using spike-in control exosomes [17]. Indeed, even in cell culture supernatant, a 5-25% exosome recovery rate following ultracentrifugation have been reported[18,19].

1.2.2 Ultrafiltration

A few groups have developed ultrafiltration as an alternative and relatively rapid method of concentrating exosomes. Ultrafiltration is also recommended and increasingly incorporated as an additional step within the differential centrifugation isolation protocol to further remove non-exosomal proteins or larger particles[20]. Briefly, this method involves using a filter of a defined size to exclude or include only particles of a particular size. A further advancement using this method was the development of a nanomembrane concentrator which is able to concentrate urinary exosomes comparable to, and as effectively as, standard ultracentrifugation[21]. Supporting this, another study combined ultrafiltration with size-exclusion chromatography and was able to consistently demonstrate a lower protein/vesicle ratio compared to ultracentrifugation methods, suggesting a higher extracellular vesicle ratio[22]. Using ultrafiltration on a complex biological fluid such as urine, however, remains challenging, as soluble proteins tend to be retained and concentrated in urine in addition to exosomes, thereby reducing the sensitivity of subsequent detection and analysis methods[23].

1.2.3 Sucrose gradient

The use of a sucrose gradient can be seen as both a purification and detection method. The method of purification using a 30% sucrose cushion, is routinely added to differential ultracentrifugation to yield an exosome pellet with less larger protein particles or aggregates[24]. This method relies on the characteristic density of exosomes which will result in them floating at a defined density on the sucrose cushion. Recent studies have indicated a large loss in the total number of particles recovered using a sucrose gradient, but a lower protein/exosome ratio, again, suggesting a more pure preparation[20]. More refined variations of this method are in development, such as OptiPrep™ (Sigma-Aldrich, Dorset, UK), which is an

iodixanol-based density gradient which better preserves all sizes of vesicles by forming iso-osmotic solutions at all densities[25].

1.2.4 Commercial exosome precipitation reagents

In attempts to address the challenges associated with exosome purification, a number of commercial products have been developed to precipitate exosomes without the need of ultracentrifugation and the large required starting volumes associated with it, for example: ExoQuick™ (System Bioscience, California, USA) and Exo-Spin™ (Cell Guidance Systems, Cambridge, UK). The exact mode-of-action for either has not been disclosed or validated[26], but these products rely on polymer interactions to precipitate the exosomal fraction from a biological fluid. However, there has been considerable evidence that these products also co-precipitate soluble RNA-binding proteins and microparticles with exosomes in plasma[26] and urine[27]. Furthermore, ExoQuick™ has been shown to also enrich the RNA-binding ribonucleotide Argonaute-2 (Ago2) complex along with exosomes. This suggests significant contamination by RNA/protein complexes [25] which greatly biases down-stream RNA analyses of "exosomal" contents. Furthermore, contamination of the exosome preparation with undisclosed chemicals from the reagent could affect assays of exosomal biological activity.

1.2.5 Immuno-isolation

Immuno-isolation is a method using immune-magnetic extraction. Briefly, this method involves magnetic beads coated with antibodies directed to specific proteins exposed on the exosomal membrane, thereby providing a simple and rapid method not involving ultracentrifugation[28]. This bead-exosome complex is then of a suitable size for analysis by standard flow cytometry, immunoblotting or electron microscopy[24]. However, the major disadvantage of this isolation method is that it only allows the analysis of a subpopulation of exosomes and not the exosome population as a whole in any given sample. This method does, however, hold great potential in recent microfluidic developments of 'on-chip' exosome capture suggesting higher specificity and a shorter isolation time[19]. Supporting this, an exosome analysis platform, using 'on-chip' immunoaffinity to isolate tumor

exosomes from plasma from cancer patients, was reported to increase sensitivity whilst decreasing sample preparation time[29].

1.2.6 Transmission electron microscopy

Transmission electron microscopy (TEM) is a type of electron microscopy which uses electron voltage instead of traditional light microscopy to visualise a sample[28]. TEM is widely used to distinguish the unique 'cup-shaped' morphology of exosomes in comparison to other extracellular vesicles or apoptotic bodies. Briefly, TEM involves a number of steps involving fixation, dehydration, resin-embedding and ultra-thin sectioning, which may prove difficult and time consuming with exosome preparations[24].

1.2.7 Western Blot

In keeping with the required minimal requirements of classification of exosomes[1], western blots are routinely used to identify specific proteins by separating protein bands by SDS-polyacrilamide gel electrophoresis (SDS-page). Several proteins have been identified and are well defined as exosomal markers, for example – tumours susceptibility 101 (TSG101), Alix[12] and flotilin[30] Furthermore, a small, glycosylated protein CD24 has been shown to be a convenient exosome marker in urine[31]. The main disadvantage of using western blots to detect and characterise exosome populations is the large starting volume required for effective protein detection. To address this challenge, real-time detection and molecular profiling of exosomes are currently being developed using immunoaffinity[29].

1.2.8 Fluorescence microscopy

Using a fluorescence microscope, exosomes conjugated to specific fluorophores can be excited and detected within specified emission ranges. This allows live cell imaging of exosomes *in vitro* [32] and *in vivo*[33] and permits tracking of exosomal uptake/internalisation by using real-time fluorescence microscopy. However, this detection method still involves the time-consuming pre-processing steps of isolating and purifying exosomes before a fluorophore can be conjugated to the exosome.

1.2.9 Nanoparticle Tracking Analyses

Nanoparticle tracking analyses (NTA) is a relatively new technology within the field of light scatter microscopy, which measures the size and total number concentration of particles in solution. This method is based on direct and real-time tracking of nano- and microparticles' Brownian movement, which results in a description of the particle size and concentration distribution of a given solution. NTA is based on the principle that at any particular temperature, the rate of Brownian motion of particles in solution is determined solely by their size. In this method, laser light is directed at a fixed angle to the vesicle suspension, and the scattered light is captured using a microscope and high-sensitivity camera. By tracking the movement of individual particles over time, the software rapidly calculates their concentration and size. NTA also has fluorescent capabilities with a single long pass filter, thereby allowing quantification of a single fluorophore population. Indeed, by using fluorescent antibodies to specific surface proteins, studies have shown that it is possible to track specific subgroups of a defined size, such as exosomes, within the whole heterogeneous vesicle population found in complex biological fluids[34,35].

1.3 Exosome content

Exosomes isolated by the above methods are shown to contain proteins, lipids, DNA and a variety of RNA species including messenger RNA (mRNA) and micro-RNA (miRNA)[36].

1.3.1 Exosomal protein content

Large scale proteomics has been used to examine the exosomal protein content in a number of biological fluids, such as plasma[17] and urine[37]. These studies consistently define exosomes as a specific subcellular compartment, containing a specific, limited subset of proteins originating from the plasma membrane, endocytic pathway and cytosol, with little representation of proteins from intracellular organelles[38]. The set of proteins include: annexins and flotilins involved in membrane transport and fusion, proteins associated with multivesicular body biogenesis (TSG101 and Alix), protein families associated with lipid domains (integrins and tetraspanins) and heat

shock proteins (HSP70 and HSP90) involved in antigenic presentation. Indeed an interesting study further revealed a potential new role for urinary exosomes based the exosomal protein content: maintaining urine sterility by virtue of their antibacterial activity. In-depth proteomic analyses of human urinary exosomes showed significant enrichment for innate immune proteins which included antimicrobial proteins and bacterial and viral receptors with a combined inherent function of inhibiting bacterial growth and inducing bacterial lysis[39]. Additionally, further studies showed, functional proteins, such as proteins associated with intracellular transport, protein folding, stress response, cellular homeostasis and lipid metabolism show significant and similar enrichment in exosomes derived from different cell types including hepatocytes[40], mast-cells[41] and B cells[42]. Although exosomes do not contain the entire proteome of the cell of origin, they do contain proteins specific to the cell of origin[43]. This characteristic allows exosomes from specific cell types to be identified from the nanoparticle mix in complex biological fluids such as urine[37] and cerebrospinal fluid (CSF)[44]. The exosomal protein can reflect the physiological condition of the cells and any changes in cellular conditions. *In vitro*, in endothelial cells, the protein content of exosomes were significantly increased similar to increases in their cell of origin, in conditions stimulating hypoxia, hyperglycaemia and inflammation[43]. The exosomal protein content of aquaporin-2 (AQP2) was also shown to be reflective of differences in the collecting duct cell following vasopressin stimulation[45]. Similarly, *in vivo*, proteins associated with the response to inflammatory stimuli were higher in serum exosomes from a mouse model of ischaemia-reperfusion injury[46]. Fewer studies have investigated the lipid composition of exosomes, but generally cholesterol and sphingomyelin are enriched[47] combined with lipid-related enzymes, suggesting exosomes may be a unit of lipid production[48]. Exosomes have different lipid profiles compared to their cell of origin, suggesting different mechanisms allowing lipid sorting into vesicles [49].

1.3.2 Exosomal mRNA content

The discovery that exosomes contain mRNA was a major finding with great consequences for the field[50]. However, a number of subsequent studies have reported that exosomes contain substantially less mRNA compared to protein and miRNA[51,52].

Indeed, it has been reported that exosomes may only contain around 8% of the total mRNA compared to donor mast cells[50]. Further studies have revealed that exosome mRNA species have clear differences compared to their cell of origin, with the majority of exosomal mRNAs being associated with intracellular transport and receptor-ligand interactions[53]. This was supported by a study that reported exosomes to contain mainly mRNA fragments and being enriched for mRNA degradation products[54]. These differences in mRNA do, however, suggest selective packaging as some gene transcripts are found to be present in exosomes, but not in the cell of origin and *vice versa*[50]. mRNA content of exosomes is further altered depending on the cellular condition that they are released under, with the key function of exosomal mRNA being cellular development, protein synthesis and RNA post-transcriptional modification[50]. The general assumption has been that exosomal delivery of mRNA to a recipient cell leads to protein translation, but there has been convincing evidence that exosomal mRNA play a regulatory role rather through mediating miRNA-binding sites[55].

1.3.3 Exosomal miRNA content

MiRNAs are short (19-25 nucleotides in length), non-protein coding RNA transcripts which regulate post-transcriptional gene expression through repression of mRNA translation or cleavage. MiRNAs are stably conserved across species, protected from RNase-dependent degradation in the circulation and can be detected in plasma, serum and urine[56]. Exosomes contain miRNAs from their cell of origin, leading to increased interest in biomarker studies[50]. Consistently, in a number of different cell types including mast cells[53] and T-lymphocytes[4], some miRNAs are significantly more abundant in exosomes compared to miRNA levels in the cell of origin, suggesting a specific sorting mechanism [4,50,53]. The mechanisms which control miRNA sorting and packaging into exosomes are still not fully defined. Recently, SUMOylation – small ubiquitin-like modifier proteins – by a specific nuclear ribonucleoprotein (HnRNPA2b1) was reported to recognise and preferentially package targeted miRNAs into exosomes[57]. Better understanding of this process is crucial for understanding exosome physiology. Changes in the exosomal miRNA cargo do reflect changes in cellular conditions. Treatment of pancreatic B cells with

pro-inflammatory cytokines showed upregulation of exosomal miRNAs associated with cell death[58]. Similarly, exosomes from mast cells exposed to reactive oxidative species showed a different miRNA profile compared to exosomes from control cells[59]. As a caveat, a number of studies have indicated that it might not be the circulating exosomal compartment that contains the majority of miRNA, but rather the Ago2 complex[60,61] with up to 90% of miRNA present in a non-vesicle form bound to a ribonucleotide protein such as the Ago2 complex[62]. The authors hypothesised that vesicle-associated versus Ago2-associated miRNA populations originate from different cell types with different release mechanisms. For example let7a associates with vesicles from cells known to release exosomes such as reticulocytes maturing into erythrocytes[63], compared to miR-122 which reports hepatocyte injury seen to be Ago2 protein associated[64]. The exosomal miRNA cargo still necessitate better understanding and definition as it consistently induces a biological effect *in vitro*, this is possibly due to the potentially high number of exosomes circulating physiologically coupled with the suggested differential cargo packaging.

1.3.4 Exosomal DNA content

Exosomes have been shown to contain both mitochondrial and genomic DNA. Mitochondrial DNA (mtDNA) is only 1 chromosome and codes for specific proteins which are used in metabolic process. Genomic DNA (gDNA) is the standard 46 chromosomes containing the genomic lineage. Exosomal mtDNA has been identified in a number of different cell types including astrocytes and gliablastoma cells[65]. In human mast cells, 75% of the secreted mtDNA could be found in the exosomal cargo[66]. Recently, gDNA, representing the entire genome, was found within exosomes[67]. Available data are currently limited, but a study in pancreatic cancer patients was able to demonstrate that serum exosomes contain double stranded genomic DNA and furthermore that mutations frequently associated with pancreatic cancer are readily detectible in exosomal gDNA[68]. This was further supported by a study showing changes in the exosomal gDNA reflecting changes in the mutational status of the parental tumour cell[67]. There are, however, differences between the

donor cancer cell and exosomal gDNA, suggesting different recycling processes sensitive to post-translational modifications[69].

1.4 Exosomes as biomarkers of disease

Exosomes have great potential as a source of disease biomarkers due to their inherent ability to contain information from their cell of origin. As they express surface markers from specific organs, there is the potential to isolate organ-specific exosomes from complex fluids such as plasma and urine. Additionally, the structural integrity of a distinctive lipid bi-layer of an exosome protects the RNA cargo from degradation by RNAses[50]. Isolation of exosomes can also significantly increase the sensitivity and specificity of the biomarker analysis when compared to whole biological fluids. Exosomes, therefore, potentially provide a minimally invasive, rapid, liquid biopsy of the tissue of origin. Here, different exosomal contents as biomarkers of disease will be discussed.

1.4.1 Exosomal protein as biomarker of disease

The protein composition and surface markers associated with exosomes provides diagnostic biomarker potential. Large-scale proteomics of exosomes derived from a number of different cell types and different biological fluids, allowed large scale identification of exosome associated proteins as potential biomarkers for a number of diseases (Table 1.2). In cancer, exosome enriched glypican-1, a cell-surface proteoglycan, reported early stages of pancreatic cancer with a high degree of specificity and sensitivity[70]. Similarly, in bowel cancer, heat HSP60 has been demonstrated to be an early biomarker of tumour formation[71]. In sarcoidosis, exosome isolation from bronchiolar lavage fluid showed neuregulin-1 to be a reliable marker of inflammation[72]. The exosome proteome is also a rich reservoir of information in neurodegenerative diseases such as Alzheimers' disease (AD) and Parkinson's disease (PD). Proteomics on neural-derived exosomes revealed different profiles for autolysosomal proteins, such as lysosome-associated membrane protein 1 (LAMP-1) in patients with AD, reflecting pathology up to 10 years before clinical onset, compared to case control patients[73]. In PD, immunophenotyping CSF and serum exosomal protein populations identified a number of proteins differentially

expressed in PD patients compared to controls, highlighting the potential of a panel of exosomal proteins as a biomarker of PD[74]. Urinary exosome proteins also hold great potential as non-invasive biomarkers of kidney disease. Urinary exosomal fetuin-A protein is increased following cisplatin-induced acute kidney injury, this increase preceding serum creatinine elevation[75]. Wilms tumor 1 (WT1) concentration in urinary exosomes are also reported to be an early biomarker of diabetic nephropathy with an increase in expression level correlated with a decrease in renal function[76].

Table 1.2 Recent exosomal proteins identified as potential biomarkers in complex biological fluids in various diseases

Biofluid	Disease	Associated proteins	Early diagnostic/prognostic/ response to treatment	Reference
Plasma	Prostate cancer	Survivin	Early diagnostic	[77]
	Ovarian carcinoma	TGF-β; MAGE-3	Prognostic, response to treatment	[78]
	Pancreatic cancer	Glypican-1	Early diagnostic	[70]
	Large bowel carcinoma	HSP-60	Therapeutic response	[71]
	Alzheimer's disease	Cathepsin D, LAMP-1 & ubiquitinylated proteins	Early diagnostic	[73]
Serum	Melanoma	MDA-9 & GRP78	Prognostic	[79]
	Pancreatic cancer	CD44v6l Tspan8, EPCAM, CD104	Early diagnosis, therapeutic response	[80]
	Breast cancer	CD95-L	Therapeutic response	[81]

Biofluid	Disease	Associated proteins	Early diagnostic/prognostic/ response to treatment	Reference
Saliva	Lung cancer	CD63 & GADPH	Early diagnostic	[82]
	Oral cancer	139 peptides	Early diagnostic	[83]
	Pancreatic cancer	ASPN, Foxp1, Ging2, Daf2	Early diagnostic	[84]
Urine	Acute kidney injury	Fetuin-A	Early diagnostic	[75]
	Diabetic nephropathy	Wilms tumour 1	Early diagnostic	[76]
	Polycystic kidney disease	Ca2+ & cytoskeleton regulating proteins TMEM2	Response to treatment	[85]
	Parkinson's Disease	DJ-1	Prognostic	[86]
	Primary Aldosteronism	Phosphorylated NCC	Early diagnostic	[87]
	Obstructive nephropathy	TGFβ & L1CAM	Early diagnostic	[88]
	Diabetic kidney disease	Dipeptidyl peptidase 1V	Prognostic	[89]

1.4.2 Exosomal mRNA as biomarkers of disease

Exosomal mRNA is not gathering as much interest as protein or miRNA as potential biomarkers of disease (Table 1.3) due to a number of challenges associated with mRNA biomarker studies. Firstly, exosomal mRNA is not reflective of the cell of origin due to the selective packaging observed and the informative value of the cargo is questionable as it has been shown to be both fragmented [55] and associated with degradation machinery[54]. Secondly, there is currently no RNA internal control available to account for different exosome yields or degradation in complex biological fluids such as plasma or urine, with standard 18S or 28S measurements yielding variable results[55,90]. A recent, exciting study was able to circumvent these challenges by using microfluidic chip-based analyses to measure exosomal mRNA levels of two enzymes known to correlate with glioblastoma multiforme treatment. The authors demonstrated a strong correlation between these mRNA candidates and levels in the parental cell and furthermore, that these changes in exosomal mRNA were able to rapidly, and minimally invasively, track changes as treatment progressed[91]. This work was building on previous work identifying specific mRNA epithelial growth factor receptor (EGFR) mutations to be specifically found in serum derived exosomes from gliablastoma patients[92]. Other studies investigating exosomal mRNA reported that melanoma-derived exosomes have differential mRNA expression associated with metastasis and cancer progression[93]. In kidney disease, specifically podocyte injury induced kidney disease, urinary exosomal cystatin-C mRNA was identified as a potential biomarker of injury[94] and urinary exosomal C2AP mRNA has been identified as a biomarker of renal function and fibrosis[95].

Table 1.3 Limited exosomal mRNA identified as biomarker of various diseases in complex biological fluids

Biofluid	Disease	Associated mRNAs	Early diagnostic/prognostic/ response to treatment	Reference
Serum	Gliablastoma multiforme	RNU6-1 – noncoding RNA	Early diagnostic	[96]
Plasma	Gliablastoma	MGMT & APNG	Early diagnostic	[91]
	Gastric cancer	RNA 152	Early diagnostic	[97]
Urine	Kidney disease	CD2AP	Prognostic	[95]
	Podocyte injury	Cystatin-C	Early diagnostic	[94]

1.4.3 Exosomal miRNA as biomarkers of disease

Considerably more studies have indicated differential exosomal miRNA concentrations in a number of disease states including various types of cancer[98], liver disease[99] and kidney disease[100]. Specific identified miRNAs have also been identified in a variety of diseases (Table 1.4). In cancer, a panel of serum derived exosomal miRNAs including miR-1246 and miR-155 has been proposed as a more sensitive and specific biomarker in acute myeloid leukemia, rather than reliance on a single miR[101]. This combined approach was supported by a study combining differential protein and miRNA expression in serum derived exosomes to allow earlier and more specific and sensitive detection of pancreatic cancer[80]. Single, potential exosomal miRNAs are being identified as potential biomarkers in a number of disease states including cancer, diabetes and kidney injury and a select few examples will be highlighted. Serum exosomal miR-19a expression levels were shown to be increased in colorectal cancer patients compared to control[98]. Similarly, serum derived exosomal miR-21 levels were upregulated in patients with oesophageal squamous cell cancer with a positive correlation shown between miR-21 levels and tumour progression[102]. In incipient diabetic nephropathy patients, urinary exosomal miR-145 was enriched and upregulated[103]. miR-143 is upregulated in patients with type 2 diabetes and this upregulation can be detected in the early stages of the disease[104]. Urinary exosome levels of miR-29c were identified as a marker of early progression of fibrosis[100] and urinary exosomal miR-146a was able to discriminate the presence of active lupus nephritis in patients with systemic lupus erythematosus[105]. A major challenge in exosome miRNA biomarker discovery, however, similar to exosomal mRNA biomarker studies, is there is currently no endogenous control for exosomal miRNA in complex biological fluids. In serum, miR-221, miR-191, let-7a, miR-181a, and miR-26a were recently identified to be an optimal gene reference set for normalising the expression of liver-specific miRNAs[106].

Table 1.4 Recent exosomal miRNAs identified as potential biomarkers in complex biological fluids in various diseases

Biofluid	Disease	Associated mRNAs	Early diagnostic/prognostic/ response to treatment	Reference
Serum	Hepatocellular carcinoma	miR-718	Prognosis	107
		miR-21	Early diagnosis	108
	Pancreatic cancer	miR-1246, miR 4644, miR-3976, miR-4306	Early diagnosis and therapeutic response	80
	Colorectal cancer	miR-17-92a	Prognostic	98
	Breast cancer	miR-373	Early diagnosis	109
	Esophageal adenocarcinoma	miR-16, miR25, miR-15b, miR-30a, miR-17	Early diagnosis	110
	Laryngeal squamous cell carcinoma	miR-21 combined with HOTAIR noncoding RNA	Early diagnosis	111
	Advanced melanoma	miR-125b	Prognosis	112
Plasma	Non-alcoholic fatty liver disease	miR-122 & miR-192	Early diagnostic and prognostic	113
	Alzheimer disease	miR-342-3p	Early diagnostic	114
	Prostate cancer	miR-1290 & miR-375	Prognostic	115

Biofluid	Disease	Associated mRNAs	Early diagnostic/prognostic/ response to treatment	Reference
	Lung cancer	miR-151a-5p, miR-200b, miR-629, miR-100 & miR-154	Early diagnostic	116
	Peripartum cardiomyopathy	miR-146a	Early diagnosis	117
	Alcoholic and inflammatory liver disease	miR-122	Prognostic	99
Urine	Prostate cancer	miR-34a	Therapeutic response	118
	Diabetic nephropathy	miR-145	Early diagnostic	103
	Type 2 diabetes	miR-143	Early diagnostic	104
	Renal fibrosis	miR-18c	Early diagnostic & prognosis	95
	Acute myocardial infarction	miR-1	Early diagnostic	119
	Renal fibrosis in IgA nephropathy	miR-21, miR29 & miR-93	Early diagnostic & prognostic	120

Biofluid	Disease	Associated mRNAs	Early diagnostic/prognostic/ response to treatment	Reference
	Lupus erythematosus	miR-146a	Prognostic	[105]
	Autoimmune encephalomyelitis	miR-155-5p	Early diagnostic & therapeutic response	[121]
	Ovarian serous adenocarcinoma	miR-30a-59	Early diagnostic	[122]
	Autoimmune glomerulonephritis	miR-26a	Early diagnostic	[123]
	Lupus nephritis	miR-29C	Prognostic	[124]
	Prostate cancer	miR-34a	Therapeutic response	[118]

1.4.4 Exosomal DNA as biomarker of disease

There are very limited data available on exosomal DNA as a biomarker of disease. A recent study was able to demonstrate that exosomal DNA reflects mutations from parental tumour cells and thereby indicated exosomal DNA as a potential biomarker the early detection of cancer and metastasis[67]. Supporting this, the methylation status of gastric juice-derived exosomal DNA was recently reported to be a potential early biomarker of gastric cancer[125]. Exosomes from prostate cancer cell lines and pancreatic patient plasma samples also contain double-stranded gDNA fragments which could be used to detect specific mutations, making exosomes potential biomarkers for cancer diagnostics and prognostics in prostate cancer[126]. In this study, exosome subpopulations differed from each other in terms of total protein and DNA content. Further analysis of gDNA fragments from the prostate cancer cell line-derived exosome subpopulations demonstrated that different exosomes contained different gDNA content, which could even harbour specific mutations. These results suggest and support previous findings that not only proteins and RNA species, but also DNA is selectively and cell-dependently packed into the exosome subtypes. DNA biomarker candidates are slowly gaining interest and research effort, with limited results currently available to corroborate these findings. The inherent stability of DNA within exosomes coupled with the ability to enrich exosomes in whole vesicle populations using specific surface markers certainly proposes this an exciting area for future development.

1.5 Exosomes as mediators of intercellular communication

Exosomes were traditionally viewed as an alternative removal pathway to lysosomal degradation for the removal of senescent or excess lipids or proteins from cells. While a definitive physiological role of exosomes remains unclear, there has been accumulating evidence in the field towards intercellular signalling involvement. Here, exosomal content - protein, RNA species and DNA- as mediators of intercellular communication will be discussed.

1.5.1 Exosomal protein as mediators of intercellular communication

Initial studies centred on exosomal protein content and the role that changes in protein expression might play in physiological events. In the immune system, the presence of molecules involved in antigen presentation gave immune-cell derived exosomes a status of potential modulators of the immune response. In epithelial cell monolayers, exosomes were shown to be released across both apical and basolateral membranes. The protein content of the apically released exosomes was suggestive of clearance processes; antigen presentation associated proteins were found in the basolaterally released exosomes. Recently, exosomes were also demonstrated to control cell mobility by promoting cell adhesion through their fibronectin rich cargo[127]. The majority of research on exosomal proteins as mediators of intercellular communication remain, however, centred on pathophysiological states. In cancer, several studies have reported that tumour derived exosomes can alter the extracellular matrix through secretion of matrix metalloproteinases (MMPs) or activators of MMPs, such as HSPs, with exosomes shown to be generally pro-tumorigenic[128]. HSP70, which has been well-characterised within the exosomal protein cargo, has been reported to be an effective inducer of inflammation following infection. Exosomal protein delivery was also shown to be central to the spread of viral disease such as human immunodeficiency virus type 1 (HIV)[129] and hepatitis C[130], and neurodegenerative diseases such as Alzheimer's disease and Parkinson's disease[73]. Even though a number of studies have indicated the function and potential of exosomes as intercellular signalling vectors, the mechanism of exosomal trafficking and specifically exosome internalisation into target cells remain unclear. Receptor-ligand interactions between both the exosome and recipient cell are widely accepted as the initial cell communication point[47]. A step further, a number of studies have indicated endocytosis as a mechanism of exosome internalisation. Endocytic mechanisms which has been identified for exosome internalisation include: clathrin-dependent endocytosis; caveolae-dependent endocytosis; phagocytosis and macropinocytosis[131,132]. An additional consideration would be the micro-environment of the cells, as a low pH was reported to be conducive to greater exosomal uptake [133]. A recent study presented real time data on exosomes attaching to the plasma

membrane through receptor binding and entering cells through endocytosis in a renal tumour cell line[134]. Whether exosomes of various cellular origins preferentially target specific cell types and how they are packaged remain unclear.

1.5.2 Exosomal mRNAs as mediators of intercellular communication

The first study to suggest a role for exosomes as intercellular messengers found that systemically injected exosomes could deliver targeted short interfering RNA to the mouse brain[135]. From this starting point, it is now clear that exosomal mRNA can be delivered into a cell where it can be transcribed into new, functional proteins, thereby changing the function of the cell. Exosomes themselves do not have the machinery for functional protein synthesis and are only capable of inducing functional protein changes when the RNA cargo is delivered into a recipient cell [50]. Indeed, by using murine cell line derived exosomes, functional delivery mediated by exosomes was demonstrated in a human mast cell line, further supporting cross species functional exosome delivery [50,136]. Further support for this is a study showing horizontal transfer of functional mRNA in glioblastoma cells. Glioblastoma-derived microvesicles including exosomes were transduced with mRNA for a secreted luciferase and, after incubation of these loaded vesicles with healthy cells, luciferase activity continued to increase over 24 hours, supporting translation of the luciferase mRNA [92].

1.5.3 Exosomal miRNA as mediators of intercellular communication

miRNAs are one of the most abundant gene regulatory molecules and are estimated to regulate the expression of more than 60% of all protein coding genes[137]. There has been considerable interest in the contribution of the exosomal miRNA cargo to the inherent physiological function of exosomes *in vitro* and *in vivo*. Recent evidence suggests that miRNAs in exosomes can be released through ceramide-dependent secretory machinery regulated by neutral sphingomyelinase 2 (nSMase2) enzyme encoded by the smpd3 gene that triggers exosome secretion[138]. In metastatic breast cancer cells, nSMase2 or ceramide were shown to promote the exosome-mediated miR-10b secretion whereas ceramide inhibitor suppressed this secretion. There are a

large number of studies focused on exosomal miRNA mediating intercellular communication (Table 1.5); examples relating to cancer, cardiovascular disease and liver disease will be discussed. In pancreatic cancer, the differential profile of exosomal miRNAs compared to the parental cell, suggest a specific sorting mechanism and a specific role of exosomes in tumour-progression. Incubation with exosomes originating from pancreatic beta-cells treated with cytokines, induced apoptosis in healthy, untreated cells. Interestingly, by inhibiting Ago2, this effect was prevented[58]. In cardiovascular disease, embryonic stem cell derived exosomes delivered a protective effect by delivering miR-294 in a myocardial infarction mouse model [139]. This protective effect delivered by exosomes is also corroborated by a study in mice where exosomes delivered a regenerative effect in cardiomyopathy to improve heart function and fibrosis through miR-146a enrichment[140] An interesting study relating to alcohol-related liver disease reported that ethanol-treated exosomes contained miRNA-122 and were able to horizontally transfer this miR to monocytes which sensitized the recipient cells to inflammatory responses[141].

Table 1.5 The role of exosomal miRNA in physiological and pathophysiological processes

miRNA	Donor cell	Recipient cell	Biological function of miRNA	Target gene	Reference
miR-155	Epstein-Barr virus positive Burkitts lymphoma cells	Retinal pigment epithelial cells (ARPE-19)	Pro-angiogenic	VEGF-A	[142]
miR-155	Synthetic miR-loaded exosomes	Primary hepatocytes and Kuppfer cells	Induction of pro-inflammatory cytokines during LPS challenge	MCP1	[143]
miR-155 miR-146a	Wild type or miR-155 or miR-146a knockdown dendritic cells	miR-155 or miR-146a knockdown primary dendritic cells	miR-155: Pro-inflammatory response to LPS miR-146a: Anti-inflammatory response to LPS	miR-155: BACH1 & SHIP1 miR-146a: IRAK1 & TRAF1	[144]
miR-146a	Cardiosphere-derived cells	In vivo Neonatal rat cardiomyocytes	Regenerative, pro-angiogenic & promoting survival and proliferation	IRAK1 and TRAF6	[140]

miRNA	Donor cell	Recipient cell	Biological function of miRNA	Target gene	Reference
miR-223	Mesenchymal stem cells	Cardiomyocytes	Cardioprotective effects by reducing inflammation and cell death	Sema3A & Stat3	[145]
miR-122	Ethanol treated hepatocytes	Monocytes (THP1)	Increased levels of pro-inflammatory cytokines	HO-1	[141]
miR-143/145	Pulmonary artery smooth muscle cells	Pulmonary endothelial cells	Pro-migratory and pro-angiogenic		[146]
miR-214	Primary hepatic stellate cells (HSC)	Day 6 Primary HSC cells	Suppression of fibrogenic signalling	Twist1	[147]
miR-15a	Biliary exosomes	Cholangiocytes	Decreased proliferation	ERK1/2	[148]
miR-221/222	MCF-7 (Tamoxifen resistant)	MCF-7wt (Tamoxifen sensitive)	Increased proliferation, decreased apoptosis, increased colony forming ability	P27 and ERα	[149]

miRNA	Donor cell	Recipient cell	Biological function of miRNA	Target gene	Reference
miR-24, miR-891a, miR-106a, miR-1908	Nasopharyngeal carcinoma derived (TWO3) cells	T-cells	Inhibiting T-cell proliferation; increased pro-inflammatory cytokines	ERK, STAT1, STAT3 phosphorylation. STAT5 phosphorylation	[150]
miR-1	Primary glioblastoma cells	Brain microvascular endothelial cells (HBMVEC)	Tumor suppressive	Annexin-2	[151]
miR-142 miR-223	Macrophages	Hepato-carcinoma cells	Inhibition of proliferation of cancerous cells	Stathmin-1	[152]
miR-133a	Myotubes	Myoblasts	Commitment of myoblasts in the process of differentiation	SIRT-1	[153]
miR-214	Endothelial cells	Endothelial cells	Represses senescence; pro-aniogenic	ATM	[154]
miR-335	Jurkat T-cells	Raji B-cells	Regulate immune synapse	SOX4	[4]

1.5.4 Exosomal DNA as mediators of intercellular communication

There is very little available research on the role the exosomal DNA cargo plays in mediating intercellular communication in either physiological or pathophysiological states, reflecting limited available knowledge on exosomal DNA content. The discovery of both single-stranded mtDNA and double-stranded gDNA will undoubtedly lead to increased research efforts into the possible roles exosomes may play in DNA regulation. One study was able to show horizontal mtDNA delivery by exosomes in human fibrosarcoma cells and human alveolar epithelial cells[155]. Whether this delivery is functional however, remains unclear. Another study reported transfer of foreign DNA by exosomes through electroporation of exogenous DNA, but functional changes in the recipient cells were not seen[156].

1.6 Exosomes and the kidney

Urine contains exosomes from all segments of the nephron. The identification and proteomic discovery of urinary exosomes containing proteins specific to each segment from the podocyte to the epithelium of the bladder[8] has led to an substantial increase in research interest to better defining the role of exosomes within the kidney. Proteomic analysis of urine can therefore potentially provide insight into the physiological and pathophysiological processes in every cell type facing the lumen. The proteins identified in large-scale proteomics are not only proteins directly involved with vesicle formation but also known proteins associated with kidney diseases (Table 1.6)[157]. This has highlighted the potential of urinary exosomes as an easily accessible, reservoir of proteomic information from the renal epithelial cell of origin and subsequent biomarker of disease.

The second wave of interest in urinary exosomes were the identification of nucleic acids in human urinary exosomes encoding all segments of the nephron and collecting duct[158]. This ground-breaking study further revealed exosome mRNA levels reflect mRNA levels in the renal tissue of origin and thereby highlighted the use of urinary exosomes for pathophysiological analysis in the kidney. Similarly,

miRNA were also identified in urinary exosomes[159]. A large number of studies are exploring urinary exosomes as kidney disease biomarkers and the role in the pathophysiology of the kidney, but little is known about its physiological relevance. The identification of CD24 – a small glycosylated protein as a convenient marker of urinary exosomes conserved across species, has helped gain some further insight into the biological relevance of the exosome secretion process[31].

Table 1.6 Segment of nephron with identified proteins and associated kidney disease

Segment of nephron	Protein	Associated kidney disease	Reference
Glomerular podocytes	Podocin and podocalyxin	Steroid-resistant nephrotic syndrome	8
Proximal tubule	Cubilin,	Imerslund-Gräsbeck syndrome	160,161
	Type IV carbonic anhydrase	Proximal renal tubular acidosis	157,162
	Aquaporin-1	Renal ischemia-reperfusion	163
Thick ascending limb of Henle	THP, CD9, Type-2-Na-K-2Cl cotransporter	Bartter syndrome type 1	162,164
Distal convoluted tubule	Sodium co-transporter	Gitelman's syndrome	162,164
Collecting duct	AQP2,	Nephrogenic diabetes insipidus	164
Transitional epithelium of urinary bladder	Uroplakin-1 and -2	Bladder cancer	165

1.7 Exosome signalling in the kidney

There has been convincing and accumulating evidence that urinary exosomes can deliver protein and RNA contents to a recipient cell and thereby change the proteome or function of a recipient cell along the length of the nephron. Combined with the unidirectional flow along the nephron, the kidney is indeed the ideal anatomical model to investigate exosome mediated intercellular signalling. However, physiological exosome signalling in the kidney remains poorly defined and understood. The roles exosomes may play in pathophysiological states, conversely, have been increasingly explored. One of the first studies to show downstream exosome uptake was a study showing real-time exosomal transfer between human proximal tubular cells and 5 different distal tubule cell lines and 3 different collecting duct cells lines. Furthermore, stimulation of the proximal tubular cells with fenoldopam, a dopamine receptor agonist, increased exosome production and reduced the basal ROS production rates in recipient, downstream cells[166], suggesting functional uptake. Here, a number of examples of exosome signalling in specifically relevant to kidney disease and renal cancer will be described. In a rodent experimental model of progressive renal disease resembling human chronic kidney disease, administration of culture media containing exosomes from human embryonic mesenchymal stem cells (MSC) rescued kidney function in rodents potentially through active DNA damage repair, proliferation and angiogenesis[167]. In acute kidney injury, human adult MSC-derived microvesicles including exosomes, mimicked the protection against AKI provided by intravenously administered MSCs[168]. This reno-protective effect has been described as a potential mechanism through which exosomes can horizontally transfer growth factors or growth factor receptors to tubular cells thereby potentiating the sensitivity of the recipient cell to locally produced growth factors[169,170]. This is supported by a separate study which was able to show exosomes can deliver genetic information and transforming growth factor-beta 1 mRNA that has the capacity to initiate tissue repair or regenerative responses in fibrotic kidneys and hypoxic epithelial cells[171]. Studies have aimed to elucidate the underlying molecular pathway involved. In a cisplatin-induced nephrotoxicity model, cisplatin-induced AKI rats treated with human MSC exosomes

showed a significant reduction in proximal tubular necrosis, oxidative stress, apoptosis and blood urea nitrogen and creatinine levels potentially through activation of the extracellular signal regulated kinase (ERK)1/2 pathway[172]. In contrast to this protective role in kidney disease, research suggests exosomes play a tumour-promoting role in renal cancer. In renal cancer cell derived exosomes were shown to promote angiogenesis through the upregulation of VEGF expression and down regulation of hepatocyte cell adhesion molecule (HepaCAM) in HUVEC cells[173]. HepaCAM is well defined to mediate cancer cell proliferation, migration and differentiation. Indeed, exosomes isolated from adenocarcinoma cells inhibited Jurkat t-cell proliferation and induced apoptosis in a dose- and time-dependent manner. This study showed exosomes contribute to immune evasion of tumours in the kidney by containing fas ligands, a type-II transmembrane protein belonging to the tumour necrosis factor family and treatment with soluble fas abolished exosome mediated Jurkat t-cell apoptosis[174].

The mechanisms of exosome uptake and release in physiological states in the kidney remain unclear. Work in our own group have identified and characterised exosomes from cell culture supernatant from a murine collecting duct cell line. The characterised exosomes were shown to express the known exosomal markers TSG101 and flotilin-1 with the characteristic and unique exosome 'cup'-shaped morphology when viewed under transmission electron microscopy. They were further able to show that stimulation with desmopressin, a vasopressin analogue, led to an increase in AQP2 expression in the exosomes which correlated with AQP2 abundance in whole cells. Functionally, they were able to show that desmopressin stimulated exosomes can deliver functional water channels to recipient cells and increase water flow significantly, thereby representing a novel physiological mechanism for cell-to-cell communication within the kidney.

1.8 Vasopressin regulation in the kidney

Arginine vasopressin (AVP) is a small neuropeptide of nine amino acids, predominately produced in the hypothalamus and, to a much lesser extent in a number of peripheral tissues[175]. AVP has an endocrine, paracrine and autocrine

effect. The most potent stimulus for AVP secretion from the posterior pituitary is change in plasma osmolality. When plasma osmolality rises above a physiologic threshold, secretion from the vasopressinergic nerve endings in the neurohypophysis increases[176]. Changes in blood volume and blood pressure will affect secretion of AVP, but this requires larger changes for hormone release compare with serum osmolality. AVP primarily acts through receptors located in the brain and periphery: V1a, V1b and V2. V1a receptors are present in many tissues including smooth muscle cells, the brain, adrenal cortex, adipose tissue, and hepatocytes. V1b receptors are mainly present in the anterior pituitary, adrenal medulla, islet of Langerhans, and white adipose tissue. V2 receptors are mainly present in the kidney on the basolateral membrane of the collecting duct and alveolar epithelial cells. AVP binding to the V2 receptor decreases water excretion, increasing the fraction of filtered water returned to the blood. In the kidney, binding of AVP to the V2 receptor leads to increased intracellular cyclic-AMP (cAMP) which in turn leads to phosphorylation and apical membrane accumulation of AQP2[176]. However, trafficking of this basolaterally located AQP2 remains poorly understood. The V2 receptor (gene symbol, AVPR2) is a G protein-coupled receptor with physiological functions mediated by heterotrimeric G-protein Gs. This results in activation of adenylyl cyclases to increase intracellular levels of cAMP. Mutations in the AVPR2 gene are responsible for X-linked nephrogenic diabetes insipidus.

1.8.1 Aquaporin 2

AQP2 is a gene coding for aquaporin 2, functional water channels expressed throughout the collecting duct system of the kidney. Under vasopressin control, AQP2 mediates apical transepithelial water transport across the collecting duct epithelium. Two forms of AQP2 regulation have been identified: short term and long term. Short term effects are the result of membrane trafficking. In non-AVP stimulated states, AQP2 is stored in vesicles in the supranuclear region in the principal cells of the collecting duct and mostly colocalised with Rab11 – a marker of apical recycling endosomes[177]. This indicates that early endosomes may play a part in its trafficking to the plasma membrane following AVP stimulation. Following AVP stimulation, AQP2 at the cell surface is rapidly retrieved to the intracellular

vesicles by endocytosis and is concentrated in the clathrin-coated pits at the plasma membrane of the collecting duct principal cells [178]. The long term effect of AVP is an increase in the total abundance of AQP2 protein, both by increasing the protein half-life and increasing transcription and translation of new protein[179].

AQP2 trafficking and its regulation within the principal collecting duct cells is an interesting field of study as it is a responsive mechanism with measurable functional effects which could provide information and insight into exosome signalling in physiological states. AQP2 has been identified to be present in urinary exosomes in a number of studies[8,21]. As discussed previously, work in our group was able to demonstrate that exosomal expression of AQP2 closely reflects cellular expression in a dose- and time dependent manner following AVP stimulation. Secondly, the functional AQP2 transfer between cells and exosomes may represent a novel physiological mechanism for cell-to-cell communication within the kidney[45]. However, the mechanisms of exosome uptake and release remain unclear.

1.9 Acute kidney injury

Acute kidney injury (AKI) is common and is seen in about 15% of adults admitted to hospital. AKI also presents poor prognosis and high mortality rates around 30-40% in the UK[180]. AKI is characterised by a rapid reduction in kidney function resulting in a failure to maintain fluid, electrolyte and acid-base homeostasis measured by changes in serum creatinine or urinary output. AKI has a myriad of causes, usually multifactorial, which can be divided and described as 'prerenal, postrenal or intrinsic'[181]. Prerenal causes include any factor which may impair blood flow to the kidney for example renal ischemia or low blood volume. Intrinsic causes include damage to the kidney itself or disease of the renal parenchyma for example glomerulonephritis, acute tubular necrosis and acute interstitial nephritis. Post renal causes of AKI, on the other hand, is a consequence of urinary tract obstruction which may be within the urinary tract itself for example blood clots or extrinsic, for example formation of tumours[181]. Contrast media induced acute kidney injury (CI-AKI) is the development of acute kidney injury (AKI) following the administration of radiographic contrast media (CM)[182] and can be described as a prerenal etiology

due to it renal vasoconstrictive effects. The definition of CI-AKI is variable, as it is challenging to exclude other causes of AKI unrelated to CM, but it is generally defined as 'a sudden alteration in renal function within 24-72 hours of the intravascular injection of CM which cannot be attributed to any other causes' [183]. The reported incidence of CI-AKI reflects the variability in definition, varying from 2-30%. Even though the direct mechanisms of CI-AKI are not yet fully understood, possible pathophysiological mechanisms of CI-AKI include: direct CM molecule tubular cell toxicity; haemodynamic effects primarily through afferent arteriolar vasoconstriction; and endogenous biochemical disturbances such as changes in nitric oxide levels and increases in oxygen-free radicals[184,185]. Investigating CI-AKI within the context of exosome mediated intercellular signalling in the kidney is of particular interest as it could potentially provide more information of disease propagation along the length of the nephron in a clinically relevant setting.

1.9.1 Biomarkers of AKI

Currently, serum creatinine is the standard index of kidney function and also the gold standard for recognising and diagnosing AKI. Serum creatinine as a biomarker of kidney injury does, however, have limitations as it is slow to reflect changes in glomerular filtration rate which can potentially delay diagnosis[186,187]. It is also non-specific and subject to renal and non-renal influences (such as hydration levels and muscle mass). Considerable research efforts aimed at discovering and developing new, accurate biomarkers of AKI are ongoing. Although this research speciality is still relatively new, a number of key points have so far became evident. Firstly, changes in concentration levels of newly identified biomarkers are detected relatively faster compared to changes in serum creatinine concentrations. Secondly, these biomarkers of AKI can be used to monitor the therapeutic response as it changes with treatment or recovery. And thirdly, the discovery of new biomarkers of AKI leads to better understanding of the pathogenesis of AKI through identifying possible mechanisms of injury. Two candidates reflecting kidney tubular damage as opposed to disturbed function are NGAL and KIM-1. NGAL (Neutrophil-gelatinase-associated lipocalin) is a protein bound to gelatinase in specific granules of the neutrophil. It was first discovered to have a ten-fold increase in expression within

only a few hours following ischaemic renal injury in a mouse model[188]. Subsequently, numerous studies have demonstrated that NGAL is a sensitive early marker for AKI in humans, preceding serum creatinine concentration increases by 1-3 days[189,190]. KIM-1 (Kidney Injury Molecule-1) is a type-1 cell membrane glycoprotein containing a unique immunoglobulin-like and mucin domain in its extracellular region. These ecto-domains are shed into urine following proximal tubular injury and can be quantified in both murine models[191] and humans[192]. A number of studies have unequivocally demonstrated both NGAL and KIM-1 to be novel, predictive biomarkers for AKI[193]. The limitations of serum creatinine and existing AKI markers, however, highlights the need for new candidates for timelier diagnosis of AKI - which will aid better prediction and stratification of injury and lead to more refined methods of safety assessment of nephrotoxic events during drug development[193]. It would also be of interest to develop a more comprehensive characterisation of kidney injury propagation along the nephron in a CI-AKI model to further elucidate the underlying pathophysiological mechanisms in AKI.

1.10 Aims of study

Accurate assessment of urinary exosomes remains challenging, in part because of a lack of consensus in methodologies to measure extracellular vesicles and the inability of most techniques to capture the entire size range of these vesicles. However, newer techniques and standardized protocols to improve the detection of exosomes are in development. A clearer understanding of the composition and biology of exosomes will provide insights into their physiological and pathophysiological roles to further aid and develop their potential as biomarkers and therapeutic agents.

We hypothesise that exosomes mediate intercellular communication in the kidney. To address this, the aims of this study were to:

1) Develop nanoparticle tracking analysis (NTA) as a technique to quantify exosomes in urine.
2) Investigate the hormonal regulation of exosome uptake *in vitro* and *in vivo*.
3) Investigate exosome excretion in a central diabetes insipidus (DI) patient and a patient group after contrast media exposure to investigate exosome excretion along the kidney in injury.

CHAPTER 2

Materials and Methods

2.1 Particle size and concentration distribution measurement by NTA

Nanoparticles in the whole urine samples and isolated exosome suspensions were analysed using the NanoSight LM 10 instrument (NanoSight Ltd, Amesbury, UK) which allowed simultaneous estimation of size, size distribution and concentration of dilute suspensions of nanoparticles. Using a 532nm (green) diode laser beam a 60 second video was taken with a frame rate of 30 frames/second and particle movement were analysed by NTA software. Each experiment was carried out in triplicate. All experiments were carried out at a 1:1000 dilution, yielding particle concentrations in the region of $1x10^8$ particles/ml in accordance with the manufacturer's recommendations. For fluorescent NTA analysis a 532nm (green) laser diode excited the Qdots with a long pass filter (430nm) so that only fluorescent particles were tracked and labelled particle concentration determined by NTA software. In each run, fresh samples were injected three times and measurements were performed following each injection. Standard deviations were determined from concentrations obtained from replicate runs.

2.2 Cell Culture

The murine cortical collecting duct cell line (CCD) was a kind gift from Hans-Peter Gaeggeler and Bernard Rossier (University of Lausanne, Lausanne, Switzerland; Gaeggeler *et al*. 2005) and was grown following Street's established method[45]. Briefly, the cells were grown in Dulbecco's modified Eagles medium (DMEM)–F12 medium, 1:1 (Gibco, Paisley, UK), supplemented with 2% fetal calf serum (FCS; Invitrogen, Paisley, UK), 1× insulin transferrin selenium (ITS) solution (Gibco), 100 I.U/ml penicillin and 100μg/ml streptomycin (Invitrogen), 50 pM dexamethasone (Sigma Aldrich), 1 nM3,3,5-triiodo-L-thyronine sodium salt (Sigma Aldrich) and 10 ng/ml epidermal growth factor (Sigma Aldrich). Passaging was achieved by two 10 min washes with 1 mM EDTA in Dulbecco's modified phosphate-buffered saline (DPBS) followed by incubation in trypsin EDTA solution (Lonza, Basel, Switzerland). The presence of exosomes in FCS would interfere with our study so they were depleted as follows. FCS was diluted to 20% with media and then ultra-

centrifuged for 2 hours at 200,000g. The supernatant was removed and filtered through a 0.22μm cellulose acetate filter.

2.3 Isolation and fluorescent labelling of exosomes

Culture media from CCD cells was vigorously vortexed then centrifuged at 15,000g for 10 min to pellet any cells, large membrane fragments and other debris. The supernatant was then centrifuged at 200,000g for 60 min to pellet the exosomal fraction. The pellet was washed with phosphate-buffered saline (PBS) and then re-centrifuged at 200,000 g for 60 min before final resuspension in PBS. Pelleted exosomes were conjugated with Cell Tracker 655 (Invitrogen) following the manufacturer's protocol. Briefly, pelleted exosomes were incubated with the Cell Tracker 655 conjugate in 200ul fresh culture media for 1hr at 37°C. The exosomal pellet suspension (Qdot-Exosome) was washed twice with fresh media before being put back on confluent cells. Exosomal size distribution was confirmed by NTA of a 1:1000 dilution of Cell Tracker 655 conjugate. Bovine serum albumin was used as a control and treated in the same way as exosomal isolation.

2.4 Antibody conjugation with quantum dots

The anti-CD24 antibody was a kind gift of Dr P. Altevogt (German Cancer Research Center, Heidelberg, Germany)[31]. Following the manufacturer's protocol, quantum dots (Qdots) were conjugated to anti-CD24 antibody with a Qdot 605 Antibody Conjugation Kit (anti-CD24 Qdots) (Invitrogen). Briefly, Qdots were activated with the cross-linker 4-(maleimidomethyl)-1-cyclohexanecarboxylic acid N-hydroxysuccinimide ester (SMCC), yielding a maleimide-nanocrystal surface. Excess SMCC was removed by size exclusion chromatography. The antibodies were then reduced by dithiothreitol to expose free sulfhydryl groups, and excess dithiothreitol was removed by size exclusion chromatography. The activated Qdots were covalently coupled with reduced antibody and the reaction quenched with mercaptoethanol. Conjugates were concentrated by ultrafiltration and purified by size exclusion chromatography. Anti-AQP2 antibody was purchased from Millipore (Billerica, MA, USA). Mouse IgG antibody was purchased from Invitrogen. Both antibodies were also conjugated to Qdots as described above. The suspension (see

above) was diluted 1:1000 and antibody-Qdots were added to give a final sample-Qdot concentration of 10 nM. After 1 hour incubation with the urine sample, at room temperature, the labelled urine samples and isolated exosomes were analysed by NTA.

2.5 Data and statistical analyses

Data were stored and analysed using GraphPad Prism Version 6 (La Jolla, California, USA) unless otherwise stated. For NTA results, data from three triplicate videos were analysed by calculating the area under the curve (AUC) for particles sized between 20-100nm. The intra-assay variability was determined by the coefficient of variability between the calculated AUC from the triplicate videos. Throughout, unless otherwise stated, differences between two experimental conditions were calculated by paired t-tests. Differences between three different experimental conditions or more were analysed by non-parametric ANOVAs with suitable post-hoc tests. Data were expressed as Tukey plots showing mean ± SD and $P < 0.05$ were seen as significant throughout. Different statistical analysis methods employed in further chapters will be discussed.

CHAPTER 3

Exosome quantification by NTA

3.1 Introduction

The potential of exosomes as biomarkers and novel therapeutic agents has been extensively highlighted in a number of disease states, including acute[75] and chronic kidney disease[194]. Exosomes are vesicles that are released from a wide range of cell types into complex biological fluids, including urine[8]. Exosomal cargo, which includes protein and nucleic acids, changes with kidney injury[195]. This presents an opportunity to track changes in intracellular pathways, which may even precede a decline in renal function, without the need for an invasive tissue biopsy. Moreover, using exosomes to deliver new information to a recipient cell further highlights their potential as therapeutic agents[135].

The first step in exploiting this two-fold potential would be the successful isolation and characterisation of exosomes to effectively measure the size and concentration of circulating exosomes in clinical biofluid specimens. Previous research has been constrained by the limitations of available measurement methods and has been hampered by lengthy isolation and characterisation methods involving ultracentrifugation, electron microscopy and flow cytometry to semi-quantify exosomes in biofluids. These methods are not only time consuming, but are also proven to lack sufficient accuracy and sensitivity at the small nanoparticle sizes characteristic of exosome[34].

There is, therefore, a pressing need for new technologies that can measure extracellular vesicles, including exosomes, in biofluids such as urine, rapidly and accurately with minimal sample preparation. This would allow excretion in animal models and humans to be quantified and the effect of physiological changes and disease on vesicle release to be defined in a more time appropriate manner. The current lack of precise quantification of urinary exosome concentration also significantly compromises RNA and protein biomarker discovery studies, as existing methods for quality control and normalization across study groups are inadequate[196].

A recent technological advancement called nanoparticle tracking analyses (NTA) use light scatter microscopy to determine the number and distribution of micro- and nanoparticles in a given solution directly and in real-time[34]. NTA is based on the

principle that at any particular temperature, the rate of Brownian motion of particles in solution is determined solely by their size. In this method, laser light is directed at a fixed angle to the vesicle suspension, and the scattered light is captured using a microscope and high-sensitivity camera. By tracking the movement of individual particles over time, the software rapidly calculates their concentration and size. Published studies have demonstrated that through the use of fluorescent antibodies, NTA can count and size specific subgroups of particles within the wider particle population[34,35], but this has not yet been applied to urine.

Therefore, the first aim of the studies presented in this chapter was to assess the capability of NTA to quantify exosomes in whole urine; the second aim was to exploit the fluorescent antibody labelling system to track specific exosome populations. And the third aim was optimise storage conditions by evaluating the preservation of exosomes in whole urine samples using NTA.

Ultimately, development and refinement of new approaches in more rapidly quantifying exosomes in complex biological fluids such as urine is crucial in further understanding the interaction between exosomes and kidney cells and to potentially deliver RNA therapies in the treatment of diseases of renal tubular dysfunction.

3.2 Methods and materials

3.2.1 Urine collection

Second morning spot urine samples were obtained from healthy volunteers recruited from the local community. Inclusion criteria were age between 20 and 40 years (25.6 ± 3.1 years); body mass index < 30 kg/m^2 (23.1 ± 2.2 kg/m^2) and no history of cardiovascular disease, diabetes, hypercholesterolemia or renal disease. None of the included volunteers were taking any medication, vitamins or nutritional supplements. The protocol agreed with the institutional ethics rules and informed consent was obtained from volunteers included in the study.

3.2.2 Exosome isolation

Exosomes were concentrated by ultra-centrifugation or commercial as per described methods in Chapter 2.

3.2.3 Antibody-specific fluorescent labelling of quantum dots

Antibody-specific fluorescent labelling with quantum dots was performed as per described methods in Chapter 2.

3.2.4 Particle size and number distribution measured by NTA

The size and number distribution of particles in solutions or urine were measured by NTA as per described methods in Chapter 2.

3.2.5 Validation and specificity of antibody-specific labelled exosome quantification by NTA

3.2.5.1 Validation by lysis of cellular membrane

Spot urine samples were obtained from five healthy male volunteers (aged 22-30) following informed consent. Exosome pellets from urine samples were isolated. Following the final centrifugation step, the remaining pellet was re-suspended in PBS and divided into two aliquots. Qiazol lysis reagent (Qiagen, Hilden, Germany) was added to one of the aliquots and the remaining aliquot left untreated. Qiazol lysis reagent is routinely used as a cell and cell membrane lysis reagent during cellular or tissue RNA extraction. All prepared samples were diluted and labelled with anti-CD24 Qdots prior to NTA measurements, as previously described.

3.2.5.2 Clinical relevance of specificity of NTA measurements

Urine samples from 10 metastatic renal clear cell (RCC) cancer patients before and after metastatic nephrectomy were kindly obtained from Dr G Stewart (Senior Lecturer in Urology, University of Edinburgh). Carbonic Anhydrase 9 (CA9) has

been shown to be a marker for metastasis and tumour formation in this patient cohort[197]. Anti-CA9 (Sigma Aldrich) antibody was conjugated to Qdots as previously described (anti-CA9 Qdots). Urine samples from patients before and after nephrectomy were incubated with the anti-CA9 Qdots and subsequently measured by NTA. Differences in CA9 positive exosome quantities before and after nephrectomy were analysed and compared by Kruskal-Wallis paired t-tests.

3.2.6 Cell culture model of exosome release

Murine kidney collecting duct (CCD) cells were grown in culture as described in Chapter 2. Briefly, following confluency, cells were stimulated with desmopressin (Sigma-Aldrich), 3.16 ng/ml for 48 and 96 hours. The cell culture medium (2 ml) was then analysed by NTA following fluorescent labelling with anti-AQP2 Qdots.

3.2.7 Urinary exosome excretion in the mouse

Mice (C57/BL6; n = 6) were individually housed in metabolic cages (model 3600M021; Techniplast, Buguggiate, Italy) with free access to food and water. After acclimation, daily food and fluid intakes were measured, as well as body weight. Each mouse received a single subcutaneous injection of 0.9% NaCl (1 µl/g body weight) on days 1 and 2 and, after each injection; a 24 hour urine collection was performed. On days 3 and 4, mice received a subcutaneous injection of desmopressin (1 µl/g body weight of 10 µg/ml drug solution), and two further 24 hour urine collections were performed. A second cohort of mice (n = 5) was used as control animals, receiving subcutaneous injections of 0.9% NaCl on all 4 days. All studies were performed with the appropriate Home Office (UK) licence.

3.2.8 Evaluating optimum storage conditions for exosomes by NTA

Freshly obtained urine samples (60 ml each) from 5 volunteers were subjected to 4 different storage protocols (6ml 1:1000 dilution per protocol in 3 x 2ml aliquots) all with and without protease inhibitors (1:10 final concentration: 0.5 mM

phenylmethylsulfonyl fluoride (PMSF; Sigma Aldrich), 20 µM leupeptin (Sigma Aldrich)). The protocols were:

a) analysed immediately with NTA;

b) stored at room temperature; 4°C; -20°C or -80 °C for 2 hours;

c) stored at room temperature; 4°C; -20°C or -80 °C for 1 day

d) stored at room temperature; 4°C; -20°C or -80 °C for 1 week.

All samples were vigorously vortexed while thawing following Zhou *et al.*'s (2006) recommendation. Each NTA measurement for the different protocols for each subject were performed as described above.

3.3 Results

3.3.1 Optimising dilutions of urine sample preparation

The analysis settings were optimised and kept constant between samples and each video was analysed to give the mean, mode, median and estimated number of particles for each particle size. Following the Sokolova *et al*. (2011) method and initial comparison between whole urine samples and 1:1000 dilution, all experiments were carried out at a 1:1000 dilution (Table 3.1), yielding equivalent particle concentrations in the region of $1x10^8$ particles/ml in accordance with the manufacturers' recommendations. Hereafter, 'whole urine sample' refer to a 1:1000 dilution of obtained sample.

A representative report obtained from the NTA software is shown in Figure 3.1a, showing the particle size concentration distribution. A screenshot of undiluted, unprocessed urine (Figure 3.1b) reveals a heterogenous, and highly concentrated particle size distribution. Heterogenous, polydisperse biological samples will normally show a log-normal particle size distribution profile unless purified or fractioned, with different amounts of light scattered and subsequent different estimates of concentration. To address this potential bias introduced into a system the lower limit of concentration was chosen (1:1000 dilution yielding a 1×10^8 equivalent particles/ml) for all further analyses (Figure 3.1c).

Table 3.1: Representative comparison of the equivalent particle concentration from serial dilutions of urine samples as measured by NTA, expressed as equivalent particles x 10^8/ml

Dilution factor	Equivalent particles x 10^8/ml
Undiluted	22.49 x 10^8/ml
1:10 dilution	15.48 x 10^8/ml
1:100 dilution	3.35 x 10^8/ml
1:1000 dilution	1.4 x 10^8/ml

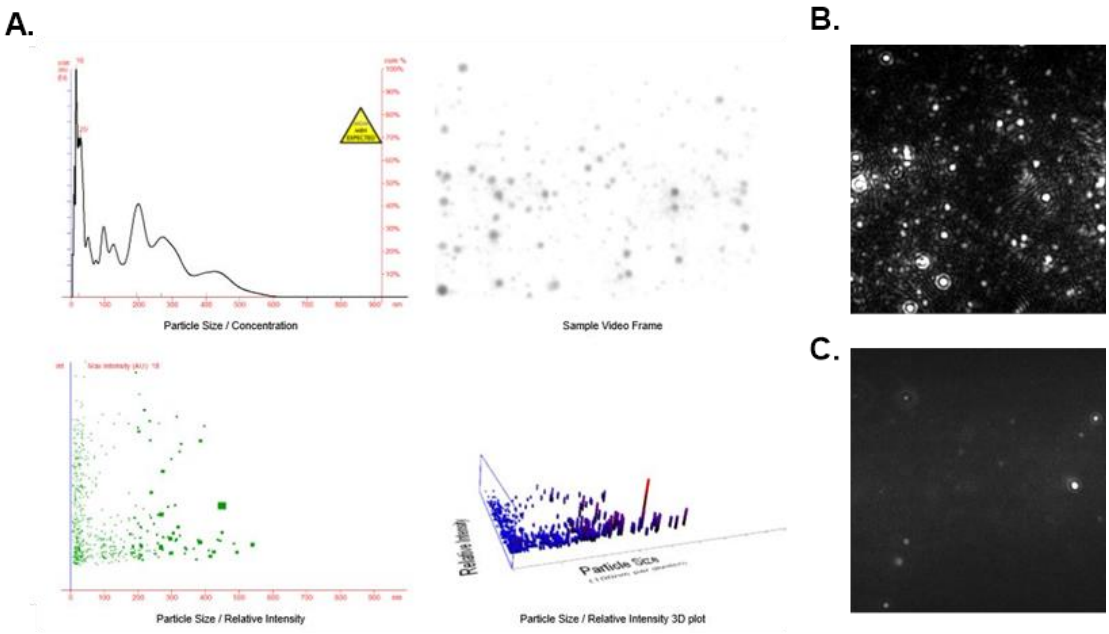

Figure 3.1: Representative NTA measurements of different urine sample dilutions

A.) NTA report for an undiluted urine sample showing the equivalent particle concentration and distribution. B.) Screenshot of NTA measurement video of an undiluted urine sample. C.) Screenshot of NTA measurement video of a 1:1000 dilution of a urine sample.

3.3.2 NTA identified nanoparticles in whole urine

Whole urine was analysed by NTA and a variable size distribution of particles was present (Figure 3.2). The NTA software was able to identify and measure particles in the expected exosome size range (20-100nm). Due to the light intensity of the larger particles causing possible over-estimation of the smaller particle size, following published recommendations[34,4] the focus was set on particles sized up to 300nm.

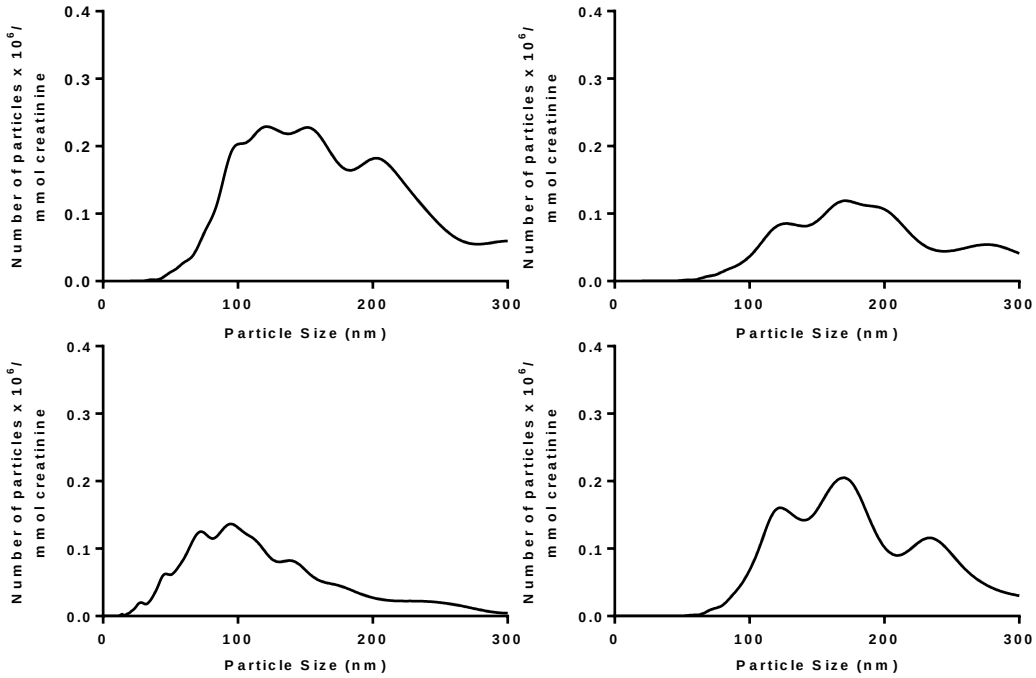

Figure 3.2: Whole urine analyses by NTA

Example NTA traces depicting the heterogeneous particle distribution profile for 4 representative volunteer urine samples. (0-300nm diameter). The number of particles is expressed per mmol urinary creatinine.

NTA software provides the number of particles of each size between 10-1000nm. As the number of particles over the size range 20-100nm was the focus, the area under the curve (AUC) was calculated using the trapezoidal rule with values increasing incrementally on the x-axis, expressed as the sum of the individual trapezoids (Figure 3.3). All values for the number of particles per ml calculated by NTA for *in vivo* urine samples were normalised with urinary creatinine values (mmol/l).

Across the five participants the median $AUC_{20–100}$ (interquartile range; IQR) was 0.02×10^6 particles/mmol creatinine ($0.01−0.05 \times 10^6$ particles/mmol creatinine). The median (IQR) particle size was 69 nm (47−92 nm) (Table 3.2).

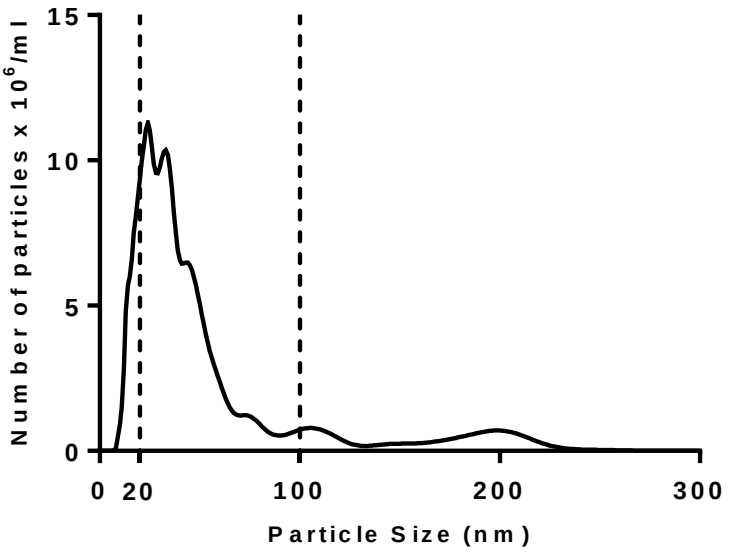

Figure 3.3: AUC area of interest

Example NTA trace showing the area of interest (particle size 20-100nm) from which the AUC is calculated.

Table 3.2: Descriptive statistics of the median particle size and the inter-quartile range across 5 volunteers following NTA measurements of whole urine samples and anti-CD24 conjugated urine samples and exosome pellets following different isolation steps

	Whole urine		**Anti-CD24 Qdot Whole urine**		**Anti-CD24 UC exosome pellet**		**Anti-CD24 Exoquick™ pellet**	
Volunteer	Median particle size (nm)	IQR (10^6part/ mmol creatinine	Median particle size (nm)	IQR (10^6part/ mmol creatinine	Median particle size (nm)	IQR (10^6part/ mmol creatinine	Median particle size (nm)	IQR (10^6part/ mmol creatinine
1	81	0.051	89	0.12	60	0.21	32	0.01
2	92	0.005	59	0.01	60	0.18	62	0.01
3	64	0.021	54	0.28	60	0.66	60	0.24
4	47	0.023	81	0.43	82	0.14	39	0.02
5	62	0.009	40	0.01	78	0.32	40	0.09
Average	**69 ± 15.7**	**0.02 ±0.02**	**64 ± 20.08**	**0.17 ± 0.18**	**68 ± 11.05**	**0.30 ± 0.21**	**46 ± 13.52**	**0.01 ± 0.01**

Data are expressed as mean ± SD. IQR, interquartile range of particles x 10^6 per urinary creatinine (mmol).

3.3.3 Fluorescent NTA identified antibody-labelled exosomes in human urine

To determine whether it is possible to track exosome particles from kidney tubular cells specifically, an antibody-specific labelling system with antibodies specifically related to urinary exosomes was developed. In the first instance, conjugating anti-CD24 to Qdots and incubating this with the urine samples, revealed differential populations by NTA measurements. The fluorescence capability of the NTA system with a long-pass filter allows tracking of fluorescently labelled particles compared to all particles in light scatter (Figure 3.4a and b). Figure 3.4c shows the representative NTA traces of 4 urine samples of all the particles in the sample, as measured by light scatter (dashed line) revealing a particle size range between 20-300nm. However, with the fluorescent long pass filter in place, the anti-CD24 positive particles were consistent with anti-CD24 binding to the urinary exosome surface marker (median size (IQR) 64nm, 89-40nm) (Table 3.2). Across the five volunteers included, the median anti-CD24 Qdot labelled AUC_{20-100} (IQR) was 0.17×10^6 particles/mmol creatinine ($0.01-0.43 \times 10^6$ particles/mmol creatinine).

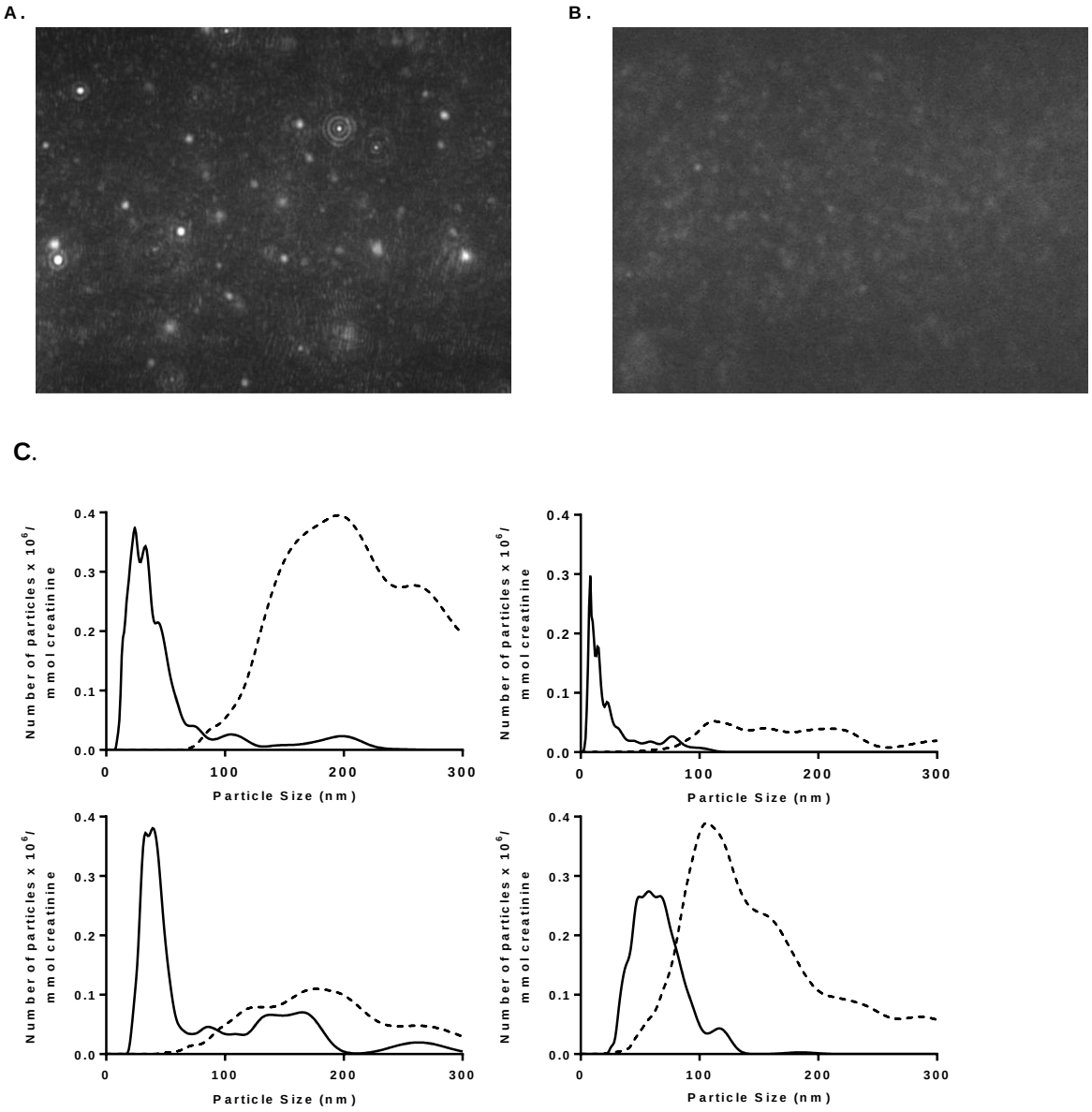

Figure 3.4: Anti-CD24 analyses by NTA

Representative screenshots from NTA measurement videos for urine samples conjugated to anti-CD24 Qdots in A.) light scatter mode and B.) with the fluorescent long-pass filter in place C.) Representative NTA traces of whole urine samples labelled with anti-CD24 Qdots indicating differential populations measured by light scatter (dashed line) and with the fluorescent filter in place (solid line). Results from 4 study participants are presented. Number of particles is expressed per mmol urinary creatinine

3.3.4 Comparison of standard exosome isolation protocols by NTA

To determine whether isolating exosomes by standardised methods from human urine would improve the purity (fewer non-CD24-positive particles of size >100 nm), two established methods were used: ultra-centrifugation (UC) and Exoquick™ reagent. Figure 3.5 demonstrates particle size vs. number of particles curves for the anti-CD24–Qdot-conjugated UC-concentrated exosomes. In light scatter mode, UC-concentrated samples still contained non-exosomal sized particles. However, with the fluorescent filter in place, the anti-CD24–Qdot-labelled particles were smaller [median size (IQR) 68 nm (60−82 nm)], consistent with anti-CD24 binding to surface markers on the urinary exosomes Across the five participants included, the median anti-CD24 labelled AUC_{20-100} (IQR) was 0.30×10^6 particles/mmol creatinine ($0.14-0.66 \times 10^6$ particles/mmol creatinine) (Table 3.2).

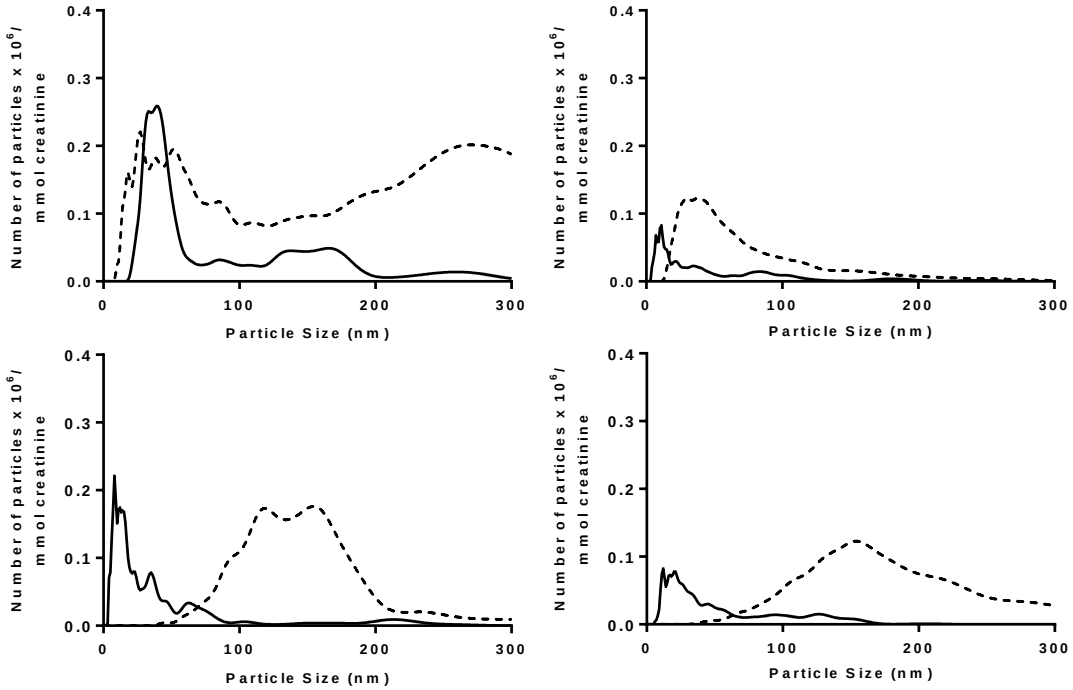

Figure 3.5: NTA analyses of exosome pellet isolated by ultra-centrifugation

Representative NTA traces of exosome pellets isolated by ultracentrifugation labelled with anti-CD24 Qdots. Differential populations as measured by light scatter mode (dashed line – all particles) and with the fluorescent filter in place (solid line – anti-CD24 Qdot labelled particles) are presented. Results from 4 study participants are presented. Number of particles is expressed per mmol urinary creatinine.

Figure 3.6 shows particle size vs. number of particles curves for the anti-CD24–Qdot-conjugated Exoquick™-isolated exosomes. Similar to the data from the UC-isolated exosomes, the light scatter trace for Exoquick™ treated samples revealed a range of particle sizes of 20−300 nm, consistent with the presence of non-exosomal particles. However, with the fluorescent filter in place, the anti-CD24–Qdot-labelled particles were smaller [median size (IQR) 46nm (32−62 nm)], again consistent with anti-CD24 selectively binding to exosomes. Across the five participants included, the median anti-CD24-labelled AUC_{20-100} (IQR) was 0.01×10^6 particles/mmol creatinine ($0.01-0.24 \times 10^6$ particles/mmol creatinine) for Exoquick™-isolated exosomes (Table 3.2).

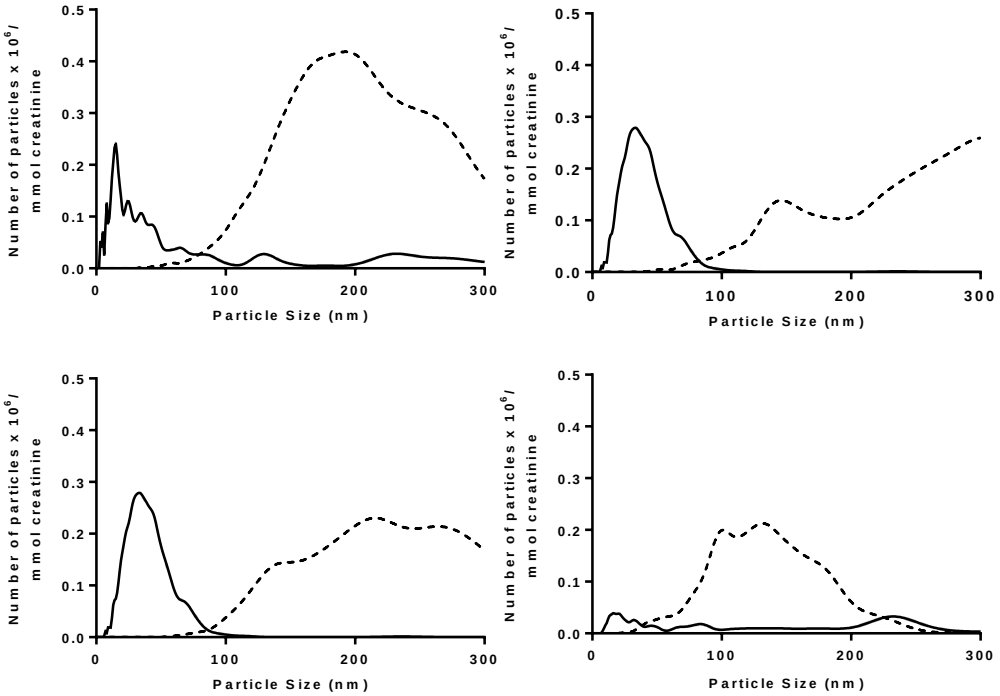

Figure 3.6: NTA analyses of exosome pellet isolated by Exoquick™ reagent

Representative NTA traces of exosome pellets isolated by Exoquick™ reagent kit labelled with anti-CD24 Qdots. Differential populations as measured by light scatter mode (dashed line – all particles) and with the fluorescent filter in place (solid line – anti-CD24 Qdot labelled particles) are presented. Results from 4 study participants are presented. Number of particles is expressed per mmol urinary creatinine.

3.3.5 Intra-assay variability of NTA measurements of different isolation methods compared to whole urine

To quantify the intra-assay variability for NTA measurements of whole urine samples, the $AUC_{20\text{-}100}$ were compared across 3 replicate measurements on the same sample (Table 3.3). The intra-assay variability expressed as the coefficient of variation (CVi) was 55.8% for $AUC_{20–100}$ for whole, unprocessed urine samples. By using the anti-CD24 Qdots coupled with the fluorescent capabilities of the NTA, the within-sample variability in $AUC_{20–100}$ was significantly less than unlabelled samples presented in (CVi = 35%, $P < 0.05$). Anti-CD24–Qdot-conjugated UC-isolated exosomes had a smaller coefficient of variation within sample (CVi = 15.6%) compared with whole urine samples ($P < 0.05$). Compared with the UC isolation method, anti-CD24–Qdot-conjugated Exoquick™-isolated exosomes had a high within-sample coefficient of variation (CVi = 55.9%, $P < 0.05$ compared to UC CVi).

Table 3.3: Comparison of the number of particles and the intra-assay variability of NTA measurements between different exosome isolation methods and whole urine samples

	Whole urine		**Anti-CD24 Qdot Whole urine**		**Anti-CD24 UC exosome pellet**		**Anti-CD24 Exoquick™ pellet**	
Volunteer	AUC_{20-100} (creatinine corrected)	CVi (%)	AUC_{20-100} (creatinine corrected)	CVi (%)	AUC_{20-100} (creatinine corrected)	CVi (%)	AUC_{20-100} (creatinine corrected)	CVi (%)
1	0.04	54.3	1.41	34.8	0.35	2.5	0.07	64.8
2	0.05	45.7	0.16	25.4	0.05	34.9	0.17	67.4
3	0.27	67.9	0.10	32.1	0.51	3.6	2.53	43.7
4	0.29	64.9	3.39	47.6	0.12	2.3	0.15	53.1
5	0.19	46.1	3.35	39.2	2.92	34.7	1.11	50.4
Average	**0.17 ± 0.12**	**55.8% ± 10.4**	**1.68 ± 1.63**	**35.2% ± 8.25 * P < 0.05**	**0.79 ± 1.22**	**15.6% ± 17.5 *¥ P < 0.05**	**0.81 ± 1.06**	**55.9% ± 9.9 ¥ P < 0.05**

Data are expressed as mean ± SD. AUC_{20-100}, Area under the curve for the number of particles sized between 20-100nm; CVi, within-sample coefficient of variation (%). * $P < 0.05$ seen as statistically significant compared to whole urine CVi; ¥ $P < 0.05$ seen as statistically significant compared to UC isolated exosome pellets.

3.3.6 Validation of antibody-specific labelling system by NTA

3.3.6.1 Validation by isotope control

As a control for the specificity of the antibody-Qdot conjugation, whole urine was labelled with mouse IgG–Qdot (Figure 3.7). The $AUC_{20\text{-}100}$ with the fluorescent filter was ~8-fold less than with anti-CD24 Qdots.

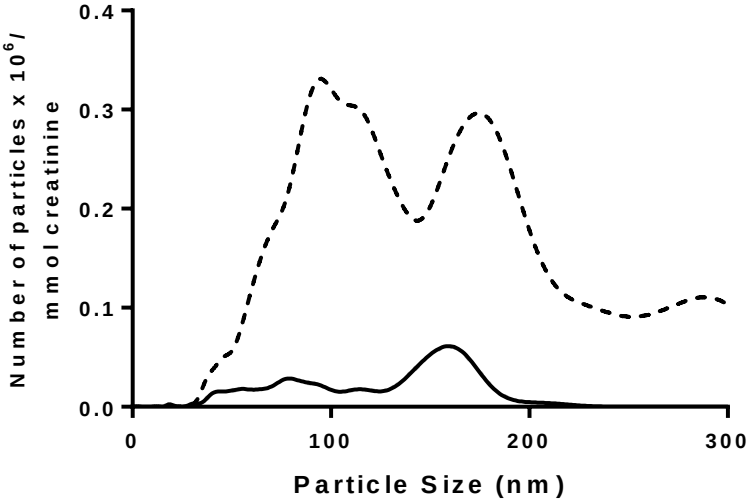

Figure 3.7: NTA analyses of mouse anti-IgG in human urine

Representative NTA trace of whole human urine labelled with mouse IgG conjugated to Qdot as isotope control, measuring differential populations in light scatter mode (dashed line) and with the fluorescent filter in place (solid line). Note the absence of a 'peak' in the particle size range 0-100nm with the fluorescent filter in place.

3.3.6.2 Validation by lysis of exosome cell membrane

As a second validation experiment, it was important to confirm whether the observed NTA signal was the result from antibody conjugation to specific surface markers on exosome membranes. UC exosome pellets were either left untreated or lysed by treatment with a lysis reagent, Qiazol™. The representative NTA trace comparing the anti-CD24 conjugated isolated exosome pellet with and without treatment with Qiazol (Figure 3.8a) demonstrated the abolition of the peak in the 20-100nm size range. For quantification, there was a 3 fold decrease in $AUC_{20\text{-}100}$ in the Qiazol treated sample compared to the isolated exosome sample (Figure 3.8b), consistent with the binding of the antibody conjugate to surface markers on the intact cellular membrane of vesicles in the expected exosome size range (20-100nm).

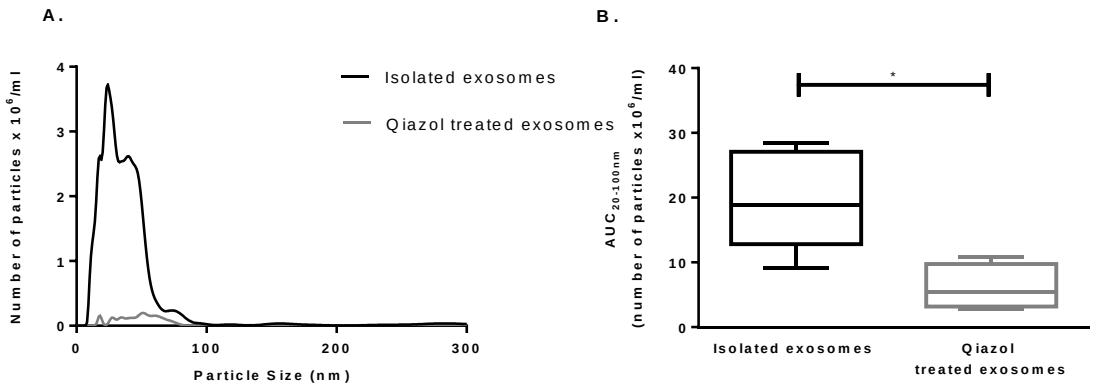

Figure 3.8: NTA analyses of membrane disrupted exosomes

A.) Representative NTA trace showing number of particles of UC-isolated exosome pellet (black line) compared to Qiazol treated exosome pellet (grey line). Figure B. $AUC_{20\text{-}100}$ of UC-isolated exosomes compared to isolated exosomes treated with Qiazol. (Values expressed as mean ± SD; n=6, *, $P < 0.05$, paired t-test.)

3.3.6.3 Validation of clinical utility of antibody-specific labelled NTA

To further develop the antibody-specific NTA method of urinary exosome quantification, the clinical relevance utility of the antibody Qdot conjugate specificity needed to be established and confirmed. Carbonic Anhydrase 9 (CA9) is a tumor-associated carbonic anhydrase isoenzyme which is highly expressed in metastatic renal clear cell carcinoma (RCC) with low expression in healthy, control kidneys. Serum or urine CA9 levels predict disease progression and is a potential RCC disease biomarker [198], with detectable levels in urine and sera of RCC patients, compared to low levels in healthy individuals[199]. Urine samples from metastatic RCC patients undergoing nephrectomy (before and after surgery) were conjugated with anti-CA9 Qdots before performing NTA measurements. Figure 3.9 shows a significant decrease in the total number of particles expressed as $AUC_{20\text{-}100}$ after nephrectomy compared to before surgery.

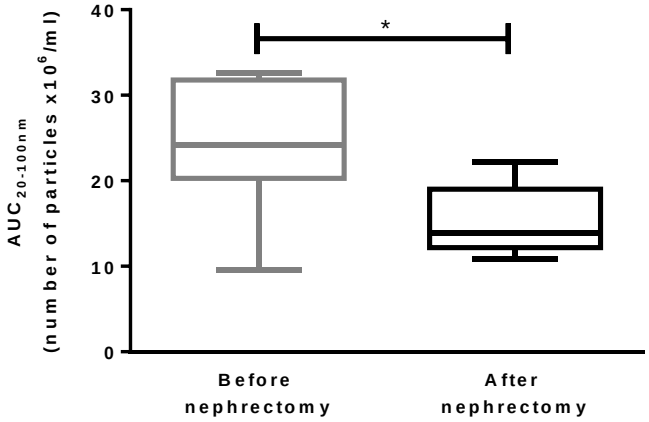

Figure 3.9: NTA analyses of patient cohort urine samples undergoing nephrectomy

$AUC_{20\text{-}100}$ values for patients before and after nephrectomy (Values expressed as mean ± SD; n=10, *, $P < 0.05$; paired t-test).

3.3.7 NTA can detect physiological changes in AQP2 expression

Previous work has demonstrated that murine kidney collecting duct (CCD) cells release AQP2-containing exosomes following stimulation with the vasopressin analogue desmopressin[45]. However, this previous study used UC processing of large volumes of cell culture medium and Western blotting to demonstrate AQP2 upregulation, which is a time-consuming, labour-intensive approach. It was now of interest to test whether NTA could detect AQP2 upregulation in exosomes *in vitro* and *in vivo*, without any pre-processing of the applied samples. NTA was indeed able to detect significant differences in AQP2-expressing exosomal concentrations following desmopressin stimulation for 96 h in the CCD cell line (Figure 3.10a). Following this, NTA was applied to urine samples collected from mice injected over consecutive days first with saline and then with desmopressin. NTA detected a significant increase in urinary AQP2-expressing exosomes following desmopressin treatment (Figure 3.10b).

To investigate the antibody-specific NTA method could be further developed to quantify changes in AQP2 expression in a clinical setting, urine samples from a central diabetes insipidus (CDI) CDI secondary to a craniopharyngioma treated with desmopressin were analysed. There was a clear increase in AQP2-expressing exosomes immediately following administration of desmopressin (Figure 3.11).

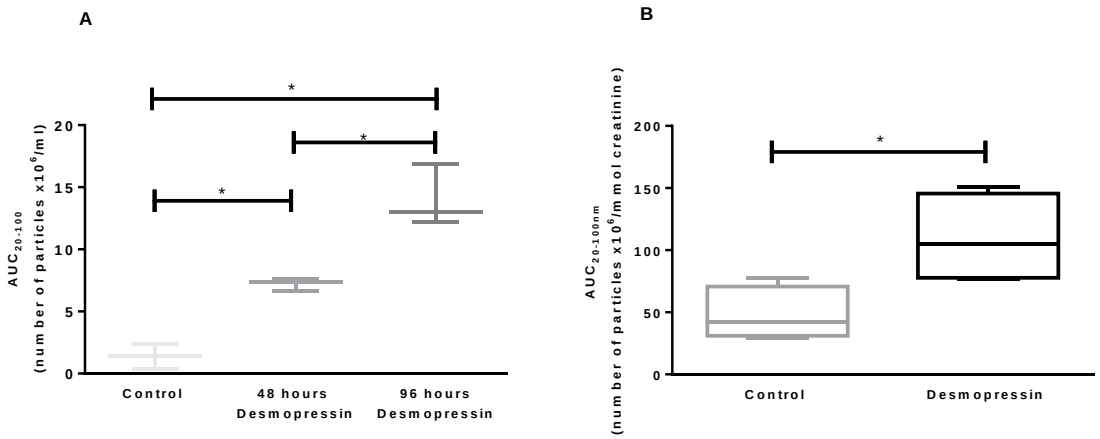

Figure 3.10: Changes in AQP2-positive exosomes following desmopressin stimulation

A.) The difference in exosome concentration in the cell culture media expressed as the area under the curve (AUC) for particles sized 20–100 nm labelled with anti-AQP2 Qdots. The cells were stimulated with desmopressin (3.16 ng/ml) for 48 or 96 h. (Values expressed as mean ± SD, n=3, *, $P < 0.05$, paired t-test). B.) The difference in exosome concentration in the urine samples from desmopressin-treated (n = 6) or control mice (n = 5), expressed as the AUC for particles sized 20–100 nm labelled with anti-AQP2 Qdots. Particle concentration is expressed per mmol urinary creatinine. (Values expressed as mean ± SD, ∗$P < 0.05$, paired t-test)

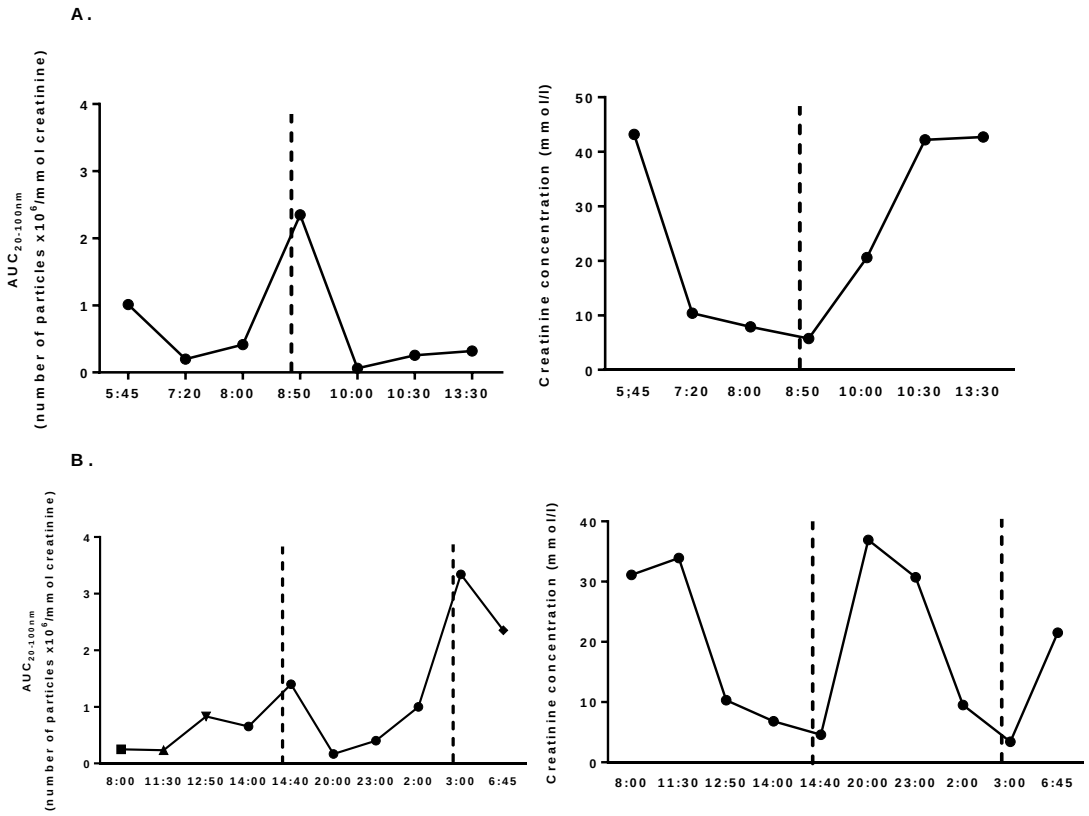

Figure 3.11: Nanoparticle tracking analysis tracked changes in AQP2-positive exosome concentration following desmopressin treatment of a patient with central diabetes insipidus

For A and B, urine aliquots were collected over 2 separate days showing paired changes in urinary creatinine. The AQP2-exosome concentration in the urine samples is expressed as the AUC for particles sized 20–100 nm that labelled with anti-AQP2 Qdots. Particle concentration is expressed per mmol urinary creatinine. The time of administration of desmopressin treatment is indicated by the dashed line.

3.3.8 Evaluation of optimal storage methods for urinary exosomes in urine

NTA was used to assess the effect of different urine storage protocols on urinary exosome number of particles. Whole urine was analysed immediately after collection, which acted as the baseline for comparison of the different storage conditions with and without addition of protease inhibitors (RT, 4, −20 and −80◦C). For each condition, the number of particles in the exosome size range ($AUC_{20\text{-}100}$) was assessed again after 2h, 1 day and 1 week. A significant decrease in the exosome yield in the $AUC_{20–100}$ range was observed with time, regardless of storage condition ($p < 0.05$ for all protocols). Indeed, the data suggests exosome degradation within 2h of urine collection. In this context, storage at −80◦C with addition of protease inhibitors resulted in substantially less reduction in $AUC_{20–100}$ compared with other storage conditions (Figure 3.12).

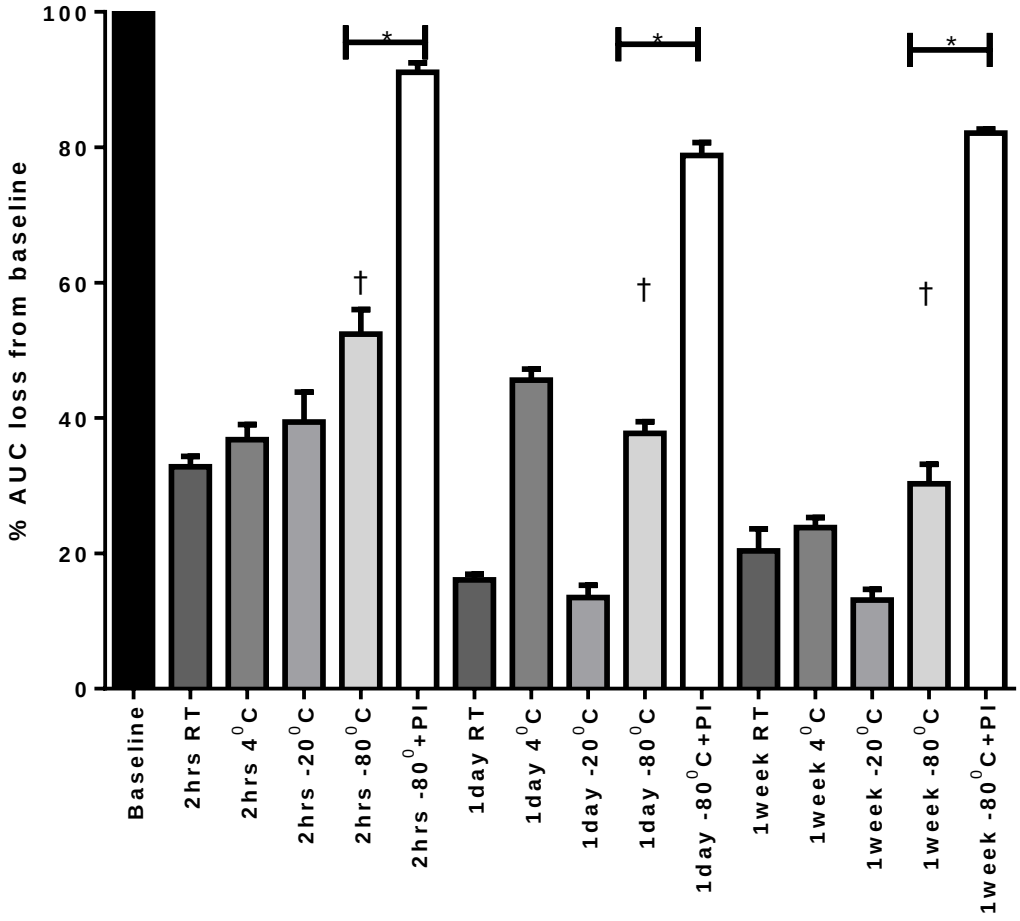

Figure 3.12: Different storage protocols and urine particle concentration

NTA was used to measure the particle concentration between 20 – 100 nm in diameter (AUC_{20-100}). The baseline was immediate measurement after sample collection. The percentage change represents decrease following storage. RT = room temperature. n=5 per group. P <0.05 for all storage conditions vs baseline values. * P <0.05 for storage at -80°C with protease inhibitors compared to other -80°C without protease inhibitor added.

3.4 Discussion

The potential of urinary exosomes as biomarkers and therapeutic agents in kidney disease has been extensively reviewed[196]. However, the inability to identify and quantify exosome populations in clinical specimens rapidly and accurately remains a translational roadblock[200]. Current, standardized methods for investigating the distributions of exosome particle size and concentration are time consuming and only semi-quantitative.

The first aim of this chapter was to determine whether a technological advancement, NTA, holds potential for the identification of exosomes in human urine samples. NTA can detect and quantify the size and concentration distribution of particles sized between 20-700nm in whole urine samples, with a significant percentage of the overall particle distribution within the expected exosome size range (20-100nm). However, unprocessed urine had a significantly higher CVi than is acceptable when measured by NTA (a CVi < 20% is deemed within the acceptable limits[201]).

To refine and further develop NTA quantification of urinary exosomes, it was of interest to see whether using the fluorescent capabilities of the NTA system, coupled with urinary exosome antibody-specific labelling, could decrease the intra-assay variability compared to unprocessed urine samples. The intra-assay variability was substantially reduced by using an anti-CD24 fluorescent label compared to unprocessed urine. CD24 has previously been described as a pan-tubule marker for the origin of urinary exosomes[31]. Antibody-specific labelling coupled with the fluorescent capabilities of NTA not only reduced variability, but also provided proof-of-concept that NTA can be used to discriminately track exosomes positive for specific, chosen antibodies. With the fluorescent filter in place, it was also possible to visualize a larger concentration of particles sized between 20 and 100 nm compared with the light scatter mode. This may be due to the intense light scatter from larger particles interfering with the accurate and reproducible measurement of smaller particles[34] whilst the use of the fluorescent filter avoided this interference in signal.

Using two standard methods of isolating urinary exosomes, i.e. UC and Exoquick™, only UC resulted in a further reduction in intra-assay variability, but it is also a labour-intensive method. Interestingly, comparing the particle size distribution of both UC and Exoquick™, light scatter mode revealed a greater than expected size distribution indicating that both UC and Exoquick™ isolated non-exosomal particles from human urine, and caution must be exercised not to assume incorrectly that these techniques result in a pure or more pure exosome preparation. This may lead to incorrect conclusions regarding the protein or RNA content of exosomes or their biological activity. The reasons for intra-assay variability include user dependent errors or inexperience, technical refinements to the NTA optics and software, and also the nanoparticle size and light refractive properties of vesicles of biological origin, such as exosomes and the associated limitations of detection NTA is aiming to overcome.

To further develop this method of quantifying urinary exosomes, a variety of approaches and controls were used. Using mouse anti-IgG conjugated to the Qdots similar to the anti-CD24 Qdot conjugation, auto fluorescence and unspecific binding of the Qdots were investigated. The decrease in the peak in anti-IgG Qdots compared to the peak seen within the 20-100nm size range when using anti-CD24 Qdots confirm that the perceived signal in the expected exosome size range in whole urine, is not emitted from unbound Qdots, thereby confirming specific binding of the antibody to the surface marker. Secondly, to investigate the specific binding of antibody-conjugated Qdots to surface markers on the cellular membranes, isolated exosome pellets were treated with a lysis reagent causing disruption of the membrane. Indeed, treatment with this reagent, led to a significant decrease in the number of particles seen within the expected exosome size range, thereby confirming that the antibody Qdot conjugate binds to specific surface markers on the intact exosome membrane. Thirdly, to validate the clinical relevance of this developed method, urine samples from metastatic renal cell carcinoma patients undergoing nephrectomy was analysed by NTA before and after the surgery. CA9 has been described as a good marker for tumour formation in renal cancer and therefore anti-CA9 was chosen as the antibody to investigate CA9 positive exosome quantities in this patient cohort. The number of CA9 positive particles before the surgery was

significantly higher than the number of particles after surgery. Taken together, this confirmed the ability of NTA to track differences the number of exosome particles in a clinically relevant and specific setting.

The protein composition of exosomes can track changes in the proteome of the cell, previously demonstrated in the laboratory by using a CCD cell line [45]. However, the measurement of exosomal AQP2 upregulation relied on Western blotting, preceded by UC to concentrate exosomes from approximately 20 ml of culture medium. In this chapter, it was shown that NTA can clearly identify AQP2 upregulation in exosomes with no sample processing, using only 2ml of culture media. Following on from the *in vitr*o results, NTA was applied to urine samples collected from mice before and after desmopressin treatment. NTA was able to report differences in urine AQP2-positive exosomal concentrations between treated and non-treated conditions. The average urine flow rate in the mouse is ∼1 ml/24 h, and this small urine volume results in low exosome yields following current protocols, such as ultracentrifugation. NTA can rapidly detect exosome protein changes in small volumes of mouse urine without extensive sample processing, which represents a significant advance for non-invasive, longitudinal physiological studies in the mouse. Applied to urine samples from a CDI patient treated with desmopressin, NTA was able to track changes in AQP2-positive exosome concentrations over time. Desmopressin resulted in a rapid increase in AQP2-expressing exosomes, which is consistent with studies that have reported rapid increases in total urinary AQP2 following subcutaneous administration of desmopressin[202]. This increase is too rapid to represent new protein synthesis and is likely to reflect cytoplasmic AQP2 transfer to the cell membrane.

Finally, by using NTA to evaluate storage methods for urinary exosomes, −80◦C with protease inhibition was shown to be the optimal approach for storage of whole urine samples, resulting in the maximal preservation of urinary exosomes compared with the other temperatures (RT, 4 and −20◦C) with or without protease inhibition. This is consistent with previous published work that used Western blotting for exosomal marker proteins as a read-out for exosome concentration[203]. Importantly, however, a significant loss of urinary exosomes for all storage conditions was seen,

even within 2h of obtaining the sample. This highlights the need for developing more rapid approaches in analysing exosome quantities in the clinical setting such as which is afforded by the developed NTA method.

In this chapter, it was demonstrated that NTA can allow rapid quantification of exosomes in urine. By combining NTA with an antibody-specific labelling system, changes in the number of relevant exosomes could be tracked, both *in vitro* and *in vivo*. This method will now be further developed and refined in the next chapters to investigate exosome excretion and uptake in health and disease.

CHAPTER 4

Vasopressin regulates exosome uptake *in vitro*

4.1 Introduction

Research has identified a potential role of exosomes in inter-cellular signalling - exosomes can deliver functional protein and RNA from one cell to another *in vitro*[50]. The mechanisms by which target cells internalise exosomes are yet to be fully elucidated and whether exosome transfer between cells occurs *in vivo* is still to be unequivocally confirmed. In cell culture studies, exosome uptake by cells has been reported via a number of mechanisms including clathrin-dependent endocytosis, caveolae-dependent endocytosis, phagocytosis and macropinocytosis[204]. However, it is not established whether exosome uptake by recipient cells is a physiologically regulated process and, if it is, which pathways or hormones are involved.

Urine contains exosome originating from the circulation and from cells that line the urinary tract[8]. Urinary exosomes contain protein, messenger RNA (mRNA), microRNA and mitochondrial DNA that originates from kidney tubular cells[8,159]. Given the unidirectional flow of urine along the nephron, the kidney is anatomically designed for potential exosome transfer from proximal to distal nephron segments. In the kidney there is evidence of exosome signaling: exosomes from injured tubular cells transfer mRNA into fibroblasts resulting in cell activation and stem cell-derived exosomes protect against acute kidney injury by transfer of RNA[171, 205].

Work in our group have previously demonstrated that vasopressin, a pituitary neuropeptide that regulates water homeostasis, modulates the aquaporin 2 (AQP2) content of these exosomes *in vitro* and this regulation translates into rodent models and humans[45, 206]. The first aim of the present study presented in this chapter was to investigate the role of vasopressin in the regulation of exosome uptake into the kidney collecting duct. The second aim was to elucidate a possible mechanism involved.

4.2 Methods

4.2.1 Cell Culture

The murine cortical collecting duct cell line (CCD) was cultured as per the described method in Chapter 2.

For the different cell type experiments, exosomes were isolated from the supernatant of an immortalised human proximal tubular cell line (HK2) and a primary murine juxtaglomerular cell line (RG1). The HK2 cell line was a kind gift from Dr Kenneth Simpson (University of Edinburgh, United Kingdom). HK2 cells were grown following the same described method as for CCD cells. The RG1 cell line was grown by supplementing 1:1 DMEM/F12 (Gibco) with 10 % heat-inactivated FCS, IFN-γ (Peprotech, London, UK) at 100 µg/ml, and 1 % ITS containing 1 mg/ml insulin, 0.55 ml/ml human transferrin and 0.5 µg/ml sodium selenite (Gibco). 1X glutamine, 1X penicillin/streptomycin (pen/strep), (Life Technologies) and 1X antioxidants (Sigma Aldrich) were added to this, as well as 10µM Y-27632 (Tocris, Bristol, UK) and filtered. The cell culture supernatant was removed from either cell type at 70-80% confluency of the cell layer for exosome isolation.

Human umbilical vein endothelial cells (HUVECs) and human microvascular endothelial cells (HMVECs) (both from Lonza) were grown in EGM-2 (EBM-2 medium supplemented with growth factors) and 2% FCS (Lonza). Lipofectamine RNAiMAX (Life Technologies) was used to transfect HUVECs with pre-miR-503 or pre-miR-control (50nM final concentration) according to the manufacturer's instructions.

4.2.2 Isolation and dye loading of exosomes

Exosomes from all cell lines were isolated and dye loaded with Cell Tracker™ as per the described method in Chapter 2.

4.2.3 CCD cell stimulation

Desmopressin (Sigma Aldrich) stimulation concentrations were based on previous work in our group[45]. For short periods of cell stimulation (1-8 hours), desmopressin and dye loaded exosomes were added simultaneously. With longer time periods of cell stimulation (24-96 hours), dye loaded exosomes were added for the final 24 hours of stimulation. At the end of the study the supernatant was collected for NTA analysis and cells removed by trypsinisation (as described in Chapter 2) for flow cytometry. In addition to desmopressin, in specific experiments for the final 24 hours the cells were treated with tolvaptan (10nM) (Sigma Aldrich), endothelin-1 (10pM) (Sigma Aldrich) or H-89 (25µM) (Sigma Aldrich)[207]. Treatment with the Dynamin Inhibitor I (Dynasore (150µM): Sigma Aldrich) was for 45 minutes immediately prior to exosome addition as per published studies[208]. Cells were treated with 10µM forskolin from *Coleus forskohlii* (Sigma Aldrich) and incubated with dye loaded exosomes overnight[209,210]. To polarise the CCD cells they were cultured on the polyester membrane of Transwell inserts (Corning Costar Co, New York, USA) at a high density to allow the cells to be confluent within three days. Desmopressin was added to the top or bottom Transwell chamber for 48 hours then dye loaded exosomes were added for the final 24 hours of the 96 hour period.

4.2.4 Particle size and concentration distribution measurement with NTA

The number of dye loaded exosome particles prior to cell incubation and remaining in the cell culture supernatant were analysed as per the described method of NTA analysis in Chapter 2.

4.2.5 Flow cytometry for total cell fluorescence

Total cell fluorescence was measured by flow cytometry on a 5LSR Fortessa cytometer (BD Biosciences, Oxford, UK). Cells were briefly stained with 1µM DAPI nucleus stain (Sigma Aldrich) and having been exposed to dye loaded exosomes as described, was excited with a violet laser (405 nm) and emission detected using 450/50 and 630/70 band pass filters respectively. Gates were set using unstained cells

and cells stained with DAPI alone. Flow cytometry data were analysed with FloJo LLC software version 8 (FlowJo LLC, Oregon, USA) and the results are presented as the percentage of total fluorescent cells.

4.2.6 Fluorescence microscopy

Using control and desmopressin-stimulated cells grown on a cover slip, internalisation of dye loaded exosomes with DAPI stained CCD cell nuclei and Phalloidin stained cell membranes (Sigma Aldrich) were visualised by an Olympus AX-70 Provis epifluorescence microscope equipped with a Hamamatsu Orca II CCD camera. Images were collected with a 60 x oil immersion objective lens and acquired by using mDaemon software (Zenn, Manchester, UK). Each picture was acquired with laser intensities and amplifier gains adjusted to avoid pixel saturation and analysed using Adobe Photoshop CC 2014 (Adobe Systems, San Jose, California).

4.2.7 RNA extraction and quantitative real time analysis

Total RNA was extracted following the manufacturer's protocol using the miReasy kit (Qiagen, Venlo, Netherlands). Real-time quantification to measure microRNAs was performed with the TaqMan microRNA reverse transcription kit and microRNA assay (hsa-miR-503: 4373228) (Applied Biosystems, Paisley, UK) with a Lightcycler 480 (Roche Diagnostics, Burgess Hill, UK). For gene expression analysis, single-strand complementary DNA (cDNA) was synthesised from 1 μg of total RNA using the High Capacity cDNA kit (Thermo Fisher Scientific, Waltham Massachusetts, USA). Quantitative PCR to measure gene expression using SYBR Green qPCR (Life Technologies) was used to measure vascular endothelial growth-factor A (VEGF-A), fibroblast growth factor-2 (FGF2), cell division cycle 25A (CDC25A), cyclin-1E (CCNE1) and 18S rRNA. The following primers were pre-designed from Sigma (KiCqStartTM Primers)[211]: VEGF-A forward: CGCAGCTACTGCCATCCAAT, reverse: GTGAGGTTTGATCCGCATAATCT; FGF2 forward: AGTGTGTGCTAACCGTTACCT, reverse ACTGCCCAGTTCGTTTCAGTG; CDC25A forward: 5'-TAAGACCTGTATCTCGTGGCTG-3', reverse: 5'-CCCTGGTTCACTGCTATCTCT-3'; CCNE1 forward: 5'-GAGCCAGCCTTGGGACAATAA-3', reverse: 5'-

GCACGTTGAGTTTGGGTAAACC-3';
18s rRNA forward: 5'- TAGAGGGACAAGTGGCGTTC -3', reverse: 5'-TGTACAAAGGGCAGGGACTT-3.

Data were normalized to 18S ribosomal RNA as an endogenous control.

4.3 Results

4.3.1 Vasopressin regulates exosome uptake in the collecting duct cell

Using fluorescent microscopy, uptake of dye loaded exosomes was shown to be under vasopressin regulation in collecting duct cells. Stimulation with desmopressin resulted in an increase in the number of red-dye loaded exosomes localising adjacent to the DAPI stained cell nuclei (Figure 4.1.B) compared to control cells (Figure 4.1.A).

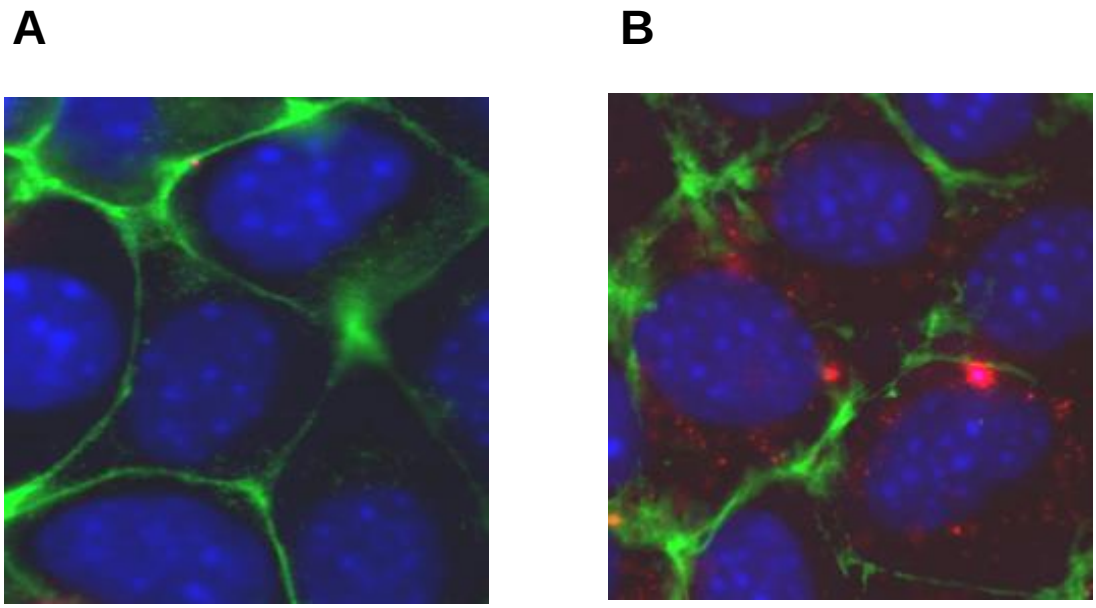

Figure 4.1: Fluorescent microscopy of control (A.) vs desmopressin stimulated cells (B)

(3.16ng/ml for 96 hours) with dye loaded exosome uptake into the cellular cytoplasm. DAPI-stained nucleus (blue), cell membrane stained with phalloidin (green).

Using different desmopressin concentrations for stimulation of CCD cells, 3.16ng/ml was the optimal. At a concentration of 3.16µg/ml there was apoptosis/necrosis of DAPI stained nuclei when viewed under confocal microscopy and 6.32pg/ml produced insignificant exosomal uptake (data not shown).

To determine whether vasopressin regulates exosome uptake in CCD cells with a short-term effect, CCD cells were incubated with desmopressin and dye loaded exosomes for a short time period (1-8 hours), showing no significant differences between control and desmopressin stimulated cells (Figure 4.2.A). However, significant exosome uptake occurred after 96 hours of desmopressin stimulation (Figure 4.2.B.). FACS analysis was able to detect differences in total cell fluorescence between control and desmopressin stimulated cells (Figure 4.2.C). At concentrations similar to the physiological concentration of vasopressin[212], 96 hours of desmopressin incubation approximately doubled the proportion of recipient cells taking up dye loaded exosomes (Figure 4.2.C and D) (desmopressin stimulated 28.01 ± 9.21% vs control 13.74 ± 6.79%; 3896 ± 1785 MFI vs control 1394 ± 254.4 MFI). Reciprocally, NTA was able to quantify the amount of dye loaded exosomes remaining in the cell culture supernatant following incubation with the CCD cells (control or desmopressin stimulated) (Figure 4.2.E). A significant decrease ($p<0.05$) in the number of dye loaded exosomes remaining in the cell culture supernatant of desmopressin cells (Mean $AUC_{20\text{-}100}$ 106.1 ± 53.75 number of particles/ml) compared to control CCD cells (Mean $AUC_{20\text{-}100}$ 376.28 ± 253.5 number of particles/ml) (Figure 4.3.F) was found.

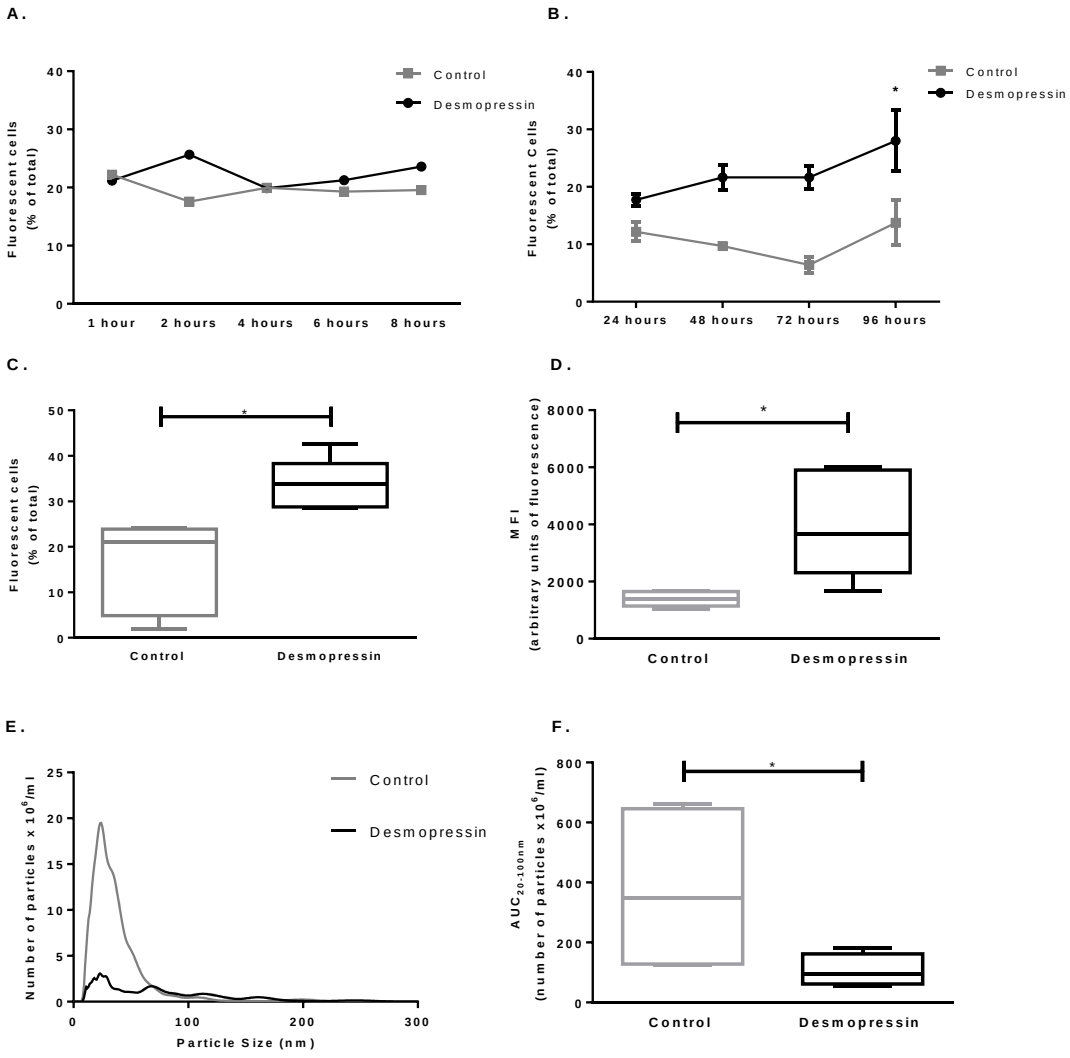

Figure 4.2: Exosome uptake by CCD cells is increased by desmopressin stimulation

A.) Flow cytometry data demonstrating no significant dye loaded exosome uptake following desmopressin stimulation (3.16ng/ml) for up to 8 hours (n=3). B.) Flow cytometry data demonstrating an effect on exosome uptake following longer desmopressin stimulation. (n=3, * $P < 0.05$: 3.16ng/ml desmopressin stimulation vs control). C.) Desmopressin (3.16ng/ml for 96 hours) stimulated CCD cells had significantly increased fluorescence after incubation with dye loaded exosomes. Fluorescent cells expressed as % of total cell number (n=6, * $P < 0.05$, paired t-test) D.) Mean fluorescence intensity of control and desmopressin stimulated cells (3.16ng/ml for 96 hours) (n=6, * $P < 0.05$, paired t-test). E.) Representative NTA trace of dye loaded exosomes in control (grey) vs desmopressin stimulated (black) cell culture supernatant. F.) NTA analyses of cell culture supernatant from control and desmopressin (3.16ng/ml for 96 hours) stimulated cells presented as the area under the concentration curve (AUC20-100) (n=6, * $P < 0.05$, paired t-test).

4.3.2 Vasopressin regulated receptor mediated exosome uptake by the collecting duct

Tolvaptan; a selective V2 receptor antagonist, abolished the increase in exosome uptake induced by desmopressin (Figure 4.3.A and B) (10nM tolvaptan + 3.16ng/ml desmopressin 11.2 ± 6.4% vs desmopressin alone 33.6 ± 5.7% fluorescent cells of total; 1090 ± 133.2 MFI vs desmopressin alone 2239 ± 578.5 MFI), combined with a reciprocal significant decrease in the number of dye loaded exosomes remaining in the cell culture supernatant (10nM tolvaptan + 3.16ng/ml desmopressin ($AUC_{20\text{-}100}$) 429.9 ± 231.3 number of particles/ml vs desmopressin alone ($AUC_{20\text{-}100}$) 106.5 ± 46.56 number of particles/ml) (Figure 4.3.D). To investigate the effect of a physiological control, we used endothelin-1, a peptide which inhibits sodium transport in the collecting duct [213]. Endothelin-1 had no effect on exosome uptake by CCD cells when applied alone, but physiologically antagonised the effect of desmopressin as could be seen in the total number of fluorescent cells (10pM endothelin-1 + 3.16ng/ml desmopressin 22.88 ± 5.19% vs desmopressin 33.6 ± 5.7% fluorescent cells of total; 2357 ± 486.7 MFI vs desmopressin alone 4207 ± 1355 MFI) (Figure 4.3. C and D) and dye loaded exosomes remaining in the cell culture supernatant as measured by NTA (10pM endothelin-1 + 3.16ng/ml desmopressin ($AUC_{20\text{-}100}$) 299.2 ± 158.1 number of particles/ml vs desmopressin alone ($AUC_{20\text{-}100}$) 113.0 ± 60.78 number of particles/ml) (Figure 4.3.F).

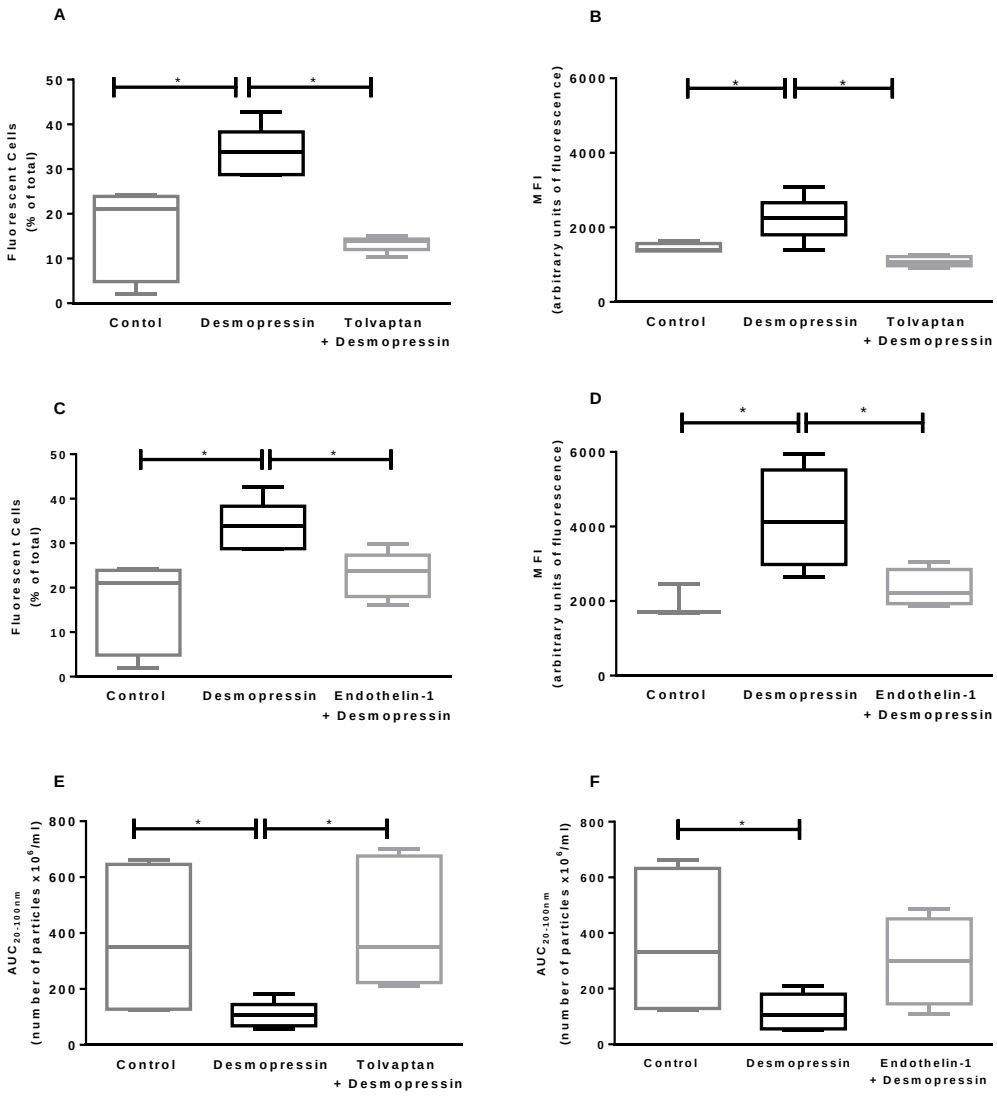

Figure 4.3: V2 receptor mediated mechanism following desmopressin stimulation

A.) Fluorescence of control and desmopressin stimulated cells (3.16ng/ml for 96 hours) in the absence and presence of tolvaptan (10nM). Expressed as % of total number of fluorescent cells. B.) Mean fluorescence intensity of control and desmopressin stimulated cells (3.16ng/ml for 96 hours) in the absence and presence of tolvaptan (10nM). C.) Fluorescence of control and desmopressin stimulated cells (3.16ng/ml for 96 hours) in the absence and presence of endothelin-1 (10pg/mL). Fluorescent cells expressed as % of total cell number. D.) Mean fluorescence intensity of control and desmopressin stimulated cells (3.16ng/ml for 96 hours) in the absence and presence of endothelin-1 (10pg/ml). E.) NTA analysis of cell culture supernatant of control, desmopressin stimulated cells (3.16ng/ml for 96 hours) in the absence and presence of tolvaptan (10nM). (, n=5. * $p < 0.05$ seen as significant between control and desmopressin stimulated cells and desmopressin and 10nM tolvaptan treated cells. Non-parametric ANOVA). E.) NTA analysis of cell culture supernatant of control, desmopressin stimulated cells (3.16ng/ml for 96 hours) in the absence and presence of endothelin-1 (10pM). (, n=5. * $p < 0.05$ seen as significant between control and desmopressin stimulated cells and desmopressin and 10pM endothelin-1 treated cells. Non-parametric ANOVA).

4.3.3 cAMP and clathrin-dependent endocytosis mediates desmopressin-induced exosome uptake

The V2 receptor is coupled with Gs proteins and causes activation of the cAMP pathway[212]. Inhibition of cAMP-dependent protein kinase A (PKA) with H-89 prevented the increase in uptake of dye loaded exosomes following desmopressin stimulation (25μM H-89 + 3.16ng/ml desmopressin 9.60 ± 1.71% vs 3.16ng/ml desmopressin 31.52 ± 10.31% fluorescent cells; 1388 ± 127.8 MFI vs desmopressin alone 2398 ± 523.5 MFI) (Figure 4.4.A and 4.5. A). Stimulation of CCD cells with forskolin increased uptake of dye loaded exosomes independent of desmopressin stimulation (forskolin 19.65 ± 4.58% vs 7.72 ± 8.82% control cells; 1477 ± 27.35 MFI vs control cells 1380 ± 69.34 MFI) (Figure 4.4.B and 4.5. B). Endocytosis can be cAMP dependent[214] and, taken together with previous studies showing that exosomes enter cells through the endocytic pathway[204], the role of clathrin-dependent endocytosis was investigated. Dynasore, a non-competitive inhibitor of GTPase dynamin activity[208,215,] significantly reduced desmopressin-stimulated exosome uptake to a level below that of control cells (150nM dynasore + 3.16ng/ml desmopressin 3.25 ± 1.85% vs control 15.71 ± 10.18% fluorescent cells; 996.0 ± 75.31 vs desmopressin alone 2044 ± 661.6 MFI) (Figure 4.4.C and 4.5. C.). In combination, these data indicate that basal and desmopressin-induced uptake of exosomes requires cAMP activation of clathrin-dependent endocytosis. As a final control to confirm whether increased exosome uptake following desmopressin stimulation is through activation of the V2 receptor and its concomitant cAMP activation, desmopressin stimulated cells (3.16ng/ml) were treated with a V1 receptor anatagonist – OPC-21268 (1μM) and exosome uptake were compared to desmopressin stimulated cells without OPC-21268 treatment. No significant differences were seen (desmopressin stimulated cells 23.2±5.2% vs desmopressin stimulated cells treated with OPC-21268 (1uM) 18.8±1.4% fluorescent cells; 1166 ± 10.54 MFI vs desmopressin alone 1182 ± 30.69 MFI) (Figure 4.4.D and 4.5. D).

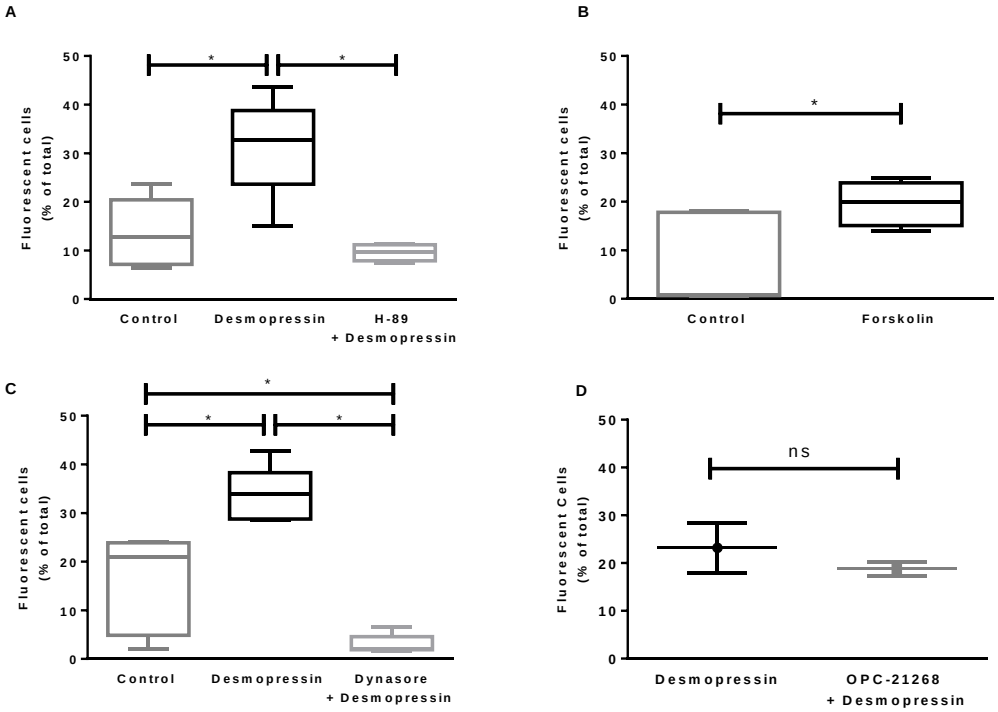

Figure 4.4: Exosome uptake following desmopressin stimulation is mediated by cAMP and clathrin-dependent endocytosis

A.) Desmopressin (3.16ng/ml for 96 hours) stimulated exosome uptake which was decreased by PKA inhibition (H-89 – 25µM) of the cAMP pathway. B.) Exosome uptake was by cAMP stimulation through forskolin (10µM). C.) Dynasore (150nM) inhibiton of dynamin activity decreased exosome uptake by desmopressin stimulated cells below that of the control cells. Fluorescent cells expressed as % of total cell number, n= 6, * P <0.05, non-parametric ANOVA. D.) No significant difference in exosome uptake between desmopressin stimulated cells and desmopressin stimulated cells treated with a V1 receptor antagonist – OPC-21268 (1µM). Fluorescent cells expressed as % of total cell number, n= 3, ns, non-significant, paired t-test.

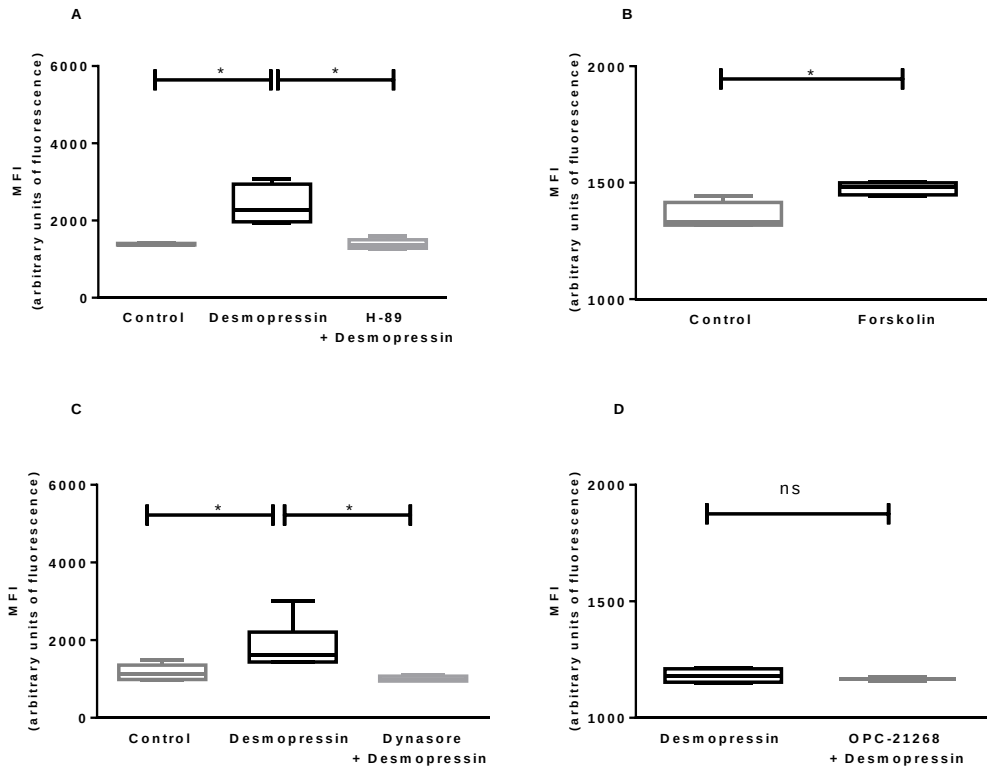

Figure 4.5: Mean fluorescent intensities for exosome uptake following desmopressin stimulation mediated by cAMP and clathrin-dependent endocytosis

A.) Mean fluorescent intensitity of increased exosome uptake of desmopressin (3.16ng/ml for 96 hours) stimulated cells which were decreased by PKA inhibition (H-89 – 25µM) of the cAMP pathway. B.) Exosome uptake was by cAMP stimulation through forskolin (10µM). C.) Dynasore (150nM) inhibiton of dynamin activity decreased exosome uptake by desmopressin stimulated cells below that of the control cells. Data expressed as mean fluorescent intensity, n= 6, * $P < 0.05$, non-parametric ANOVA. D.) No significant difference in exosome uptake between desmopressin stimulated cells and desmopressin stimulated cells treated with a V1 receptor antagonist – OPC-21268 (1µM). n= 3, ns, non-significant, Kruskal-Wallis t-test.

4.3.4 Functional delivery of miRNA by exosomes following desmopressin stimulation

To complement and confirm the data from fluorescence-based exosome tracking, exosomes loaded with a specific microRNA were used with cellular target mRNA suppression as the readout of functional exosome uptake. Exosomes were harvested from a HUVEC line transduced to over-express miR-503 and a control cell HUVEC line. This cell line was chosen as the mRNA targets of miR-503 are well-described[211,216]. The expression of miR-503 in the isolated exosome pellet was confirmed by qPCR (overexpressing Ct value 26.6 vs control Ct value >35, Figure 4.6.A). Using NTA, exosome uptake regulated by vasopressin was confirmed by the number of exosome particles remaining in the cell culture supernatant of desmopressin stimulated and control cells (Figure 4.6.B). Exosomes from both cell lines were added to control or desmopressin-stimulated CCD cells. Target genes influenced by miR-503 identified: mRNA expression of VEGF-A, FGF2, CDC25A and CCNE1 were measured. Data is expressed as the delta delta Ct value or Livak method, which computes the ratio of the target gene in a specific condition (no exosomes, control HUVEC exosomes or miR-503 HUVEC exosomes) in a treated sample (desmopressin stimulation) relative to an untreated sample (control). In the absence of added exosomes, desmopressin stimulation increased target gene expression in CCD cells. However, with the addition of miR-503 overexpressing exosomes, we found a significant down-regulation of these target genes in the presence of desmopressin stimulation compared to cells which were subjected to control HUVEC exosome (i.e. not miR-503 overexpressing) addition. (Figure 4.6C-F)

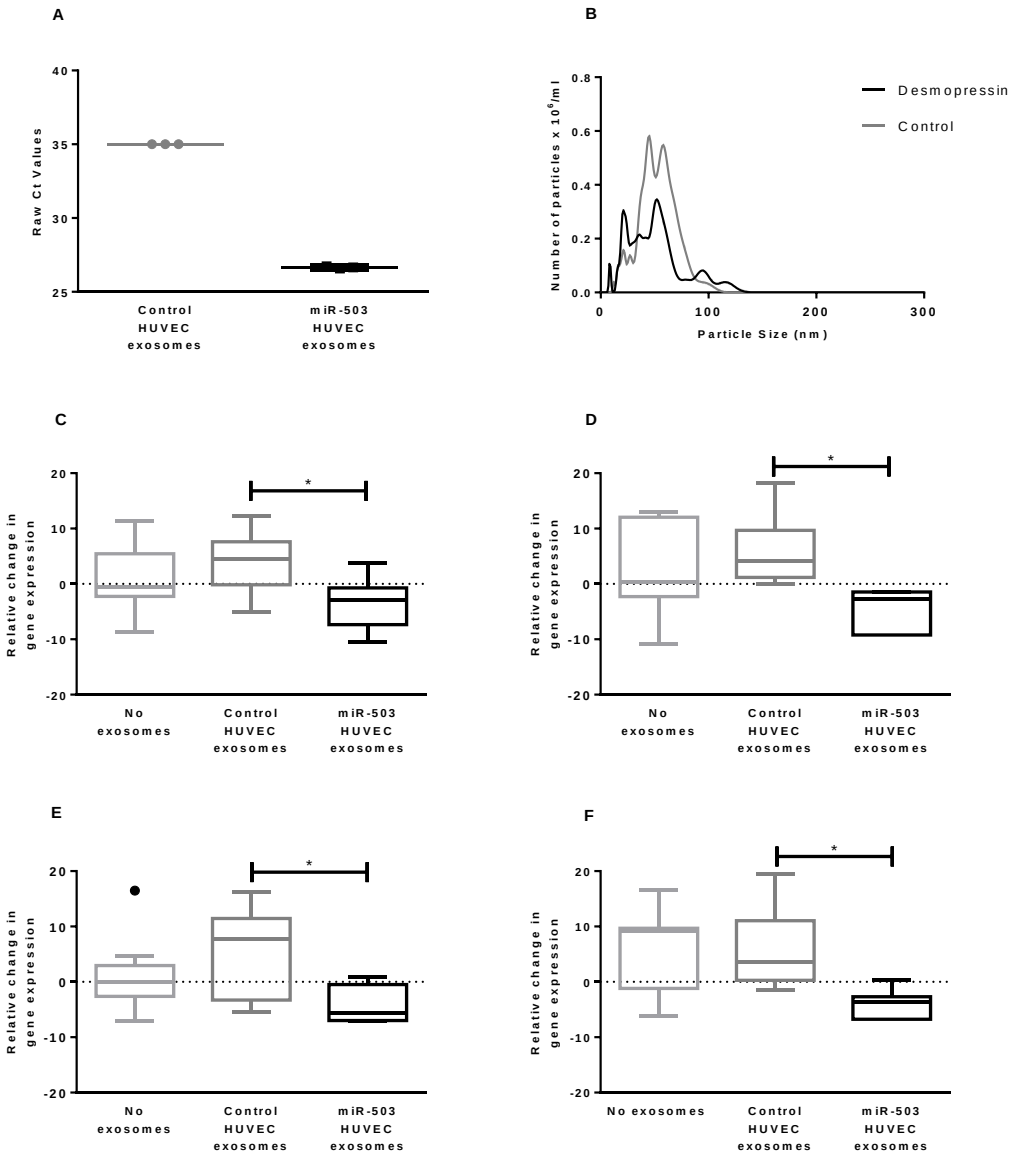

Figure 4.6: Exosomes deliver functional microRNA into desmopressin-stimulated CCD cells

A.) Raw Ct values of miR-503 in control and miR-503 loaded exosomes. B.) Representative NTA trace of differential miR-503 exosome uptake regulated by desmopressin stimulation. Relative change in gene expression following desmopressin treatment in the absence of ECVs, with control HUVEC derived ECVs and miR-503 loaded ECVs. C.) vascular endothelial growth factor-A (VEGF-A), D.) fibroblast growth-factor 2 (FGF2), E.) cyclin E-1 (CCNE1) and F.) cell division cycle 25A (CDC25A) using ΔΔCt method relative to control cells. Values are expressed as the difference between Ct values of control cells – Ct value of desmopressin simulated cells with 18S as endogenous control. Negative values indicate down-regulation and positive values indicate up-regulation of target genes following desmopressin treatment. n=9, * $p < 0.05$, paired t-test.

4.3.5 Cell specific derived exosome uptake in collecting duct cells

Next, we determined whether exosomes derived from different cell types are also internalised by CCD cells under vasopressin regulation. CCD cells (without and with desmopressin stimulation) were incubated with equal numbers of exosomes isolated from the following renal cell types: CCD (mouse); proximal tubule (HK2 - human); and juxtaglomerular (RG1 - mouse). The exosomes from all cell types had similar size distributions, as quantified by NTA (Figure 4.7A). Treating recipient CCD cells with desmopressin increased uptake of the proximal tubule and collecting duct-derived exosomes but not of those from juxtaglomerular cells (Figure 4.7B). This tubular cell selectivity was confirmed by NTA analysis, which demonstrated decreased proximal and collecting duct exosomes in the CCD cell culture supernatant, but no change in exosomes from juxtaglomerular cells (Figure 4.7C).

The V2 receptor is expressed on the basolateral membrane of the renal principal cell. Therefore exosome uptake in CCD cells was investigated by using polarised CCD cells grown on transwell plates and stimulated with desmopressin on either the apical or basolateral side. Basolateral desmopressin stimulated uptake of apically applied exosomes, whereas desmopressin applied to the apical membrane had no effect (Figure 4.7D).

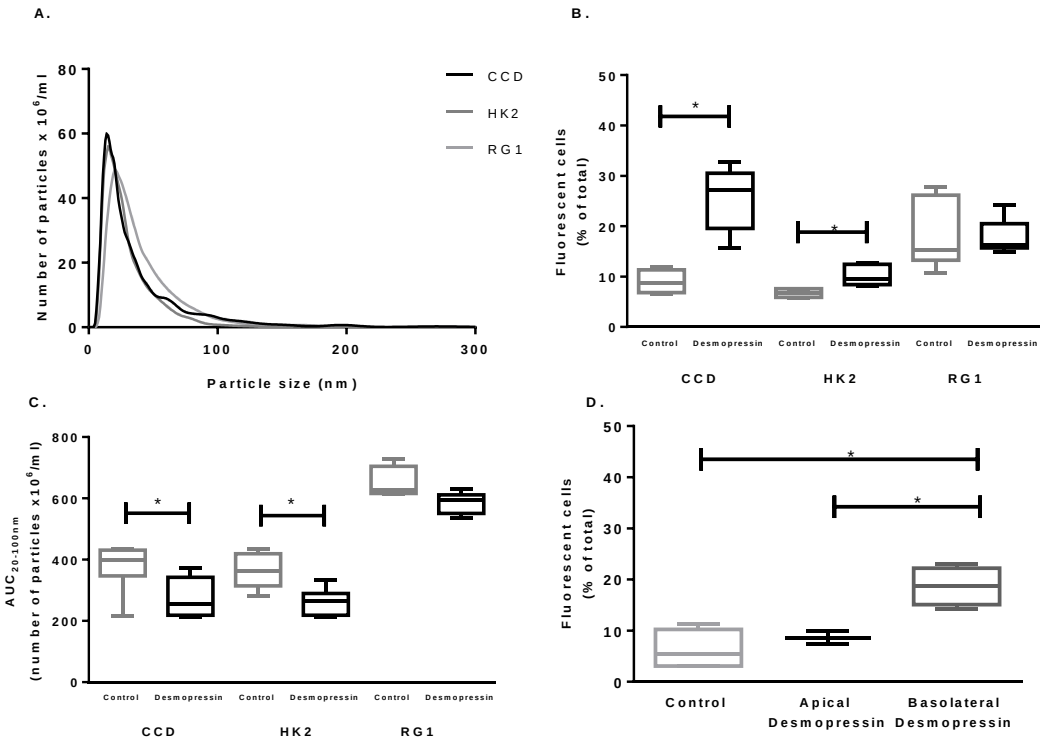

Figure 4.7: Cell type specificity for exosome uptake

A.) NTA measurement of exosomes from different cell types prior to incubation with CCD cells. CCD = collecting duct, HK2 = proximal tubule and RG1 = juxtaglomerular cell derived B.) Comparing total cell fluorescence between control and desmopressin (3.16ng/ml for 96 hours) stimulated CCD cells following labelled exosome incubation from 3 cell types: CCD, HK2 (human proximal tubular cell line) and RG1 (murine juxtaglomerular cell line). Equal numbers of exosomes were added to all experiments (n=6. * $p < 0.05$, non-parametric ANOVA). C.) NTA analyses of cell culture supernatant incubated with different cell type derived exosomes (CCD, HK2 and RG1) from control and desmopressin (3.16ng/ml for 96 hours) stimulated cells presented as the area under the concentration curve (AUC) for particles sized between 20-100nm. Desmopressin stimulation reduced the concentration of CCD and HK2 exosomes in the supernatant but not in cells incubated with RG1 exosomes. D.) Polarised cells take up exosomes under desmopressin regulation. Total cell fluorescence of CCD cells stimulated with desmopressin (3.16ng/ml for 96 hours) either apically or basolaterally compared to unstimulated cells. Labelled exosomes were applied to apical compartment of Transwell (n=6. * $p < 0.05$, non-parametric ANOVA).

4.4 Discussion

Vasopressin is released from the posterior pituitary in response to an elevation in blood osmolality[212]. Its principal role is to stimulate water reabsorption by the renal collecting duct. This is achieved through activation of the V2 receptor on the basolateral membrane of renal principal cells which, via a cAMP/PKA cascade, phosphorylates the water channel AQP2 permitting trafficking to the apical cell membrane from sub-apical recycling endosomes. In parallel, vasopressin stimulates endocytosis of vesicles from the cellular plasma membrane to maintain membrane equilibrium.

In this chapter, vasopressin as a hormonal regulator of exosome uptake in collecting duct cells was demonstrated. 4 complementary read-outs of exosome uptake were used – fluorescent microscopy, flow cytometry and microRNA transfer into cells, combined with NTA of exosomes remaining in the culture medium. The data generated by these different methodologies consistently demonstrated that desmopressin stimulated exosome uptake into CCDs. The mechanism was V2 receptor-mediated and cAMP/PKA dependent, in keeping with the established physiological pathway that increases water uptake. In the cell model, desmopressin-induced exosome uptake was reduced by endothelin-1, suggesting that exosome uptake is under opposing physiological regulation by vasopressin and endothelin-1. Thus, the mechanism of vasopressin-induced exosome uptake into CCDs is consistent with the known physiology of this hormone and is likely to be a consequence of hormone-induced plasma membrane endocytosis. Hormonal regulation of exosome entry into cells has not been demonstrated in any cell line and provides support for exosome inter-cellular signalling being a tightly regulated process.

In conclusion, in this chapter, vasopressin regulation of exosome uptake in kidney collecting duct cells was shown. Vasopressin regulation occurs in collecting duct cells through a regulated process which can result in intra-cellular modulation of target mRNA species. This finding will now be investigated *in vivo* in the studies presented in the following chapter.

CHAPTER 5

Vasopressin regulation of urinary exosome excretion *in vivo*

5.1 Introduction

Exosomes derived from different segments of the nephron have been well characterised in urine. In depth proteomic analysis of the urinary exosomal compartment has demonstrated the presence of proteins specific to each cell along the nephron epithelium: the podocyte/glomerular epithelial cell, proximal tubule, distal tubules and the collecting duct[8].

The development of urinary exosomes as biomarkers has mainly been focussed on renal pathologies such as acute kidney injury[196], diabetic nephropathy[103] and bladder cancer[217]. However, other studies have suggested that the urinary exosome cargo may contain proteins from non-renal cells. Large-scale proteomic analysis of podocyte-specific urinary exosomes revealed 14 new, previously unidentified brain-specific proteins[218]. Similarly, in a mouse model for acute and chronic liver injury, urinary exosomes showed differential expression of specific proteins[219]. Urinary exosomes may therefore provide a reservoir of information about renal and non-renal proteins and RNA species, which presents the opportunity for developing urinary exosomes biomarkers for multiple diseases.

Studies have demonstrated that exosome uptake is mediated through various forms of endocytosis including clathrin-dependent endocytosis and macropinocytosis with resultant delivery of proteins and RNA species[135,220] to the recipient cell. The mechanisms of exosome uptake and exosome mediated intercellular communication remain unclear and need to be elucidated to develop exosomes as possible therapeutic agents.

In Chapter 4, *in vitro* exosome uptake in the kidney collecting duct was demonstrated to be regulated by vasopressin in a cell type specific, receptor mediated, clathrin-dependent process of endocytosis. The aims of this chapter were to build upon this work and examined whether exosome uptake occurs *in vivo*. Two complementary approaches were used: first, the effect of tolvapatan on urinary exosome excretion in the mouse was assessed; second the effect of desmopressin on urinary exosome excretion in a patient with central diabetes insipidus was examined.

5.2 Methods

5.2.1 Cell culture

Cells were grown and cultured as per described method in Chapter 2.

5.2.2 Exosome isolation

Exosomes from CCD cell culture supernatant were isolated as per described ultra-centrifugation method in Chapter 2. The isolated exosome pellet was labelled with Cell Tracker™ (dye-labelled exosomes) followed by quantification of the number of particles in the exosome preparation per the described NTA method in Chapter 2.

5.2.3 Animals

All experiments were conducted in accordance with UK Home Office regulations and the Animals (Scientific Procedures) Act 1986 and complied with the ethical regulations of the institution. The study design was a crossover study which consisted of three experimental groups. The group of animals in each separate experimental group was seen as the experimental unit.

Adult wild type (C57BL6/J and CD1) mice were sex and age matched across experiments. Before experimentation, mice were housed in standard cages with free access to water and standard chow containing 0.25% Na^+, 0.38% Cl^-, and 0.67% K^+. A total number of 15 mice were included with 5 mice in each of the experimental groups. The number of mice used were kept to the advised minimum [221] as no previous data were available to calculate an applicable sample size for this proof of concept study.

The weight of the animals ranged from 20.8g to 36.4g (median 30.84g). General anaesthesia was induced by intra-peritoneal injection of 100mg/kg Inactin (thiobutabarbital sodium salt hydrate, Sigma, Paisley, UK). The anaesthesia was chosen for its limited effect on renal function in mice [222] combined with its inhibitory effect on proximal tubular reabsorption [223] which was ideal for this study design investigating exosome uptake in the collecting duct. Venous access was gained via

the jugular vein. Urine flow was maintained throughout with a 0.9% saline infusion (0.2mL/10gbw/hour i.v). For each experimental group, dye-labelled exosomes from CCD cells were injected in a final volume of 0.1ml (i.v). The injection of exosomes was repeated without or with preceding tolvaptan administration (0.3mg/kg i.v) or furosemide (1mg/1kg, i.v). The injected tolvaptan dose was consistent with previous published murine studies with the injected furosemide dose adjusted to yield a similar increase in urine flow rate comparable to tolvaptan. Urine was collected via a urinary catheter for 30 minutes following different conditions. Following the final time point, the mouse was euthanized by cervical dislocation. All experiments were performed during similar times of the day, within the local designated surgical laboratory.

The primary experimental outcome was to measure the urinary output of dye-labelled exosomes by NTA (as per described method in Chapter 2). Secondary, it was of importance to determine whether tolvaptan or furosemide treatment would have an effect on the urinary output of dye-labelled exosomes.

5.2.4 Clinical case study

Repeated urine samples were obtained from a 16-year-old male with stable central diabetes insipidus (CDI) secondary to a craniopharyngioma, who was being routinely treated with daily desmopressin (dDAVP nasal spray; 0.1ml (10mcg) desmopressin acetate per spray). The CDI patient samples were initially stored at 4°C then frozen at -80 °C. Analysis of the CDI patient samples were performed by a researcher blinded to the timing of desmopressin treatment. The protocol was agreed by the institutional ethical review body and informed consent was obtained. Urinary creatinine was analysed as per described method in Chapter 2. Antibodies to each segment of the nephron were identified and labelled with quantum dots (antibody-Qdots) as per described in Chapter 2.

5.2.5 Measurement of particle size and concentration distribution with NTA

Mouse urine samples were collected for 30 minutes following treatment and diluted 1:100. The diluted urine samples were then analysed using the Nanosight LM 10 instrument (Nanosight Ltd.) with the fluorescent long-pass filter in place as previously described in Chapter 2.

Human urine samples were diluted 1:100, divided into five aliquots and then labelled with different antibody-Qdots to yield a final particle concentration in the region of 1 x 10^8 particles / ml as per the manufacturer's recommendations. The diluted urine samples were then analysed using the Nanosight LM 10 instrument (Nanosight Ltd.) as previously described in Chapter 2.

5.2.6 Statistical analyses

Except where stated otherwise, data are presented as means and standard deviation. Experimental groups were compared by Student's t-test or ANOVA with appropriate post hoc testing using GraphPad Prism (version 6).

5.3 Results

5.3.1 Intravenous injection of labelled exosomes measured in mouse urine

Firstly, it was of interest to determine whether intravenously injected dye-labelled exosomes would appear in the urine and whether this could be detected and quantified by NTA. NTA quantification of urine prior to dye-loaded exosome injection yielded no signal. Prior to i.v injection, all dye-loaded exosomes were quantified by NTA (Figure 5.1A). Figure 5.1B presents a representative NTA trace of a urine sample, showing the dye-loaded exosome population in urine detected and quantified using the fluorescent filter capabilities of NTA. The median particle size of fluorescently labelled particles in whole urine for this representative sample were 64nm, indicative of particles within the expected exosomal size range.

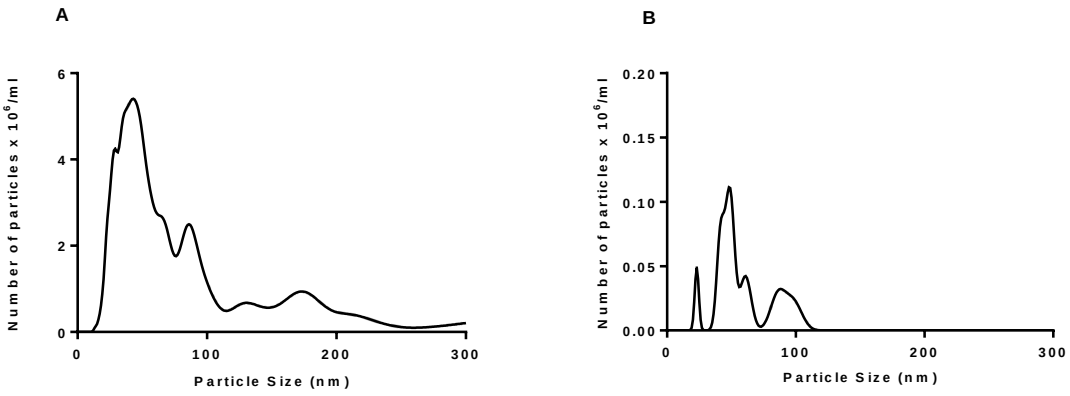

Figure 5.1: Representative NTA trace of dye-labelled exosomes in exosome preparation compared to urinary output

Representative NTA analysis of the labelled isolated exosome preparation derived from CCD cells (A) compared to urine sample from one mouse following i.v injection of labelled exosomes (B).

5.3.2 Vasopressin regulation of exosome uptake in a mouse model

As a control, mice were intravenously injected with exosome free Cell Tracker™ nanocrystals in solution and there was no signal detected in their urine by NTA. Mice were subsequently intravenously injected with dye-labelled exosomes derived from CCD cells. The urinary excretion of these fluorescent exosomes was measured by NTA. Qiazol treatment of the urine substantially reduced the number of particles measured by NTA which is consistent with the presence of dye-labelled membrane bound exosomes (Figure 2A)**.** Comparing the area under the curve for particles sized between 20-100nm, revealed a significant decrease following Qiazol treatment of urine (501.5 ± 624.8 compared to 101.8 ± 106.9 x 10^6 particles/ml) confirming a decrease in number of particles of dye-labelled exosomes (Figure 5.2B).

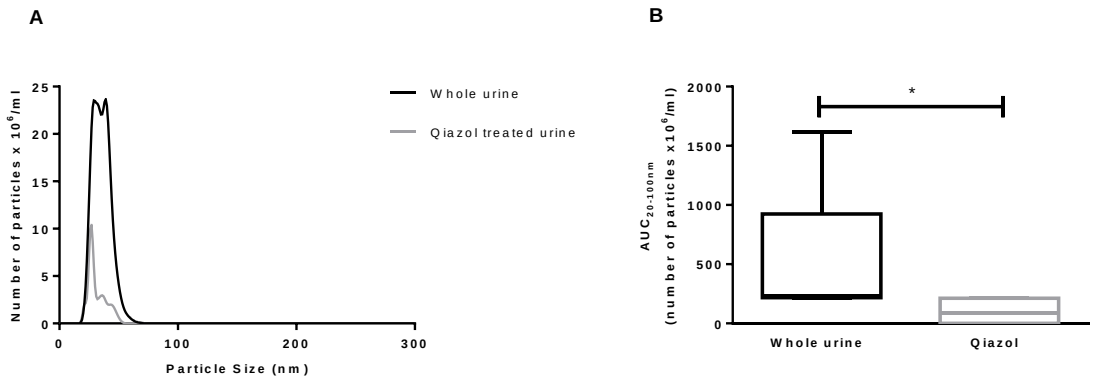

Figure 5.2: NTA analyses of membrane disrupted exosomes

A.) Representative NTA traces showing number of particles of whole urine (black line) compared to Qiazol treated urine (grey line). B). $AUC_{20 - 100}$ of whole urine compared to Qiazol treated urine. (Values expressed as mean ± SD; n=5, *, $P < 0.05$, unpaired t-test.)

Following confirmation of the integrity of dye-labelled membrane bound exosomes, mice in the control group received two consecutive injections of labelled exosomes and a similar percentage were recovered in the urine (3.82% vs 3.85%). The area under the curve for particles sized between 20-100nm (AUC_{20-100}) was also similar between two consecutive i.v injections of labelled exosomes (11.40 ± 9.56 vs 12.55 ± 17.65 x 10^6 particles/ml) (Table 5.1, Figure 5.3).

In the experimental groups, mice were first injected with dye-labelled exosomes and urine was collected to determine the basal excretion. Then the mice were treated with either tolvaptan or furosemide followed by a second i.v injection of the same number of exosomes. Tolvaptan treatment increased the exosome excretion from 2.75% to 20.34%, (Table 5.1, Figure 5.3), whereas treatment with furosemide (n=4) had no effect (3.24% compared to 3.98%), despite inducing a similar diuresis.

Table 5.1: Comparison of urinary exosome excretion (urine collection for 30 minutes) in control, tolvaptan and furosemide treated mice following 2 consecutive i.v injections of dye-labelled exosomes

	Control (n=5)		**Tolvaptan treated (n=5)**		**Furosemide (n=4)**	
	1st i.v injection	2nd i.v injection	1st i.v injection	2nd i.v injection	1st i.v injection	2nd i.v injection
Number of particles (AUC_{20-100})	11.40 ± 9.56	12.55 ± 17.65	3.72 ± 4.98	35.96 ± 20.35	1.33 ± 1.54	2.18 ± 1.59
Urine volume in 30 min collection (uL)	55	60	60.05	79	22.5	30
Fold Change in urine flow	~	1.09	~	1.3	~	1.33
Percentage exosomes recovered in 30 minute collection	3.82± 3.21%	3.86 ± 5.42%	2.75 ± 3.68% ***P < 0.05**	20.34± 11.45% ***P < 0.05**	3.24 ± 3.75%	3.98 ± 2.92%

Data are expressed as mean ± SD. *, P < 0.05 defines statistical significance between 2 consecutive i.v injections of exosomes within the same experimental group.

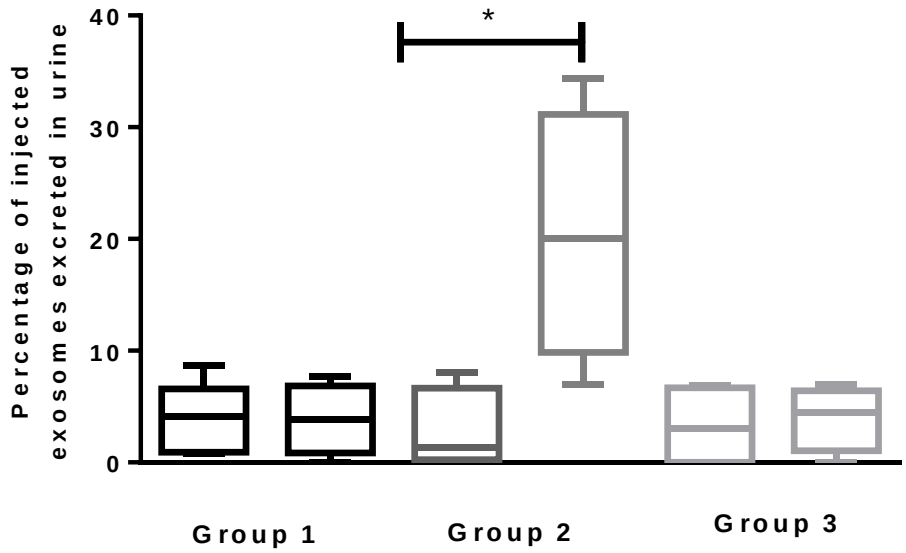

Figure 5.3: Vasopressin V2 receptor regulates urinary exosome excretion in mice

A.) Urinary excretion of i.v injected exosomes in mice. Group 1 – control group (n=5); urine exosome excretion following 2x i.v injections of dye-labelled exosomes. Group 2 – urine exosome excretion after 2 i.v injections of dye-labelled exosomes of mice treated with tolvaptan (0.3mg/kg) (n=5) between injections. Group 3 – Urinary exosome excretion after 2 i.v injections of dye-labelled exosomes of mice treated with furosemide (1mg/kg) (n=4) between injections. Data are expressed as percentage of the total number of injected exosomes excreted in the urine over 30 minute urine collection (mean ± SD, * $P < 0.05$, non-parametric Mann-Whitney t-test).

5.3.3 Vasopressin regulation of exosome uptake in a clinical case study

In a complementary *in vivo* proof-of-concept study, the urinary excretion of nephron segment specific exosomes was measured in a patient with central diabetes insipidus. In this approach Qdot labelled antibodies were used to target segment specific proteins and these populations of exosomes were measured by NTA combined with Qdot labelled antibodies for segment specific proteins[206]. Changes in urinary creatinine following intra-nasal desmopressin administration are shown in Figure 5.4A. Following self-directed desmopressin intra-nasal administration, there was a decrease in both glomerular (podocalyxin-like) and proximal tubular (cubilin) protein-expressing exosomes (Figure 5.4B).

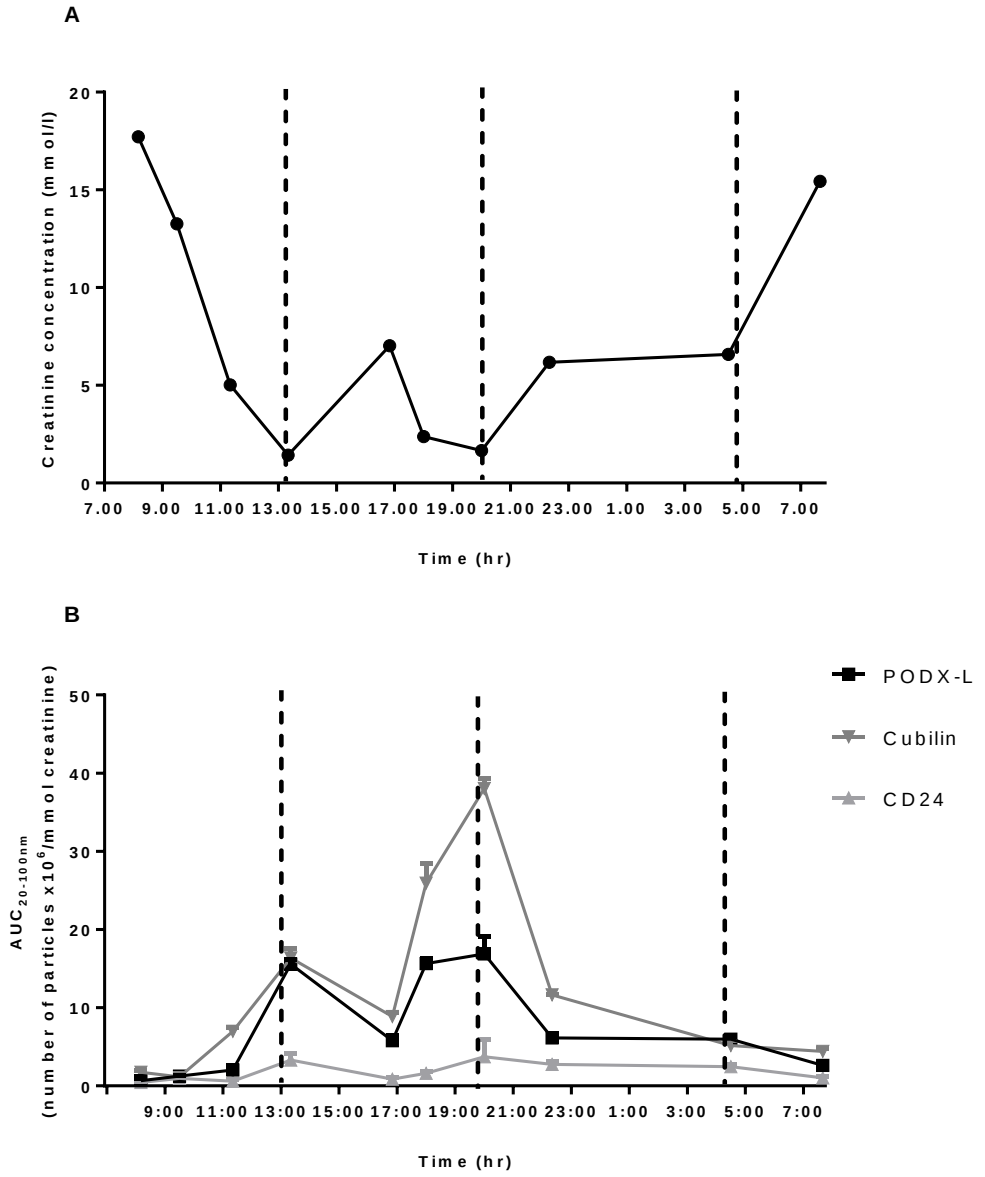

Figure 5.4: NTA analysis of 24 hour exosome excretion by a patient with central diabetes insipidus

A.) Changes in urinary creatinine concentration (mmol/l) following administration of desmopressin treatment over time. B.) Changes in the number of particles (AUC_{20-100}) of urinary creatinine and exosomes expressing nephron-segment specific proteins: glomerular (podocalyxin-like protein, PODX-L), proximal tubular (cubilin), and CD24 (pan-segment urinary exosome marker) over time. Exosome urine concentration measured by NTA and normalised by urinary creatinine concentration. NTA measurements were taken in triplicate for each time point. Lines represent the time of desmopressin treatment (dashed line).

5.4 Discussion

There has been a substantial increase in publications on the biology of exosomes, particularly relating to their signalling potential as mediators of intercellular communication. However, in the kidney and other organs there is little evidence that regulated signalling occurs *in vivo*. To test whether vasopressin is important for renal exosome uptake and excretion *in vivo*, dye-labelled exosomes were systemically injected into mice. After injection these exosomes appeared in urine which is consistent with previous published studies [119]. The small percentage recovery of dye-labelled exosomes found in the mice urine is consistent with other research showing the majority of dye-labelled particles may be sequestered or transported to the lung, spleen or liver [224].

The unique structure and filtration pathway of the nephron, including the slit diaphragm and meshwork structure of the glomerular basement membrane only allows particles with a hydrodynamic diameter size up to 6nm to be filtered [225]. Exosomes are theoretically above the cut-off size for successful glomerular filtration, however, recently, trans-renal transport of exosomes[119] has been reported. The mechanism of systemic exosome entry into urine remains to be determined. A process of trancystosis as possible mechanism have been proposed but it still remains to be elucidated[226].

In this chapter, it was demonstrated that tolvaptan, a selective V2 receptor antagonist, substantially increased the urinary excretion of systemically administered exosomes. The V2 receptor is located on the basolateral membrane of the principal collecting duct; therefore a possible explanation of the mechanisms involved with increased systemic exosome uptake following tolvaptan treatment, could be reduced intracellular shuttling of vesicles and reabsorption by the collecting duct and therefore increased excretion in the urine of dye-labelled exosomes. These are the first data that demonstrate vasopressin is a regulator of urinary exosome excretion and confirms the findings in Chapter 4 of vasopressin regulation of exosome uptake *in vitro* translating *in vivo*.

Combining antibodies to nephron segment-specific proteins with NTA can identify the cellular origin of urinary exosomes. Urine from a patient with central diabetes insipidus – a condition defined by lack of vasopressin – were collected and determined the effect of intra-nasal desmopressin on glomerular and proximal tubule derived exosomes. Following desmopressin stimulation, the urinary number of particles of these exosomes was decreased, which is consistent with vasopressin regulation of urinary exosomes excretion in humans. While these human data are hypothesis-generating, they are consistent with the data from cells and mice. An indirect limitation of this study to consider is the effect vasopressin has on exosome release and the influence this might have on the total exosome population, as shown in our findings in Chapter 3. An additional limitation is that the concentration of urinary creatinine changed as a result of desmopressin treatment making the normalisation of spot urine exosome numbers a challenge. In the future larger validation studies should be performed to confirm the human data.

Additionally, future work should include confirming the endosomal origin and cargo of the dye-labelled exosomes found in the urinary output. Control experiments conducted, including injection of dye without exosomes present, NTA trace representatives of the size distribution of dye-labelled particles and confirming the membrane bound integrity by lysis of the urine sample, combined, proved the size and shape of dye-labelled exosomes in the urinary output. However, further experiments should be aimed at confirming the contents and functional delivery of the recovered exosomes. This could be achieved through the addition of an exogenous miRNA-species and by measuring its target gene effects. Histology of the kidney and other tissue samples would also be beneficial to further elucidate the distribution of systemically injected dye-labelled exosomes.

In conclusion, in this chapter, vasopressin regulation of exosome uptake in a mouse model and clinical case study were shown. Furthermore, exosome uptake could be increased by inhibition of the V2 receptor. This is an important concept as a greater understanding of exosome uptake may allow exosome manipulation to increase their urinary excretion and opens further exciting avenues of urinary exosomal biomarker discovery and more refined therapeutic targeting of interventions in the kidney.

CHAPTER 6

Quantification of nephron-specific human urinary exosomes in Acute Kidney Injury

6.1 Introduction

The unique exosomal proteome reflective of all the different segments of the nephron highlights the potential of urinary exosomes to provide information of cell specific physiological and pathophysiological changes that may occur along the nephron. This ability subsequently highlights the potential of urinary exosomes as nephron-specific biomarkers of kidney injury.

Contrast media induced acute kidney injury (CI-AKI) is the development of acute kidney injury (AKI) following the administration of radiographic contrast media (CM)[182]. Previous exposure to CM still remains among the top 3 aetiological factors for AKI in hospital. Even though the direct mechanisms of CI-AKI are not yet fully understood, possible pathophysiological mechanisms of CI-AKI include: direct CM molecule tubular cell toxicity; haemodynamic effects primarily through afferent arteriolar vasoconstriction; and endogenous biochemical disturbances such as changes in nitric oxide levels and increases in oxygen-free radicals[184,185].

Currently, serum creatinine is the standard index of kidney function and also the gold standard for recognising AKI. Serum creatinine as a biomarker of kidney injury does, however, have limitations as it is slow to reflect changes in glomerular filtration rate which can potentially delay diagnosis[186,187]. This limitation has led to considerable, ongoing research efforts aimed at discovering and developing new, accurate biomarkers of AKI. Two promising candidates reflecting kidney tubular damage as opposed to disturbed function are NGAL (Neutrophil-gelatinase-associated lipocalin) and KIM-1 (Kidney Injury Molecule-1). A number of studies have unequivocally demonstrated both NGAL and KIM-1 to be novel, predictive biomarkers for AKI[193]. Whilst these two candidates are promising as early biomarkers of AKI, both are still variable and dependent on the underlying clinical context[227], therefore there is still a need for new candidates for timelier diagnosis of AKI - which in turn will aid better prediction and stratification of injury and lead to more refined methods of safety assessment of nephrotoxic events during drug development[193]. It would also be of interest to develop a more comprehensive characterisation of kidney injury

propagation along the nephron and further elucidate the underlying pathophysiological mechanisms in AKI.

Building upon the developed method of quantifying urinary exosomes by NTA using an antibody-specific labelling system (Chapter 3), the first aim of this chapter was to determine whether this method could quantify nephron-specific exosomes in a human AKI model of CM exposure, and how this would compare to standardised biomarkers of AKI. The second aim was to determine whether nephron-specific exosome populations in AKI could provide more insights into the role exosomes might play in pathophysiology of the kidney.

In this chapter, urinary exosomes positive for a panel of proteins characteristic of each segment of the nephron (podocyte, proximal and distal tubule, collecting duct and a pan-tubule surface marker) were measured and compared against the established and standardised biomarkers for kidney tubular injury: KIM-1 and NGAL. It was determined whether NTA measurements of nephron-specific exosomes could reflect changes in patients comparable to standard kidney injury markers in a CI-AKI model.

6.2 Methods

6.2.1 Patient group, sample collection and sample processing

Samples for this study were kindly obtained from Prof M Eddleston (Professor of Clinical Toxicology, University of Edinburgh) from a clinical trial (Protocol No NAC0606) investigating the mechanisms for an effect of acetylcysteine on renal function after exposure to radio-graphic contrast material[228]. The study was performed simultaneously in four groups of participants. Studies 1-3 were randomised, placebo-controlled, three-way, crossover human volunteer studies of eight participants. All studies were performed at the Wellcome Trust Clinical Research Facility, Royal Infirmary of Edinburgh. The applicable arm of this 4-arm study was Study 4: a randomised, placebo-controlled, three-way parallel group study in patients undergoing elective coronary angiography. Patients in this group were

randomised to receive either oral acetylcysteine (1200 mg twice daily for two days), IV acetylcysteine (200 mg/kg over 7 hours), or placebo. Patients were subsequently followed up 24 hours and 72 hours after acetylcysteine-administration. The local ethics committee approved the study and written informed consent was obtained from each participant. All participants were male, non-smoking and aged over 45 with a body mass index of 22 - 40 kg/m^2. Exclusion criteria for this study were thyroid disease, asthma, atopy or myasthenia gravis, a history of allergy or sensitivity to acetylcysteine or CM and current intake of metformin. The primary outcome of this study was a change in renal blood flow, with secondary outcomes including changes in glomerular filtration rate, tubular function, urinary proteins and oxidative balance.

The study described in this chapter included 32 chronic kidney disease (CKD) stage III patients, who were exposed to CM. Participants in study 4 received doses of *Visipaque 320* as prescribed by the consultant cardiologist performing angiography to adequately visualise the coronary arteries and perform any procedure judged to be necessary. A baseline spot urine sample was collected before the administration of CM. Two spot urine samples were collected after CM exposure: 24 hours and 72 hours after administration. The patient samples were initially stored at 4°C and then frozen at -80°C.

6.2.2 Creatinine, KIM-1 and NGAL

Urinary creatinine concentration was measured for every spot urine sample by a colorimetric method using a commercial kit from Alpha Laboratories Ltd. (Eastleigh, UK). KIM-1 and NGAL concentrations were also measured for every sample. Both KIM-1 and NGAL were assayed using a commercial kit from R&D systems, Inc. (Minneapolis, USA) following the manufacturer's protocol with calibration ranges of 0 - 2500 pg/mL. Urine was assayed undiluted for KIM-1 and diluted 1:20 with deionised H_2O for NGAL.

6.2.3 Fluorescent labelling with antibody conjugated to quantum dots

Proteomic analysis by Pisitkun *et al*. (2004) identified nephron segment-specific proteins in human urinary exosomes. Specific proteins relating to each segment of the nephron were chosen for further analyses. As per the described method in Chapter 2, quantum dots (Qdots) were conjugated to the different antibodies: Anti-CD24; Anti-AQP2 (Millipore); Anti-NCC (Stressmarq biosciences Inc., Victoria, Canada); Anti-CU (Abcam); Anti-PODXL (Milipore) (Table 6.1). The conjugated Qdots were diluted to 1:1000 with deionised water.

Table 6.1: Nephron specific urinary exosome protein markers

Nephron segment	Protein identified in urinary exosomes
Podocyte/Glomerulus	Podocalyxin-like protein (PODXL)[21]
Proximal tubules	Cubilin (CU)[39]
Distal tubules	Sodium-chloride co-transporter (NCC)[87]
Collecting duct	Aquaporin-2[45]
Pan-tubule surface marker	CD24[31]

6.2.4 Measurement of particle size and concentration distribution with NTA

All urine samples were diluted 1:100, divided into five aliquots and then labelled with different antibody-Qdots to yield a final particle concentration in the region of 1 x 10^8 particles/ml as per the manufacturer's recommendations. The diluted antibody-Qdot urine samples were then analysed using the Nanosight LM 10 instrument (Nanosight Ltd., Amesbury, UK) as previously described in Chapter 2.

6.2.5 Statistical analysis

The data from triplicate NTA results were analysed using GraphPad Prism Version 6 as previously described in Chapter 2. Wilcoxon matched pairs signed rank tests were performed to determine significant differences between time points for each antibody-Qdot exosome concentration expressed as the area under the curve for particles sized between 20-100nm as measured by NTA. Data are shown with and without urinary creatinine correction. A non-parametric Spearman correlation test was performed to determine correlations between KIM-1 or NGAL and the different antibody-Qdot exosome concentrations. After correlations had been found, the data was analysed using a linear regression analysis to compare NGAL and KIM-1 with antibody-Qdot NTA values. Finally, as the study is currently still blinded, patients were divided into 3 tertile groups according to the final KIM-1 and NGAL values (72 hours post-exposure) and changes in antibody-Qdot exosome NTA values in the different tertile groups over time were compared using non-parametric Kruskal-Wallis ANOVA.

6.3 Results

6.3.1 Patient demographics

Table 6.2 summarises the demographics of the patients. In total, urine samples from 32 patients were included, all male, with a mean age of 76 years. The average dose of CM was 165ml (Table 6.2).

Table 6.2: Patient demographics

Factor	Mean
Age (years)	76 (60-91)
Height (cm)	173 (156.5–186)
Weight (kg)	90 (64–127.6)
Average dose (mL)	165 (50-520)

Data are represented as the mean and range, n = 32.

6.3.2 Urinary levels of characterised biomarkers of kidney injury

Comparing urinary creatinine levels pre- and post-exposure to CM across all patients, revealed a significant increase following contrast media exposure (*Table* 6.3). This negated using urinary creatinine as an analyte normaliser for differences in concentrations in subsequent analyses. For the total study group, KIM-1 values were significantly higher post-exposure (24 and 72 hours) compared to the initial pre-exposure measurements (Table 6.3; Figure 6.1A). Figure 6.1B shows the non-significant differences once KIM-1 values are corrected for urinary creatinine values. NGAL showed a significant increase 24 hours post-exposure compared to pre-exposure values (Table 6.3; Figure 6.1C). Similarly, once NGAL values were corrected with urinary creatinine values, the significant differences seen pre-correction were diminished (Figure 6.1D).

Table 6.3: Biomarker characteristics pre- and post (24 hours and 72 hours) exposure to contrast media

Biomarker	Pre-exposure	Post-exposure 24 hours	Post-exposure 72 hours
Urinary creatinine (µg/ml)	546.6 ± 212.3	1208 ± 602.8***	1058 ± 127.6***
Urinary KIM-1 (pg/ml)	535.6 ± 381.9	1629 ± 1820*	1376 ± 1498*
Urinary NGAL (ng/ml)	7.7 ± 11.6	19.7 ± 21.4*	14 ± 20.8 ns
Corrected KIM-1 (pg/µg creatinine)	0.94 ± 0.84	1.55 ± 2.11	1.45 ± 1.38
Corrected NGAL (pg/µg creatinine)	14.49 ± 20.43	19.05 ± 30.96	15.60 ± 31.57

Comparison of the biomarker characteristics measured in patient urine samples obtained before (pre-exposure) and after (24 hours and 72 hours post-exposure) contrast media exposure. Data are represented as mean ± SD. Statistical significance is indicated as * $P < 0.05$; *** $P < 0.001$; and ns, non-significant for post-exposure biomarker characteristics compared to pre-exposure characteristics.

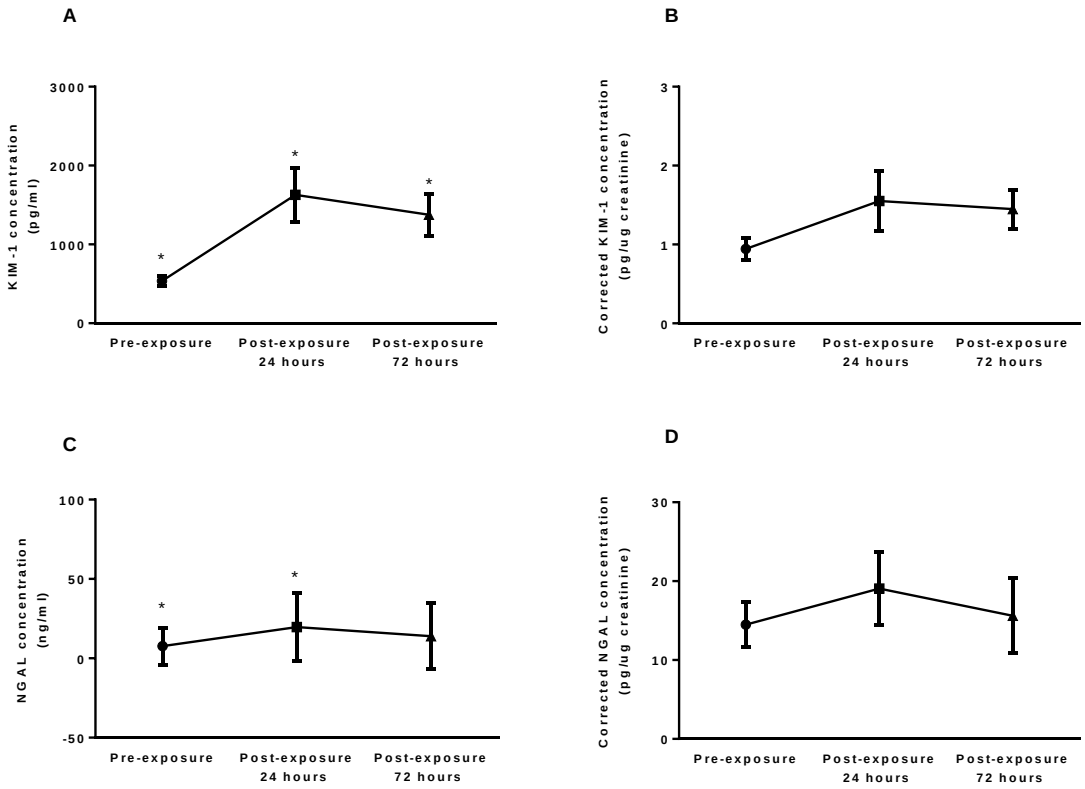

Figure 6.1: Change in urinary tubular injury biomarkers after contrast exposure

KIM-1 (A), urinary creatinine corrected KIM-1 (B), and NGAL (C) and urinary creatinine corrected NGAL (D) pre- and post-exposure to CM (24hours & 72 hours). (Mean ± SEM, *** $P < 0.001$ seen as highly significant, * $P < 0.05$ seen as significant compared to pre-exposure values, n = 32).

6.3.3 Comparison of protein-exosome conjugates concentration and urinary KIM-1 and NGAL

The relationship between the concentration of each nephron-specific protein-exosome conjugate and urinary KIM-1 and NGAL concentration was explored (both exosomes and biomarkers expressed per mL urine) (Table 6.4).

Interestingly, 24 hours post-exposure PODXL showed a significant relationship with both biomarkers, KIM-1 and NGAL at the final time point, 72 hours post exposure to CM (Table 6.4). A linear regression analysis of the relationship between PODXL (72hours post-exposure) NTA values and KIM-1 and NGAL also showed a small, but significant fit of line (Figure 6.2).

However, once the protein-exosome conjugate concentrations were corrected for urinary creatinine values, the previous statistical significance was negated (Table 6.5) highlighting the confounding effect creatinine correction may have on this study.

Table 6.4: Correlations between protein-exosome conjugates (24 and 72 hour post-exposure) compared to urinary KIM-1 and NGAL (72 hours post-exposure)

Biomarker	KIM-1		NGAL	
	R^2	P	R^2	P
Podocalyxin-like				
24 hours	0.19	**0.03***	0.24	**0.01***
72 hours	0.25	**0.01***	0.13	**0.03***
Cubilin				
24 hours	0.00	0.78	0.01	0.58
72 hours	0.11	0.10	0.11	**0.05***
NCC				
24 hours	0.13	0.073	0.08	0.09
72 hours	0.12	0.09	0.09	0.08
Aquaporin-2				
24 hours	-0.26	0.81	0.01	0.51
72 hours	-0.18	0.99	0.01	0.54
CD24				
24 hours	0.03	0.42	0.18	**0.04***
72 hours	0.02	0.52	0.02	0.45

Comparison of relationship between different time points post-exposure (24 and 72 hours) to CM and the 72 hours post-exposure time point for biomarkers, KIM-1 and NGAL. Data is expressed as the R^2 value of the interaction with * $P < 0.05$ seen as statistically significant.

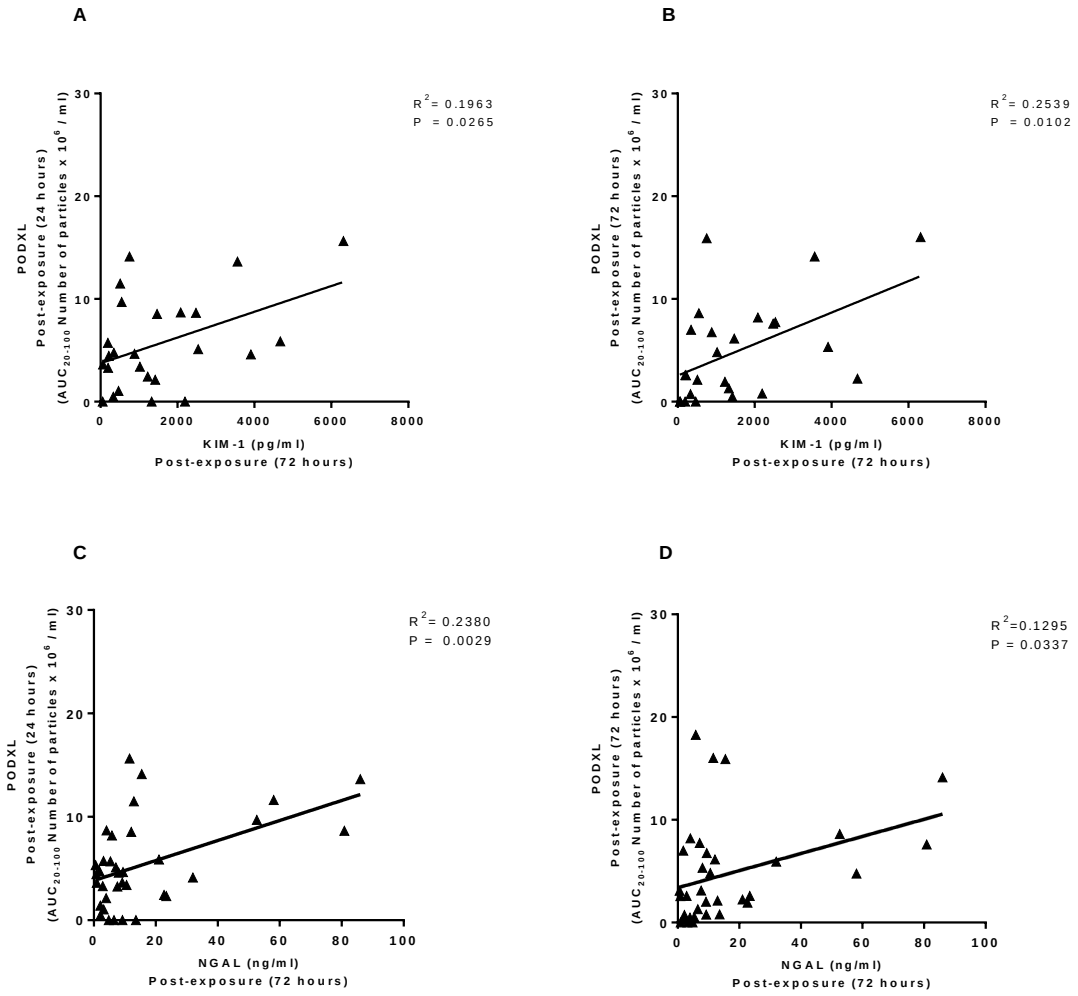

Figure 6.2: Relationship between PODXL (24 and 72 hours post-exposure) and urinary KIM-1 and NGAL (72 hours post-exposure)

Linear regression analyses between PODXL and markers KIM-1 and NGAL following significant correlations for 24 and 72 hours post-exposure respectively. A.) PODXL (24 hours post-exposure) correlated with KIM-1 (72 hours post exposure). B.) PODXL (72 hours post-exposure) correlated with KIM-1 (72 hours post-exposure). C.) PODXL (24 hours post-exposure) correlated with NGAL (72 hours post exposure) D.) PODXL (72 hours post-exposure) correlated with KIM-1 (72 hours post-exposure). PODXL values expressed as the AUC for particles sized between 20-100nm. R^2 value given with statistical significance (* $P < 0.05$, n=32).

Table 6.5: Correlations between urinary creatinine corrected protein-exosome conjugates (24 and 72 hour post-exposure) compared to urinary KIM-1 and NGAL (72 hours post-exposure)

Biomarker	KIM-1		NGAL	
	R^2	P	R^2	P
Podocalyxin-like				
24 hours	0.15	0.06	0.28	**0.001**
72 hours	0.05	0.26	0.07	0.10
Cubilin				
24 hours	0.03	0.33	0.05	0.18
72 hours	0.00	0.93	0.09	0.06
NCC				
24 hours	0.13	0.073	0.05	0.19
72 hours	0.12	0.09	0.02	0.34
Aquaporin-2				
24 hours	0.00	0.95	0.02	0.43
72 hours	0.05	0.30	0.03	0.33
CD24				
24 hours	0.02	0.49	0.01	0.48
72 hours	0.10	0.11	0.00	0.77

Comparison of relationship between different time points post-exposure (24 and 72 hours) to CM and the 72 hours post-exposure time point for urinary creatinine corrected biomarker concentrations, KIM-1 and NGAL. Data is expressed as the R^2 value of the interaction with * $P < 0.05$ seen as statistically significant

6.3.4 Comparing protein-exosome conjugate levels in different KIM-1 and NGAL tertiles before and after CM exposure

The patients included in this particular study were subsequently divided into tertile groups based on final biomarker levels – both KIM-1 and NGAL (72 hours post-exposure). Following this allocation, the third tertile based on KIM-1 values resulted in a sub-group (n=11) with a mean value of 3013 ± 1482 pg/ml urinary KIM-1 (Table 6.6, Figure 6.4A). Urinary creatinine correction of protein-exosome conjugates in different tertile groups for KIM-1 (Table 6.7) and NGAL (Table 6.9) values are shown. To investigate the relationship of the panel of exosome protein markers with the AKI biomarkers in the different tertile groups, the final PODXL values (72hours post-exposure) showed a significant difference between the first tertile (low KIM-1 values) compared to the third tertile group (high KIM-1 values). No significant differences were found in any of the other nephron-specific protein-exosome conjugates following allocation into tertile groups (Table 6.6, Figure 6.3B). Only PODXL from the panel of nephron-specific protein exosome conjugates showed a significant difference between different KIM-1 tertile groups (Figure 6.3C-E).

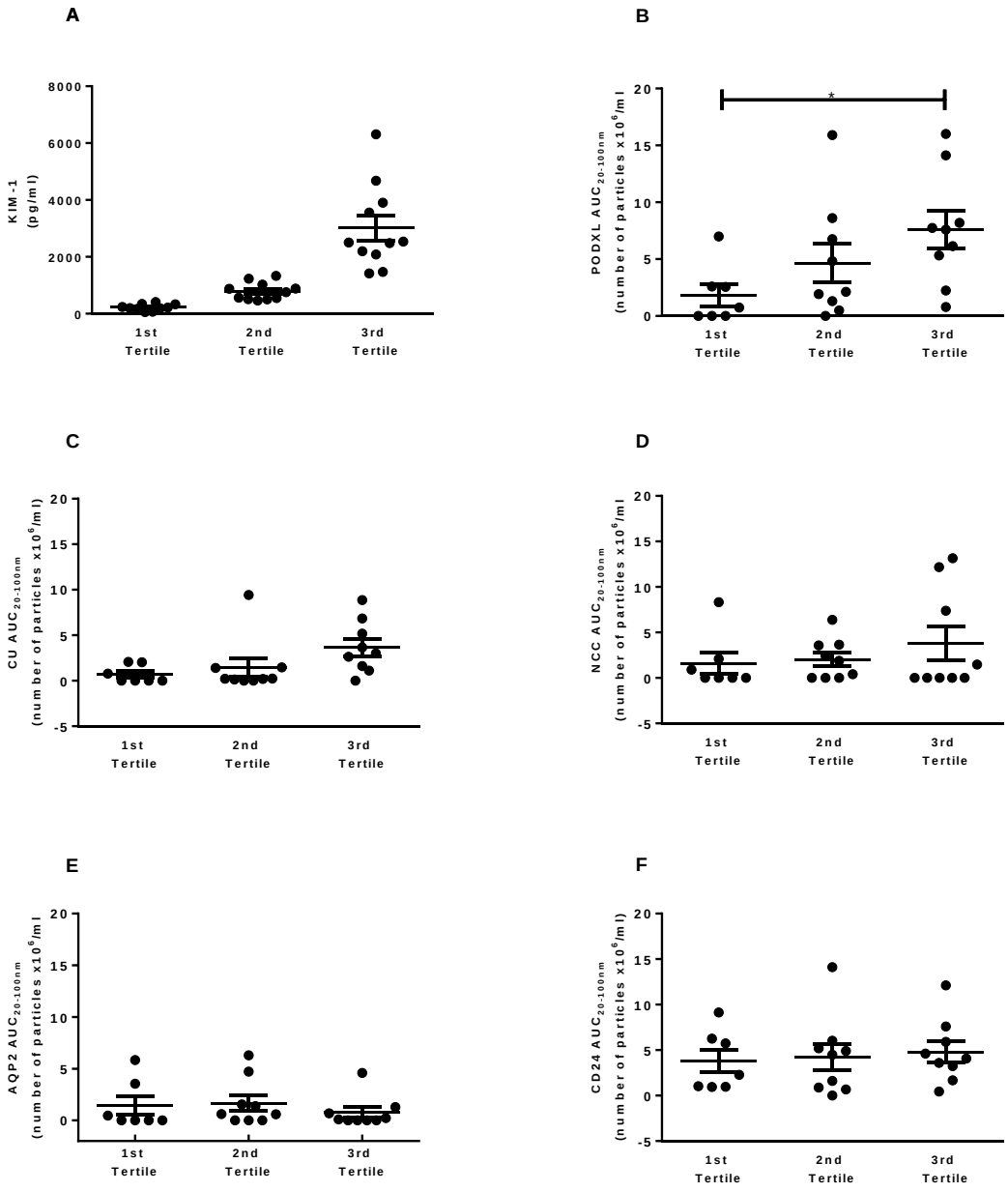

Figure 6.3: Changes in NTA values of nephron-specific protein-exosome following allocation in tertile groups based on final KIM-1 value (72 hours post-exposure)

A.) Tertile groups based on KIM-1 values. Graphs are representative of $AUC_{20\text{-}100}$ for B.) Podocalyxin-like (PODXL) C.) Cubilin (CU); D.) Sodium-chloride co-transporter (NCC); E.) Aquaporin-2 (AQP2) and F.) CD24 positive urinary exosomes number of particles, comparing different tertile groups as indicated. Data is expressed as the area under the curve for particles sized between 20-100nm ($AUC_{20\text{-}100}$), expressed as mean ± SEM; * $P < 0.05$.

Table 6.6: Comparison of NTA measurements of nephron-specific protein-exosomes pre- and post-exposure to CM following allocation of patient group into tertile subgroups based on 72 hours post-exposure KIM-1 values

	1st Tertile			**2nd Tertile**			**3rd Tertile**		
KIM-1									
n	10			11			11		
Mean (pg/ml)	221.8 ± 115.6			789.6 ± 304.8			3013 ± 1482		
AUC_{20-100}	**Pre-exposure**	**Post-exposure (24 hours)**	**Post-exposure (72 hours)**	**Pre-exposure**	**Post-exposure (24 hours)**	**Post-exposure (72 hours)**	**Pre-exposure**	**Post-exposure (24 hours)**	**Post-exposure (72 hours)**
CD24	8.9 ± 8.0	3.5 ± 2.6	3.8 ± 3.3	5.0 ± 4.6	5.2 ± 8.1	4.2 ± 4.3	7.2 ± 5.7	6.0 ± 5.6	4.8 ± 3.5
PODXL	2.5 ± 3.9	3.2 ± 2.2	1.8 ± 2.5 *** P < 0.05**	5.0 ± 5.1	5.4 ± 5.0	4.7 ± 5.1	5.5 ± 3.0	7.9 ± 4.7	7.6 ± 4.9 *** P < 0.05**
CU	0.9 ± 1.5	0.7 ± 0.8	0.7 ± 0.9	2.8 ± 4.7	3.1 ± 4.6	1.5 ± 3.0	3.1 ± 2.5	3.4 ± 2.5	3.7 ± 2.8
NCC	2.4 ± 3.2	1.9 ± 2.7	1.6 ± 3.1	2.7 ± 3.7	1.9 ± 2.3	2.0 ± 2.2	2.7 ± 4.2	3.8 ± 5.0	3.8 ± 5.6
AQP2	1.4 ± 1.7	2.1 ± 2.6	1.4 ± 2.3	0.8 ± 1.1	1.9 ± 2.5	1.7 ± 2.2	0.5 ± 0.9	1.4 ± 2.1	0.8 ± 1.5

Comparison of NTA measurements of nephron-specific protein-exosome conjugates following allocation of whole patient group into different tertile groups based on the final KIM-1 values (72 hours post-exposure). (Dara are expressed as the mean AUC of particles sized between 20-100nm (AUC_{20-100}) ± SD. * P < 0.05 seen as statistically significant. n as indicated. Non-parametric ANOVA Kruskal-Wallis test)

Table 6.7: Comparison of NTA measurements of creatinine corrected nephron-specific protein-exosomes pre- and post-exposure to CM following allocation of patient group into tertile subgroups based on 72 hours post-exposure KIM-1 values

	1st Tertile			2nd Tertile			3rd Tertile		
KIM-1									
n	10			11			11		
Mean (pg/ml)	221.8 ± 115.6			789.6 ± 304.8			3013 ± 1482		
AUC_{20-100}	**Pre-exposure**	**Post-exposure (24 hours)**	**Post-exposure (72 hours)**	**Pre-exposure**	**Post-exposure (24 hours)**	**Post-exposure (72 hours)**	**Pre-exposure**	**Post-exposure (24 hours)**	**Post-exposure (72 hours)**
CD24	0.01 ± 0.01	0.003 ± 0.002	0.01 ± 0.008	0.016 ± 0.022	0.005 ± 0.008	0.007 ± 0.008	0.016 ±0.012	0.005 ± 0.003	0.003 ± 0.002
PODXL	0.003 ± 0.004	0.003 ± 0.002	0.005 ± 0.006	0.015 ± 0.015	0.003 ± 0.004	0.004 ± 0.006	0.016 ± 0.023	0.007 ± 0.008	0.006 ± 0.006
NCC	0.002 ± 0.004	0.001 ± 0.001	0.003 ± 0.006	0.008 ± 0.012	0.002 ± 0.002	0.003 ± 0.004	0.015 ± 0.03	0.004 ± 0.006	0.002 ± 0.003
CU	0.001 ± 0.002	0.001 ± 0.001	0.002 ± 0.003	0.008 ± 0.012	0.002 ± 0.004	0.002 ± 0.003	0.007 ± 0.005	0.003 ± 0.003	0.003 ± 0.002
AQP2	0.002 ± 0.002	0.002 ± 0.002	0.002 ± 0.002	0.002 ± 0.002	0.002 ± 0.002	0.002 ± 0.002	0.002 ± 0.002	0.002 ± 0.002	0.002 ± 0.002

Comparison of NTA measurements of creatinine corrected nephron-specific protein-exosome conjugates following allocation of whole patient group into different tertile groups based on the final KIM-1 values (72 hours post-exposure). (Dara are expressed as the mean AUC of particles sized between 20-100nm (AUC_{20-100}) ± SD. * $P < 0.05$ seen as statistically significant. n as indicated. Non-parametric ANOVA Kruskal-Wallis test)

Similarly, allocation based on NGAL values, resulted in a third sub-group with a final NGAL value of 31.9 ± 27.9ng/ml (Table 6.8, Figure 6.4A).Comparable to the differences seen between PODXL (72 hours post-exposure) in the different KIM-1 based tertile groups, based on NGAL values: PODXL also revealed a significant difference between the first tertile group (low NGAL values) compared to the third NGAL group (high NGAL values). Interestingly, the same pattern was revealed with significant differences found between high and low NGAL tertile groups based on 24 hours post-exposure PODXL NTA values (Table 6.8, Figure 6.4B). Similarly, only PODXL from the panel of nephron-specific protein exosome conjugates showed a significant difference between different KIM-1 tertile groups (Figure 6.4C-E). No significant differences were seen following creatinine correction of the protein-exosome conjugate concentrations in their respective tertile groups (Table 6.7 and 6.9).

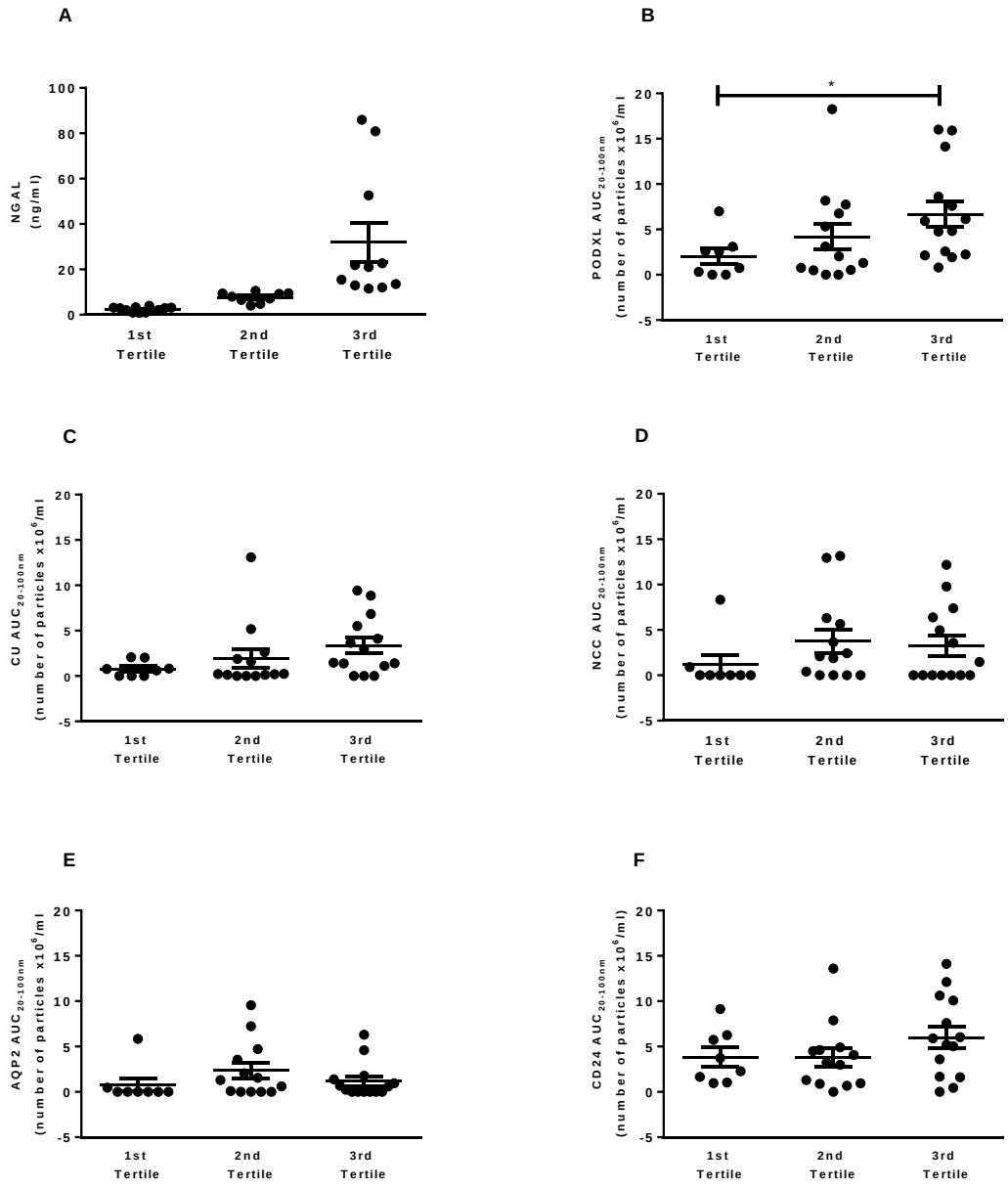

Figure 6.4: Changes in NTA values of nephron-specific protein-exosome following allocation in tertile groups based on final NGAL value (72 hours post-exposure)

A.) Tertile groups based on NGAL values. Graphs are representative of $AUC_{20\text{-}100}$ for B.) Podocalyxin-like (PODXL) C.) Cubilin (CU); D.) Sodium-chloride co-transporter (NCC); E.) Aquaporin-2 (AQP2) and F.) CD24 positive urinary exosomes number of particles, comparing different tertile groups as indicated. Data is expressed as the area under the curve for particles sized between 20-100nm ($AUC_{20\text{-}100}$), expressed as mean ± SEM; * $P < 0.05$.

Table 6.8: Comparison of NTA measurements of nephron-specific protein-exosomes pre- and post-exposure to CM following allocation of patient group into tertile subgroups based on 72 hours post-exposure NGAL

	1st Tertile			2nd Tertile			3rd Tertile		
NGAL									
n	12			9			11		
Mean (pg/ml)	2.3 ± 1.0			7.7 ± 2.2			31.9 ± 27.9		
AUC_{20-100}	**Pre-exposure**	**Post-exposure (24 hours)**	**Post-exposure (72 hours)**	**Pre-exposure**	**Post-exposure (24 hours)**	**Post-exposure (72 hours)**	**Pre-exposure**	**Post-exposure (24 hours)**	**Post-exposure (72 hours)**
CD24	5.5 ± 3.9	3.1 ± 2.4	3.6 ± 2.7	10.7 ± 12.3	7.1 ± 7.1	4.1 ± 3.8	7.5± 5.1	6.1 ± 7.7	5.9 ± 4.6
PODXL	3.1 ± 3.5	3.4 ± 2.2 ***P< 0.05**	2.4 ± 2.9 **¥ P< 0.05**	4.2 ± 3.6	3.7 ± 2.8	4.4 ± 4.9	5.4 ± 4.8	8.1 ± 5.2 *** P < 0.05**	6.4 ± 5.7 **¥P < 0.05**
CU	1.1 ± 1.4	0.7 ± 0.7	0.7 ± 0.8	2.8 ± 5.4	2.9 ± 3.6	2.2 ± 3.8	3.5 ± 4.1	4.1 ± 3.9	3.5 ± 3.3
NCC	1.3 ± 1.9	1.2 ± 2.4	1.2 ± 2.6	2.9 ± 4.3	3.9 ± 4.2	4.1 ± 4.7	3.7 ± 4.4	3.5 ± 4.7	3.2 ± 4.4
AQP2	0.9 ± 1.5	1.5 ± 2.4	0.7 ± 1.8	1.7 ± 2.5	3.4 ± 3.8	2.6 ± 3.1	0.6 ± 0.9	1.3 ± 1.6	1.2 ± 2.0

Comparison of NTA measurements of nephron-specific protein-exosome conjugates following allocation of whole patient group into different tertile groups based on the final NGAL values (72 hours post-exposure). (Dara are expressed as the mean AUC of particles sized between 20-100nm (AUC_{20-100}) ± SD. ¥ $P < 0.05$ statistically significant between 24 hours post-exposure values. * $P < 0.05$ statistically significant between 72 hours post-exposure values. n as indicated. Non-parametric ANOVA Kruskal-Wallis test)

Table 6.9: Comparison of NTA measurements of nephron-specific protein-exosomes pre- and post-exposure to CM following allocation of patient group into tertile subgroups based on 72 hours post-exposure KIM-1 values

	1st Tertile			2nd Tertile			3rd Tertile		
NGAL									
n	10			11			11		
Mean (pg/ml)	221.8 ± 115.6			789.6 ± 304.8			3013 ± 1482		
AUC_{20-100}	**Pre-exposure**	**Post-exposure (24 hours)**	**Post-exposure (72 hours)**	**Pre-exposure**	**Post-exposure (24 hours)**	**Post-exposure (72 hours)**	**Pre-exposure**	**Post-exposure (24 hours)**	**Post-exposure (72 hours)**
CD24	0.009 ± 0.009	0.003 ± 0.002	0.01 ± 0.008	0.025 ± 0.021	0.007± 0.008	0.004 ± 0.003	0.017 ±0.017	0.006 ± 0.007	0.006 ± 0.006
PODXL	0.004 ± 0.003	0.003 ± 0.002	0.005 ± 0.006	0.013 ± 0.021	0.003 ± 0.003	0.003 ± 0.005	0.013 ± 0.013	0.007 ± 0.007	0.006 ± 0.007
NCC	0.003 ± 0.004	0.001 ± 0.002	0.003 ± 0.006	0.013± 0.031	0.004 ± 0.004	0.004 ± 0.004	0.009± 0.012	0.004 ± 0.006	0.003 ± 0.006
CU	0.002 ± 0.003	0.008 ± 0.008	0.002 ± 0.003	0.007 ± 0.009	0.002 ± 0.004	0.002 ± 0.003	0.008 ± 0.010	0.004 ± 0.004	0.003 ± 0.004
AQP2	0.002 ± 0.005	0.001 ± 0.000	0.002 ± 0.004	0.007 ± 0.009	0.003 ± 0.005	0.003 ± 0.005	0.003 ± 0.004	0.001 ± 0.002	0.001 ± 0.001

Comparison of NTA measurements of nephron-specific protein-exosome conjugates following allocation of whole patient group into different tertile groups based on the final KIM-1 values (72 hours post-exposure). (Dara are expressed as the mean AUC of particles sized between 20-100nm (AUC_{20-100}) ± SD. * $P < 0.05$ seen as statistically significant. n as indicated. Non-parametric ANOVA Kruskal-Wallis test)

6.4 Discussion

The development of acute kidney injury (AKI) following the administration of contrast media remains one of the main aetiological factors of AKI in-hospital while the exact pathophysiological mechanisms of injury propagation along the nephron remain unclear. This chapter aimed to investigate whether the method developed in Chapter 3 could track changes in nephron-specific urinary exosomes in a patient group exposed to contrast media as a model of AKI and how this would relate to established kidney injury markers, KIM-1 or NGAL. Secondly, this chapter also aimed to discover whether NTA measurements of nephron-specific protein-exosome populations could provide some insights into the role exosomes may play during the development or progression of kidney injury along the nephron.

Patient urine samples were obtained from a patient group exposed to contrast media, a known cause of AKI, pre- and post-exposure. The significant differences seen in urinary creatinine values pre- and post-exposure negated the use of urinary creatinine as an analyte and concentration normaliser for subsequent analyses in this study and also highlighted the importance of developing and refining a viable and more applicable urinary normaliser to lessen the variation usually seen and associated with urine analyses. The standard biomarkers of AKI, KIM-1 and NGAL both significantly increased in the whole study group 24 hours post-exposure. KIM-1 however, also showed a significant increase 72 hours post-exposure to contrast media, which was not mirrored by NGAL. The increase in NGAL 24 hours post-exposure, however, served to confirm NGAL as an early marker for AKI[190].

KIM-1 is released from the proximal tubules only during injury and the increase in KIM-1 across the whole study group confirmed that contrast media exposure may exert its damaging nephrotoxic effects through direct proximal tubule damage[191]. The evidence on KIM-1 as a biomarker of CI-AKI is limited with varying conclusions, but urinary KIM-1 levels have been shown to increase 12 hours following CM administration[229]. NGAL has been shown to be upregulated in kidney tubules during ischemic AKI and is seen as an indicator of kidney damage, showing an increase even 6 hours post-CM administration[230]. Additionally, NGAL has been suggested as

a therapeutic agent, through its protective or regenerative role in AKI by induced proliferation and inhibition of apoptosis of tubule epithelial cells[188]. Despite the numerous studies showing the biomarker potential of both KIM-1 and NGAL in CI-AKI, there is still limitations that preclude their clinical utility as they do not provide information of injury or injury propagation for the whole nephron, with KIM-1 localised to the proximal tubules and NGAL to distal tubular segments of the injured nephron[231]. Attempting to address these limitations, a combination, or panel, of these two biomarkers and the concomitant relationships with the panel of nephron-specific exosome proteins would therefore potentially provide information of tubular damage but also disease propagation along the nephron in an AKI model.

Patient samples were analysed for glomerular/podocyte (PODXL), proximal- (CU) – and distal tubular (NCC), collecting duct (AQP2) and overall tubular (CD24) - positive particles in the exosome size range of 20 - 100 nm by NTA quantification of antibody-specific fluorescently labelled particles. To investigate how NTA measurements of the panel of nephron-specific protein-exosome conjugates would compare to KIM-1 and NGAL as standard biomarkers of kidney injury, small but significant relationships were found, with podocalyxin-like protein correlating with both KIM-1 and NGAL. The significant correlation of the podocalyxin-like protein with both biomarkers as opposed to only one provided confidence which was further confirmed by podocalyxin-like protein showing significant differences between low and high biomarker tertile groups post-exposure, for both KIM-1 and NGAL.

The positive correlation of the podocyte/glomerular marker (podocalyxin-like protein) with both AKI biomarkers, KIM-1 and NGAL, supports previous findings in Chapter 4 indicating increased exosome uptake in physiological states. In pathophysiological states, such as CM-induced AKI, the inverse should hypothetically be true with a decrease in exosome uptake along the nephron. Alternatively, this positive relationship of podocalyxin-like protein with the AKI biomarkers may indicate possible podocyte involvement during contrast media induced AKI. The understanding however is currently limited, but emerging research suggests the protective role podocytes play in injury progression[232,233] and

podocalyxin-like protein being shown to be an indicator of the severity of disease and disease progression in AKI[234].

In this chapter it was demonstrated that NTA can rapidly quantify nephron-specific exosome populations in a patient group with increases comparable to other standardised biomarkers of AKI. Podocalyxin-like protein, as a podocyte marker, showed a relationship with two biomarkers of AKI, possibly providing more information of exosome uptake along the nephron in an AKI model, but also potentially highlighting glomerular involvement during contrast media induced AKI. This warrants further development and refinement, to not only develop podocalyxin-like protein exosomes as a biomarker of AKI, but to provide further explanation of the exosomal mechanisms involved with disease propagation along the nephron.

CHAPTER 7

Conclusions

The studies presented in this thesis aimed to better understand the role of exosomes in inter-cellular signalling in physiological and pathophysiological states in the kidney, both through the development of a new urinary exosome quantification method and investigating the hormonal regulation of exosome uptake in the collecting duct, *in vitro* and *in vivo*. The potential role of nephron segment-specific exosomes was also elucidated in an acute kidney injury model, highlighting the potential of urinary exosomes as biomarkers of kidney disease.

7.1 Urinary exosome quantification using NTA

The studies in Chapter 3, showed the development of a method for rapidly quantifying urinary exosomes. We were able to demonstrate that NTA can be used as a method to quantify exosome-sized particles in whole urine samples. Combining the fluorescent capabilities of NTA with an antibody-specific fluorescent labelling system reduced intra-assay variability, but also provided evidence that NTA can be used to differentially track exosome populations through the use of nephron segment specific antibodies. Furthermore, by using this newly developed method of urinary exosome quantification, we were able to show changes in AQP2 expression *in vitro* and *in vivo*, similar to previous findings relying on more standard methods of exosome quantification such as Western blotting[45]. Supporting this cell culture and rodent data, we were able to show that this method was able to rapidly track changes in AQP2 levels in a diabetes insipidus patient. The newly developed method further corroborated challenges within the field by highlighting the need for optimised and standardised methods of exosome isolation. Indeed, comparing the yield from two standard isolation methods: ultracentrifugation and ExoQuick™, revealed a large number of non-exosomal particles. This finding supports other research which showed that ExoQuick™ may also precipitate non-exosomal particles, larger proteins and aggregates and yield an altogether less pure exosome pellet[159]. NTA was also used to evaluate storage methods for urinary exosomes and revealed -80°C to be the optimal temperature for storage of whole urine samples, resulting in preservation of an increased total number of urinary exosomes, consistent with previous work[203].

7.2 Vasopressin regulation of exosome uptake

The studies in Chapter 4 and 5 were aimed at understanding the hormonal regulation of exosome uptake in the collecting duct to potentially better define the role of exosomes in inter-cellular signalling in the kidney and elucidate the underlying mechanisms involved. In collecting duct cells, the role of vasopressin, as a hormonal regulator of exosome uptake was demonstrated for the first time. Using 4 different read-outs of exosome uptake – fluorescent microscopy, flow cytometry and miRNA transfer into cells, combined with NTA of the labelled exosomes remaining in the cell culture supernatant, consistently showed that desmopressin stimulation of collecting duct cells stimulated exosome uptake. Furthermore, we were able to demonstrate that the mechanism is V2-receptor mediated and cAMP/PKA dependent, which is in keeping with the established physiological pathway of vasopressin stimulation on the principal cells of the collecting duct[176]. Exosomes isolated from different cell types had different uptake patterns into collecting duct cells. Combining these data with the opposing effect endothelin-1 had on exosome uptake compared to desmopressin stimulation, suggests that exosome uptake in cells is a tightly regulated, cell type specific process. To investigate whether vasopressin regulates exosome uptake *in vivo*, we were able to show systemic exosome uptake in a mouse model by measuring urinary output using NTA. Exosome excretion could be increased by inhibition of the V2 receptor, increasing the exosome recovery in the urine from 2% - 25%. This finding of systemically injected exosomes appearing in the urine is important for two reasons. First, investigators performing proteomic and transcriptomic analysis of urinary exosomes cannot assume that new biomarkers have originated from the kidney, and urinary non-renal exosomes may offer a non-invasive way to assess the physiology and pathology on other (non-renal) organs. Second, the presence of plasma-derived exosomes in urine provides proof-of-concept that systemically administered novel therapeutic interventions, delivered within exosomes, could gain access to renal tubules. By using a clinical case study of a diabetes insipidus patient, we were able to track changes in urinary exosome populations following exogenous desmopressin administration. By using NTA combined with antibody-specific fluorescent tags, a decrease in upstream exosomes, i.e glomerular and proximal tubular occurred, suggesting decreased uptake in the

downstream tubules. These data are therefore consistent with our cell and mouse data revealing exosome uptake to be regulated by vasopressin.

7.3 Quantification of nephron-specific human urinary exosomes in acute kidney injury

In Chapter 6, in a cohort of patients treated with contrast media – a known cause of acute kidney injury - we were able to measure exosome populations from all different segments of the nephron using antibody specific NTA. In this chapter it was demonstrated that NTA can rapidly quantify nephron-specific exosome populations in this patient group. Podocalyxin-like protein, a podocyte-specific marker, was shown to correlate with two standard biomarkers of AKI: KIM-1 and NGAL. The biomarker potential of podocalyxin-like protein has been shown in a number of diseases, including bladder and colorectal cancer[235] and diabetic nephropathy[236]. Additionally, podocalyxin-like protein was shown to be increased in during the recovery phase of AKI[232]. Our findings therefore possibly provides more information of exosome uptake along the nephron in pathophysiological states such as AKI, but may also highlight glomerular involvement during contrast media induced AKI.

7.4 Future work

The findings of the studies in this thesis have raised further questions that need to be answered and will be discussed below.

7.4.1 Nomenclature of exosomes

Despite the exponential increase in exosome research efforts, correct and definitive nomenclature of an ‘exosome’ remains unclear and contentious. Recent guidelines from within the field have attempted to address this by setting a number of minimal requirements for defining an extracellular vesicle as an ‘exosome’[1]. Within the scope of those guidelines we have endeavoured to define our population of vesicles based on their size predominantly, but also by surface markers known to be expressed on exosomal membranes, for example CD24 as a surface marker of urinary exosomes[31]. By using this approach we were able to develop a new method of rapidly tracking

changes in specific exosome populations, relevant to specific changes in the cell of origin. Development of this method will further the development of urinary exosomes as a biomarker of kidney injury and disease, but will undoubtedly be met with comparisons to more standard and time consuming methods of exosome quantification such as Western blotting. Therefore, it would be interesting to further develop NTA by using recent advances in other technologies as a complimentary approach to better define our vesicle population. Indeed, increased transmission electron microscopy capabilities should theoretically allow direct visualisation of an exosome containing our chosen fluorescent Cell Tracker™ quantum dots[237]. Similarly, increased confocal microscopy capabilities allow real-time visualisation of exosome uptake[134,204]. Combined, these advances should benefit the clear definition of an exosome and strengthen the relevancy of antibody-specific NTA to quantify exosomes within the field.

7.4.2 Internal control for NTA quantification

The development of tracking specific urinary exosome populations using antibody-specific NTA holds great potential for rapidly quantifying changes in exosome concentrations. This may further develop urinary exosomes as a biomarker of kidney disease, but may also provide more information about the underlying physiological mechanisms of exosome-mediated cell signalling. We were able to discriminately track specific exosome populations. Whilst the measurements were comparable to changes measured by other standardised methods as highlighted in Chapter 3, development of an internal control will greatly refine and reduce the variability seen with this method. Currently, urinary creatinine is the standard normaliser for analyte concentration differences in urine. The assumption, however, that urinary creatinine remains constant between individuals is not true, indeed studies have shown the inter-assay variability of urinary creatinine values to be between 10 to 14% between individuals with marked diurnal variation[238]. Our findings supported this by revealing that urinary creatinine values were variable between our test volunteers even within a relatively similar demographic background with the data further suggesting urinary creatinine as a read-out of renal function[239], might not be an applicable normaliser for changes in nephron segment-specific exosome release. A

normaliser is, however, crucial to account for differences in spot urine concentration. A possible approach would be to develop a panel of potential biomarkers of AKI and measuring quantitative and relative abundances across the panel, which will in theory, provide both absolute data regarding kidney function and information of the underlying inter-cellular communication and propagation of disease along the nephron. A second possible approach for this challenge would be the identification and development of an internal control – for example CD24 as a pan-tubular marker, which could provide a baseline value to correct for concentration differences. Whether this exists in urinary exosomes, however, remains elusive.

7.4.3 Pharmacological inhibitors of endocytosis

The studies presented here provided a clathrin-dependent endocytic inhibition approach. Indeed by using Dynasore, described as an inhibitor of dynamin – a large GTPase necessary for clathrin-coated pit formation - we were able to demonstrate a significant decrease in exosome uptake even below that of the control, unstimulated cells (Chapter 4). Recently, however, Dynasore was also reported to inhibit lipid-raft organisation, a different endocytic pathway[240]. The use of pharmacological agents as inhibitors of the endocytic pathway will always be contentious with challenges of sensitivity and specificity coupled with unknown off-target effects[241]. The next step would be to include a variety of different pharmacological inhibitors for all the different endocytic pathways identified: clathrin-mediated, lipid raft/caveolae-mediated endocytosis and macropinocytosis/phagocytosis, and measure not only their effect on exosome uptake but also on the function and structure of our specific cell type. For instance, by using amiloride as an inhibitor of macropinocytosis there was a large amount of cell death. To further address the challenges associated with the use of pharmacological inhibitors of endocytic pathways, a more specific approach may be the use of short-interfering RNA (siRNA) that could knockdown expression of proteins known to be involved with endocytosis such as clathrin heavy chain (CLTC), caveolin-1, and Rab34, respectively[242]. Once this method is better defined, it could potentially open exciting avenues of targeting exosome uptake and subsequent exosomal content delivery to a specific cell.

7.4.4 Targeted functional exosome uptake

We were able to show hormonal regulation of exosome uptake in the collecting duct *in vitro* and *in vivo*. Subsequently, we were able to identify a possible mechanism involved with exosome uptake and showed it to be consistent with vasopressin action of plasma membrane endocytosis and vesicle shuttling inside the principal cells of the collecting duct[176]. However, it would be interesting to elucidate how exosomes preferentially target cells for uptake in the kidney – as we demonstrated different exosome uptake patterns from different cell type derived exosomes. Previous studies have reported exosome uptake to be dependent on the protein signature of the vesicle coupled with the signalling status of receptors on the recipient cell[128,243,244]. Recent improvements in available techniques will allow us to visually track exosome uptake in real-time whilst providing more quantitative read-outs in terms of increased flow cytometry capabilities and combined, should provide a better understanding of the interaction between exosome and recipient cell. A better understanding will provide evidence of the role of exosomes in physiological and pathophysiological states. The majority of exosome research efforts are currently centred on pathophysiological states. It is therefore crucial to employ these methods to investigate whether exosome uptake is functionally relevant in a physiological state and the mechanisms involved. Understanding exosome uptake physiologically, will help to better target exosomes as therapeutic agents – delivering specific content to a defined site of action.

7.4.5 Podocalyxyin-like protein as biomarker of AKI

Contrast media exposure have been shown to be a direct cause of AKI specifically through its nephrotoxic effects on the renal tubular cells[245]. Using our newly developed method of antibody-specific NTA, we however, found podocalyxin-like protein as a podocyte specific marker, to be well correlated with both KIM-1 and NGAL as standard biomarkers of AKI. It may suggest we were able to track propogation of AKI along the nephron by increased podocalyxin-like protein indicating recovery from AKI in a previous study[236] and may similarly suggest tubular injury leading to reduced exosome uptake capabilities of downstream segments of the nephron. This, however, needs to be elucidated. It is important to

consider as caveats not only the small patient group, but also the researchers still being blinded to the patient outcome at time of study. Whether stratification of patients into groups who ultimately developed AKI would provide further information or a different exosomal pattern remains to be elucidated.

The development of urinary exosomes as not only a biomarker, but also as a therapeutic agent in kidney disease is an exciting and valuable field to focus research efforts. To exploit this inherent potential in pathophysiological states, it is crucial to understand the role exosomes play in intercellular signalling in physiological states. The work presented in this thesis has highlighted the limitations and challenges related to exosome research and have addressed this with the development of a new, rapid method of exosome quantification. Furthermore, the work has also showed physiological regulation of exosome uptake in the kidney collecting duct by vasopressin stimulation and has elucidated the mechanism involved. Combined with exosome secretion in an AKI model, this provide a clearer understanding of regulation of exosome uptake along the nephron in both physiological and pathophysiological states and should support further research within the field of urinary exosomes.

REFERENCES

1. Lötvall, J. O. *et al.* Minimal experimental requirements for definition of extracellular vesicles and their functions: a position statement from the International Society for Extracellular Vesicles. *J. Extracell. Vesicles* **3,** (2014).

2. Van Niel, G. *et al.* Intestinal epithelial cells secrete exosome-like vesicles. *Gastroenterology* **121,** 337–349 (2001).

3. Van Balkom, B. W. M., Pisitkun, T., Verhaar, M. C. & Knepper, M. A. Exosomes and the kidney: prospects for diagnosis and therapy of renal diseases. *Kidney Int.* **80,** 1138–1145 (2011).

4. Mittelbrunn, M. *et al.* Unidirectional transfer of microRNA-loaded exosomes from T cells to antigen-presenting cells. *Nat. Commun.* **2,** 282 (2011).

5. Caby, M.-P., Lankar, D., Vincendeau-Scherrer, C., Raposo, G. & Bonnerot, C. Exosomal-like vesicles are present in human blood plasma. *Int. Immunol.* **17,** 879–887 (2005).

6. Almqvist, N., Lonnqvist, A., Hultkrantz, S., Rask, C. & Telemo, E. Serum-derived exosomes from antigen-fed mice prevent allergic sensitization in a model of allergic asthma. *Immunology* **125,** 21–27 (2008).

7. Lässer, C. *et al.* Human saliva, plasma and breast milk exosomes contain RNA: uptake by macrophages. *J. Transl. Med.* **9,** 9 (2011).

8. Pisitkun, T., Shen, R.-F. & Knepper, M. A. Identification and proteomic profiling of exosomes in human urine. *Proc. Natl. Acad. Sci. U. S. A.* **101,** 13368–13373 (2004).

9. Thery, C. *et al.* Molecular Characterization of Dendritic Cell-Derived Exosomes. *J. Cell Biol.* **147,** 599–610 (1999).

10. Rana, S., Malinowska, K. & Zoller, M. Exosomal Tumor MicroRNA Modulates Premetastatic Organ Cells. *Neoplasia N. Y. N* **15,** 281–295 (2013).

11. Stoorvogel, W., Kleijmeer, M. J., Geuze, H. J. & Raposo, G. The biogenesis and functions of exosomes. *Traffic Cph. Den.* **3,** 321–330 (2002).

12. Théry, C., Zitvogel, L. & Amigorena, S. Exosomes: composition, biogenesis and function. *Nat. Rev. Immunol.* **2,** 569–579 (2002).

13. Bobrie, A., Colombo, M., Raposo, G. & Théry, C. Exosome secretion: molecular mechanisms and roles in immune responses. *Traffic Cph. Den.* **12,** 1659–1668 (2011).

14. Raposo, G. & Stoorvogel, W. Extracellular vesicles: Exosomes, microvesicles, and friends. *J. Cell Biol.* **200,** 373–383 (2013).

15. Lobb, R. J. *et al.* Optimized exosome isolation protocol for cell culture supernatant and human plasma. *J. Extracell. Vesicles* **4,** (2015).

16. Musante, L., Saraswat, M., Ravidà, A., Byrne, B. & Holthofer, H. Recovery of urinary nanovesicles from ultracentrifugation supernatants. *Nephrol. Dial. Transplant.* **28,** 1425–1433 (2013).

17. Kalra, H. *et al.* Comparative proteomics evaluation of plasma exosome isolation techniques and assessment of the stability of exosomes in normal human blood plasma. *Proteomics* **13,** 3354–3364 (2013).

18. Lamparski, H. G. *et al.* Production and characterization of clinical grade exosomes derived from dendritic cells. *J. Immunol. Methods* **270,** 211–226 (2002).

19. Liga, A., Vliegenthart, A. D. B., Oosthuyzen, W., Dear, J. W. & Kersaudy-Kerhoas, M. Exosome isolation: a microfluidic road-map. *Lab. Chip* **15,** 2388–2394 (2015).

20. Muller, L., Hong, C.-S., Stolz, D. B., Watkins, S. C. & Whiteside, T. L. Isolation of biologically-active exosomes from human plasma. *J. Immunol. Methods* **411,** 55–65 (2014).

21. Cheruvanky, A. *et al.* Rapid isolation of urinary exosomal biomarkers using a nanomembrane ultrafiltration concentrator. *Am. J. Physiol. Renal Physiol.* **292,** F1657–F1661 (2007).

22. Nordin, J. Z. *et al.* Ultrafiltration with size-exclusion liquid chromatography for high yield isolation of extracellular vesicles preserving intact biophysical and functional properties. *Nanomedicine Nanotechnol. Biol. Med.* **11,** 879–883 (2015).

23. Rood, I. M. *et al.* Comparison of three methods for isolation of urinary microvesicles to identify biomarkers of nephrotic syndrome. *Kidney Int.* **78,** 810–816 (2010).

24. Théry, C., Amigorena, S., Raposo, G. & Clayton, A. in *Current Protocols in Cell Biology* (John Wiley & Sons, Inc., 2001).

25. Van Deun, J. *et al.* The impact of disparate isolation methods for extracellular vesicles on downstream RNA profiling. *J. Extracell. Vesicles* **3,** (2014).

26. Huang, X. *et al.* Characterization of human plasma-derived exosomal RNAs by deep sequencing. *BMC Genomics* **14,** 319 (2013).

27. Zubiri, I. *et al.* Diabetic nephropathy induces changes in the proteome of human urinary exosomes as revealed by label-free comparative analysis. *J. Proteomics* **96,** 92–102 (2014).

28. Park, J. & Choi, Y. Exosome identification for personalized diagnosis and therapy. *Biomed. Eng. Lett.* **4,** 258–268 (2014).

29. Im, H. *et al.* Label-free detection and molecular profiling of exosomes with a nano-plasmonic sensor. *Nat. Biotechnol.* **32,** 490–495 (2014).

30. Fevrier, B. *et al.* Cells release prions in association with exosomes. *Proc. Natl. Acad. Sci. U. S. A.* **101,** 9683–9688 (2004).

31. Keller, S. *et al.* CD24 is a marker of exosomes secreted into urine and amniotic fluid. *Kidney Int.* **72,** 1095–1102 (2007).

32. Tian, T., Wang, Y., Wang, H., Zhu, Z. & Xiao, Z. Visualizing of the cellular uptake and intracellular trafficking of exosomes by live-cell microscopy. *J. Cell. Biochem.* **111,** 488–496 (2010).

33. Suetsugu, A. *et al.* Imaging exosome transfer from breast cancer cells to stroma at metastatic sites in orthotopic nude-mouse models. *Adv. Drug Deliv. Rev.* **65,** 383–390 (2013).

34. Dragovic, R. A. *et al.* Sizing and phenotyping of cellular vesicles using Nanoparticle Tracking Analysis. *Nanomedicine Nanotechnol. Biol. Med.* **7,** 780–788 (2011).

35. Gardiner, C., Ferreira, Y. J., Dragovic, R. A., Redman, C. W. G. & Sargent, I. L. Extracellular vesicle sizing and enumeration by nanoparticle tracking analysis. *J. Extracell. Vesicles* **2,** (2013).

36. Mathivanan, S. & Simpson, R. J. ExoCarta: A compendium of exosomal proteins and RNA. *Proteomics* **9,** 4997–5000 (2009).

37. Gonzales, P. A. *et al.* Large-Scale Proteomics and Phosphoproteomics of Urinary Exosomes. *J. Am. Soc. Nephrol.* **20,** 363–379 (2009).

38. Kowal, J., Tkach, M. & Théry, C. Biogenesis and secretion of exosomes. *Curr. Opin. Cell Biol.* **29,** 116–125 (2014).

39. Conde-Vancells, J. *et al.* Characterization and Comprehensive Proteome Profiling of Exosomes Secreted by Hepatocytes. *J. Proteome Res.* **7,** 5157–5166 (2008).

40. Laulagnier, K. *et al.* Mast cell- and dendritic cell-derived exosomes display a specific lipid composition and an unusual membrane organization. *Biochem. J.* **380,** 161–171 (2004).

41. Wubbolts, R. *et al.* Proteomic and Biochemical Analyses of Human B Cell-derived Exosomes POTENTIAL IMPLICATIONS FOR THEIR FUNCTION AND MULTIVESICULAR BODY FORMATION. *J. Biol. Chem.* **278,** 10963–10972 (2003).

42. De Jong, O. G. *et al.* Cellular stress conditions are reflected in the protein and RNA content of endothelial cell-derived exosomes. *J. Extracell. Vesicles* **1,** (2012).

43. Rastaldi, M. P. *et al.* Glomerular podocytes possess the synaptic vesicle molecule Rab3A and its specific effector rabphilin-3a. *Am. J. Pathol.* **163,** 889–899 (2003).

44. Street, J. M. *et al.* Exosomal transmission of functional aquaporin 2 in kidney cortical collecting duct cells. *J. Physiol.* **589,** 6119–6127 (2011).

45. Yang, J. C.-S. *et al.* Altered exosomal protein expression in the serum of NF-κB knockout mice following skeletal muscle ischemia-reperfusion injury. *J. Biomed. Sci.* **22,** 40 (2015).

46. Colombo, M., Raposo, G. & Théry, C. Biogenesis, Secretion, and Intercellular Interactions of Exosomes and Other Extracellular Vesicles. *Annu. Rev. Cell Dev. Biol.* **30,** 255–289 (2014).

47. Record, M., Carayon, K., Poirot, M. & Silvente-Poirot, S. Exosomes as new vesicular lipid transporters involved in cell-cell communication and various pathophysiologies. *Biochim. Biophys. Acta* **1841,** 108–120 (2014).

48. Carayon, K. *et al.* Proteolipidic Composition of Exosomes Changes during Reticulocyte Maturation. *J. Biol. Chem.* **286,** 34426–34439 (2011).

49. Valadi, H. *et al.* Exosome-mediated transfer of mRNAs and microRNAs is a novel mechanism of genetic exchange between cells. *Nat. Cell Biol.* **9,** 654–659 (2007).

50. Zomer, A. *et al.* Exosomes. *Commun. Integr. Biol.* **3,** 447–450 (2010).

51. Pegtel, D. M. *et al.* Functional delivery of viral miRNAs via exosomes. *Proc. Natl. Acad. Sci.* **107,** 6328–6333 (2010).

52. Ekström, K. *et al.* Characterization of mRNA and microRNA in human mast cell-derived exosomes and their transfer to other mast cells and blood CD34 progenitor cells. *J. Extracell. Vesicles* **1,** (2012).

53. Van Balkom, B. W. M., Eisele, A. S., Pegtel, D. M., Bervoets, S. & Verhaar, M. C. Quantitative and qualitative analysis of small RNAs in human endothelial cells and exosomes provides insights into localized RNA processing, degradation and sorting. *J. Extracell. Vesicles* **4,** 26760 (2015).

54. Batagov, A. O. & Kurochkin, I. V. Exosomes secreted by human cells transport largely mRNA fragments that are enriched in the 3′-untranslated regions. *Biol. Direct* **8,** 12 (2013).

55. Alvarez, S. *et al.* Urinary exosomes as a source of kidney dysfunction biomarker in renal transplantation. *Transplant. Proc.* **45,** 3719–3723 (2013).

56. Villarroya-Beltri, C. *et al.* Sumoylated hnRNPA2B1 controls the sorting of miRNAs into exosomes through binding to specific motifs. *Nat. Commun.* **4,** 2980 (2013).

57. Guay, C., Menoud, V., Rome, S. & Regazzi, R. Horizontal transfer of exosomal microRNAs transduce apoptotic signals between pancreatic beta-cells. *Cell Commun. Signal.* **13,** 17 (2015).

58. Eldh, M. *et al.* Exosomes Communicate Protective Messages during Oxidative Stress; Possible Role of Exosomal Shuttle RNA. *PLoS ONE* **5,** e15353 (2010).

59. Chevillet, J. R. *et al.* Quantitative and stoichiometric analysis of the microRNA content of exosomes. *Proc. Natl. Acad. Sci.* **111,** 14888–14893 (2014).

60. Turchinovich, A., Weiz, L., Langheinz, A. & Burwinkel, B. Characterization of extracellular circulating microRNA. *Nucleic Acids Res.* **39,** 7223–7233 (2011).

61. Arroyo, J. D. *et al.* Argonaute2 complexes carry a population of circulating microRNAs independent of vesicles in human plasma. *Proc. Natl. Acad. Sci. U. S. A.* **108,** 5003–5008 (2011).

62. Johnstone, R. M., Adam, M., Hammond, J. R., Orr, L. & Turbide, C. Vesicle formation during reticulocyte maturation. Association of plasma membrane activities with released vesicles (exosomes). *J. Biol. Chem.* **262,** 9412–9420 (1987).

63. Szabo, G. & Bala, S. MicroRNAs in liver disease. *Nat. Rev. Gastroenterol. Hepatol.* **10,** 542–552 (2013).

64. Guescini, M. *et al.* C2C12 myoblasts release micro-vesicles containing mtDNA and proteins involved in signal transduction. *Exp. Cell Res.* **316,** 1977–1984 (2010).

65. Zhang, B., Asadi, S., Weng, Z., Sismanopoulos, N. & Theoharides, T. C. Stimulated Human Mast Cells Secrete Mitochondrial Components That Have Autocrine and Paracrine Inflammatory Actions. *PLoS ONE* **7,** (2012).

66. Thakur, B. K. *et al.* Double-stranded DNA in exosomes: a novel biomarker in cancer detection. *Cell Res.* **24,** 766–769 (2014).

67. Kahlert, C. *et al.* Identification of Double-stranded Genomic DNA Spanning All Chromosomes with Mutated KRAS and p53 DNA in the Serum Exosomes of Patients with Pancreatic Cancer. *J. Biol. Chem.* **289,** 3869–3875 (2014).

68. Montermini, L. *et al.* Inhibition of Oncogenic Epidermal Growth Factor Receptor Kinase Triggers Release of Exosome-like Extracellular Vesicles and Impacts Their Phosphoprotein and DNA Content. *J. Biol. Chem.* **290,** 24534–24546 (2015).

69. Melo, S. A. *et al.* Glypican-1 identifies cancer exosomes and detects early pancreatic cancer. *Nature* **523,** 177–182 (2015).

70. Campanella, C. *et al.* Heat shock protein 60 levels in tissue and circulating exosomes in human large bowel cancer before and after ablative surgery. *Cancer* **121,** 3230–3239 (2015).

71. Qazi, K. R. *et al.* Proinflammatory exosomes in bronchoalveolar lavage fluid of patients with sarcoidosis. *Thorax* (2010).

72. Goetzl, E. J. *et al.* Altered lysosomal proteins in neural-derived plasma exosomes in preclinical Alzheimer disease. *Neurology* (2015).

73. Tomlinson, P. R. *et al.* Identification of distinct circulating exosomes in Parkinson's disease. *Ann. Clin. Transl. Neurol.* **2,** 353–361 (2015).

74. Zhou, H. *et al.* Exosomal Fetuin-A identified by proteomics: a novel urinary biomarker for detecting acute kidney injury. *Kidney Int.* **70,** 1847–1857 (2006).

75. Kalani, A. *et al.* Wilm's tumor-1 protein levels in urinary exosomes from diabetic patients with or without proteinuria. *PloS One* **8,** e60177 (2013).

76. Khan, S. *et al.* Plasma-Derived Exosomal Survivin, a Plausible Biomarker for Early Detection of Prostate Cancer. *PLoS ONE* **7,** (2012).

77. Szajnik, M. *et al.* Exosomes in Plasma of Patients with Ovarian Carcinoma: Potential Biomarkers of Tumor Progression and Response to Therapy. *Gynecol. Obstet. Sunnyvale Calif* **Suppl 4,** 3 (2013).

78. Guan, M. *et al.* MDA-9 and GRP78 as potential diagnostic biomarkers for early detection of melanoma metastasis. *Tumour Biol. J. Int. Soc. Oncodevelopmental Biol. Med.* **36,** 2973–2982 (2015).

79. Madhavan, B. *et al.* Combined evaluation of a panel of protein and miRNA serum-exosome biomarkers for pancreatic cancer diagnosis increases sensitivity and specificity. *Int. J. Cancer* **136,** 2616–2627 (2015).

80. Olimón-Andalón, V. *et al.* Proapoptotic CD95L levels in normal human serum and sera of breast cancer patients. *Tumour Biol. J. Int. Soc. Oncodevelopmental Biol. Med.* **36,** 3669–3678 (2015).

81. Yang, J., Wei, F., Schafer, C. & Wong, D. T. W. Detection of Tumor Cell-Specific mRNA and Protein in Exosome-Like Microvesicles from Blood and Saliva. *PLoS ONE* **9,** (2014).

82. Sivadasan, P. *et al.* Human salivary proteome — a resource of potential biomarkers for oral cancer. *J. Proteomics* **127, Part A,** 89–95 (2015).

83. Lau, C. *et al.* Role of pancreatic cancer-derived exosomes in salivary biomarker development. *J. Biol. Chem.* **288,** 26888–26897 (2013).

84. Choi, D.-S., Kim, D.-K., Kim, Y.-K. & Gho, Y. S. Proteomics of extracellular vesicles: Exosomes and ectosomes. *Mass Spectrom. Rev.* n/a–n/a (2014). doi:10.1002/mas.21420

85. Ho, D. H., Yi, S., Seo, H., Son, I. & Seol, W. Increased DJ-1 in urine exosome of Korean males with Parkinson's disease. *BioMed Res. Int.* **2014,** 704678 (2014).

86. Van der Lubbe, N. *et al.* The phosphorylated sodium chloride cotransporter in urinary exosomes is superior to prostasin as a marker for aldosteronism. *Hypertension* **60,** 741–748 (2012).

87. Trnka, P., Ivanova, L., Hiatt, M. J. & Matsell, D. G. Urinary biomarkers in obstructive nephropathy. *Clin. J. Am. Soc. Nephrol. CJASN* **7,** 1567–1575 (2012).

88. Sun, A. *et al.* Dipeptidyl peptidase-IV is a potential molecular biomarker in diabetic kidney disease. *Diab. Vasc. Dis. Res.* **9,** 301–308 (2012).

89. Jenjaroenpun, P. *et al.* Characterization of RNA in exosomes secreted by human breast cancer cell lines using next-generation sequencing. *PeerJ* **1,** e201 (2013).

90. Shao, H. *et al.* Chip-based analysis of exosomal mRNA mediating drug resistance in glioblastoma. *Nat. Commun.* **6,** (2015).

91. Skog, J. *et al.* Glioblastoma microvesicles transport RNA and protein that promote tumor growth and provide diagnostic biomarkers. *Nat. Cell Biol.* **10,** 1470–1476 (2008).

92. Xiao, D. *et al.* Identifying mRNA, MicroRNA and Protein Profiles of Melanoma Exosomes. *PLoS ONE* **7,** e46874 (2012).

93. Spanu, S., van Roeyen, C. R. C., Denecke, B., Floege, J. & Mühlfeld, A. S. Urinary Exosomes: A Novel Means to Non-Invasively Assess Changes in Renal Gene and Protein Expression. *PLoS ONE* **9,** e109631 (2014).

94. Lv, L.-L. *et al.* CD2AP mRNA in urinary exosome as biomarker of kidney disease. *Clin. Chim. Acta Int. J. Clin. Chem.* **428,** 26–31 (2014).

95. Manterola, L. *et al.* A small noncoding RNA signature found in exosomes of GBM patient serum as a diagnostic tool. *Neuro-Oncol.* **16,** 520–527 (2014).

96. Li, Q. *et al.* Plasma long noncoding RNA protected by exosomes as a potential stable biomarker for gastric cancer. *Tumour Biol. J. Int. Soc. Oncodevelopmental Biol. Med.* **36,** 2007–2012 (2015).

97. Matsumura, T. *et al.* Exosomal microRNA in serum is a novel biomarker of recurrence in human colorectal cancer. *Br. J. Cancer* **113,** 275–281 (2015).

98. Bala, S. *et al.* Circulating microRNAs in exosomes indicate hepatocyte injury and inflammation in alcoholic, drug-induced, and inflammatory liver diseases. *Hepatol. Baltim. Md* **56,** 1946–1957 (2012).

99. Lv, L.-L. *et al.* MicroRNA-29c in urinary exosome/microvesicle as a biomarker of renal fibrosis. *Am. J. Physiol. Renal Physiol.* **305,** F1220–1227 (2013).

100. Hornick, N. I. *et al.* Serum Exosome MicroRNA as a Minimally-Invasive Early Biomarker of AML. *Sci. Rep.* **5,** 11295 (2015).

101. Tanaka, Y. *et al.* Clinical impact of serum exosomal microRNA-21 as a clinical biomarker in human esophageal squamous cell carcinoma. *Cancer* **119,** 1159–1167 (2013).

102. Barutta, F. *et al.* Urinary Exosomal MicroRNAs in Incipient Diabetic Nephropathy. *PLoS ONE* **8,** (2013).

103. Gallagher, I. J. *et al.* Integration of microRNA changes in vivo identifies novel molecular features of muscle insulin resistance in type 2 diabetes. *Genome Med.* **2,** 9 (2010).

104. Perez-Hernandez, J. *et al.* Increased Urinary Exosomal MicroRNAs in Patients with Systemic Lupus Erythematosus. *PloS One* **10,** (2015).

105. Li, Y. *et al.* Identification of Endogenous Controls for Analyzing Serum Exosomal miRNA in Patients with Hepatitis B or Hepatocellular Carcinoma, Identification of Endogenous Controls for Analyzing Serum Exosomal miRNA in Patients with Hepatitis B or Hepatocellular Carcinoma. *Dis. Markers Dis. Markers* **2015, 2015,** e893594 (2015).

106. Sugimachi, K. *et al.* Identification of a bona fide microRNA biomarker in serum exosomes that predicts hepatocellular carcinoma recurrence after liver transplantation. *Br. J. Cancer* **112,** 532–538 (2015).

107. Wang, H. *et al.* Expression of serum exosomal microRNA-21 in human hepatocellular carcinoma. *BioMed Res. Int.* **2014,** 864894 (2014).

108. Eichelser, C. *et al.* Increased serum levels of circulating exosomal microRNA-373 in receptor-negative breast cancer patients. *Oncotarget* **5,** 9650–9663 (2014).

109. Chiam, K. *et al.* Circulating Serum Exosomal miRNAs As Potential Biomarkers for Esophageal Adenocarcinoma. *J. Gastrointest. Surg. Off. J. Soc. Surg. Aliment. Tract* **19,** 1208–1215 (2015).

110. Wang, J. *et al.* Combined detection of serum exosomal miR-21 and HOTAIR as diagnostic and prognostic biomarkers for laryngeal squamous cell carcinoma. *Med. Oncol. Northwood Lond. Engl.* **31,** 148 (2014).

111. Alegre, E. *et al.* Study of circulating microRNA-125b levels in serum exosomes in advanced melanoma. *Arch. Pathol. Lab. Med.* **138,** 828–832 (2014).

112. Povero, D. *et al.* Circulating Extracellular Vesicles with Specific Proteome and Liver MicroRNAs Are Potential Biomarkers for Liver Injury in Experimental Fatty Liver Disease. *PLoS ONE* **9,** (2014).

113. Lugli, G. *et al.* Plasma Exosomal miRNAs in Persons with and without Alzheimer Disease: Altered Expression and Prospects for Biomarkers. *PloS One* **10,** e0139233 (2015).

114. Huang, X. *et al.* Exosomal miR-1290 and miR-375 as prognostic markers in castration-resistant prostate cancer. *Eur. Urol.* **67,** 33–41 (2015).

115. Cazzoli, R. *et al.* microRNAs derived from circulating exosomes as noninvasive biomarkers for screening and diagnosing lung cancer. *J. Thorac. Oncol. Off. Publ. Int. Assoc. Study Lung Cancer* **8,** 1156–1162 (2013).

116. Halkein, J. *et al.* MicroRNA-146a is a therapeutic target and biomarker for peripartum cardiomyopathy. *J. Clin. Invest.* **123,** 2143–2154 (2013).

117. Corcoran, C., Rani, S. & O'Driscoll, L. miR-34a is an intracellular and exosomal predictive biomarker for response to docetaxel with clinical relevance to prostate cancer progression. *The Prostate* **74,** 1320–1334 (2014).

118. Cheng, Y. *et al.* A translational study of urine miRNAs in acute myocardial infarction. *J. Mol. Cell. Cardiol.* **53,** 668–676 (2012).

119. Wang, G. *et al.* Urinary miR-21, miR-29, and miR-93: novel biomarkers of fibrosis. *Am. J. Nephrol.* **36,** 412–418 (2012).

120. Singh, J., Deshpande, M., Suhail, H., Rattan, R. & Giri, S. Targeted Stage-Specific Inflammatory microRNA Profiling in Urine During Disease Progression in Experimental Autoimmune Encephalomyelitis: Markers of Disease Progression and Drug Response. *J. Neuroimmune Pharmacol. Off. J. Soc. NeuroImmune Pharmacol.* (2015).

121. Zhou, J. *et al.* Urinary microRNA-30a-5p is a potential biomarker for ovarian serous adenocarcinoma. *Oncol. Rep.* **33,** 2915–2923 (2015).

122. Ichii, O. *et al.* Decreased miR-26a expression correlates with the progression of podocyte injury in autoimmune glomerulonephritis. *PloS One* **9,** e110383 (2014).

123. Solé, C., Cortés-Hernández, J., Felip, M. L., Vidal, M. & Ordi-Ros, J. miR-29c in urinary exosomes as predictor of early renal fibrosis in lupus nephritis. *Nephrol. Dial. Transplant. Off. Publ. Eur. Dial. Transpl. Assoc. - Eur. Ren. Assoc.* **30,** 1488–1496 (2015).

124. Yoshida, Y., Yamamoto, H. & Morita, R. Detection of DNA methylation of gastric juice-derived exosomes in gastric cancer. *Integr. Mol. Med.* (2014).

125. Lázaro-Ibáñez, E. *et al.* Different gDNA content in the subpopulations of prostate cancer extracellular vesicles: apoptotic bodies, microvesicles, and exosomes. *The Prostate* **74,** 1379–1390 (2014).

126. Sung, B. H., Ketova, T., Hoshino, D., Zijlstra, A. & Weaver, A. M. Directional cell movement through tissues is controlled by exosome secretion. *Nat. Commun.* **6,** (2015).

127. Hannafon, B. N. & Ding, W.-Q. Intercellular Communication by Exosome-Derived microRNAs in Cancer. *Int. J. Mol. Sci.* **14,** 14240–14269 (2013).

128. Lenassi, M. *et al.* HIV Nef is secreted in exosomes and triggers apoptosis in bystander CD4+ T cells. *Traffic Cph. Den.* **11,** 110–122 (2010).

129. Bukong, T. N., Momen-Heravi, F., Kodys, K., Bala, S. & Szabo, G. Exosomes from Hepatitis C Infected Patients Transmit HCV Infection and Contain Replication Competent Viral RNA in Complex with Ago2-miR122-HSP90. *PLoS Pathog* **10,** e1004424 (2014).

130. Feng, D. *et al.* Cellular Internalization of Exosomes Occurs Through Phagocytosis. *Traffic* **11,** 675–687 (2010).

131. Frühbeis, C. *et al.* Neurotransmitter-Triggered Transfer of Exosomes Mediates Oligodendrocyte–Neuron Communication. *PLoS Biol* **11,** e1001604 (2013).

132. Parolini, I. *et al.* Microenvironmental pH Is a Key Factor for Exosome Traffic in Tumor Cells. *J. Biol. Chem.* **284,** 34211–34222 (2009).

133. Lai, C. P. *et al.* Visualization and tracking of tumour extracellular vesicle delivery and RNA translation using multiplexed reporters. *Nat. Commun.* **6,** 7029 (2015).

134. Alvarez-Erviti, L. *et al.* Delivery of siRNA to the mouse brain by systemic injection of targeted exosomes. *Nat. Biotechnol.* **29,** 341–345 (2011).

135. Lotvall, J. & Valadi, H. Cell to Cell Signalling via Exosomes Through esRNA. *Cell Adhes. Migr.* **1,** 156–158 (2007).

136. Friedman, R. C., Farh, K. K.-H., Burge, C. B. & Bartel, D. P. Most mammalian mRNAs are conserved targets of microRNAs. *Genome Res.* **19,** 92–105 (2009).

137. Kosaka, N. & Ochiya, T. Unraveling the mystery of cancer by secretory microRNA: horizontal microRNA transfer between living cells. *RNA* **2,** 97 (2012).

138. Khan, M. *et al.* Embryonic stem cell-derived exosomes promote endogenous repair mechanisms and enhance cardiac function following myocardial infarction. *Circ. Res.* **117,** 52–64 (2015).

139. Ibrahim, A. G.-E., Cheng, K. & Marbán, E. Exosomes as Critical Agents of Cardiac Regeneration Triggered by Cell Therapy. *Stem Cell Rep.* **2,** 606–619 (2014).

140. Momen-Heravi, F., Bala, S., Kodys, K. & Szabo, G. Exosomes derived from alcohol-treated hepatocytes horizontally transfer liver specific miRNA-122 and sensitize monocytes to LPS. *Sci. Rep.* **5,** 9991 (2015).

141. Yoon, C. *et al.* Delivery of miR-155 to retinal pigment epithelial cells mediated by Burkitt's lymphoma exosomes. *Tumour Biol. J. Int. Soc. Oncodevelopmental Biol. Med.* (2015).

142. Bala, S. *et al.* Biodistribution and function of extracellular miRNA-155 in mice. *Sci. Rep.* **5,** 10721 (2015).

143. Alexander, M. *et al.* Exosome-delivered microRNAs modulate the inflammatory response to endotoxin. *Nat. Commun.* **6,** 7321 (2015).

144. Wang, X. *et al.* Exosomal miR-223 Contributes to Mesenchymal Stem Cell-Elicited Cardioprotection in Polymicrobial Sepsis. *Sci. Rep.* **5,** 13721 (2015).

145. Deng, L. *et al.* miR-143 Activation Regulates Smooth Muscle and Endothelial Cell Crosstalk in Pulmonary Arterial Hypertension. *Circ. Res.* (2015).

146. Chen, L., Chen, R., Kemper, S., Charrier, A. & Brigstock, D. R. Suppression of fibrogenic signaling in hepatic stellate cells by Twist1-dependent microRNA-214 expression: Role of exosomes in horizontal transfer of Twist1. *Am. J. Physiol. - Gastrointest. Liver Physiol.* **309,** G491–G499 (2015).

147. Masyuk, A. I. *et al.* Biliary exosomes influence cholangiocyte regulatory mechanisms and proliferation through interaction with primary cilia. *Am. J. Physiol. Gastrointest. Liver Physiol.* **299,** G990–999 (2010).

148. Wei, Y. *et al.* Exosomal miR-221/222 enhances tamoxifen resistance in recipient ER-positive breast cancer cells. *Breast Cancer Res. Treat.* **147,** 423–431 (2014).

149. Ye, S.-B. *et al.* Tumor-derived exosomes promote tumor progression and T-cell dysfunction through the regulation of enriched exosomal microRNAs in human nasopharyngeal carcinoma. *Oncotarget* **5,** 5439–5452 (2014).

150. Bronisz, A. *et al.* Extracellular vesicles modulate the glioblastoma microenvironment via a tumor suppression signaling network directed by miR-1. *Cancer Res.* **74,** 738–750 (2014).

151. Aucher, A., Rudnicka, D. & Davis, D. M. MicroRNAs transfer from human macrophages to hepato-carcinoma cells and inhibit proliferation. *J. Immunol. Baltim. Md 1950* **191,** 6250–6260 (2013).

152. Forterre, A. *et al.* Myotube-derived exosomal miRNAs downregulate Sirtuin1 in myoblasts during muscle cell differentiation. *Cell Cycle Georget. Tex* **13,** 78–89 (2014).

153. Van Balkom, B. W. M. *et al.* Endothelial cells require miR-214 to secrete exosomes that suppress senescence and induce angiogenesis in human and mouse endothelial cells. *Blood* **121,** 3997–4006, S1–15 (2013).

154. Esquilin, Y., Queenan, C., Calabro, A. & Leonardi, D. mtDNA Migration and the Role of Exosomes in Horizontal Gene Transfer. *Microsc. Microanal.* **18,** 286–287 (2012).

155. Lamichhane, T. N., Raiker, R. S. & Jay, S. M. Exogenous DNA Loading into Extracellular Vesicles via Electroporation is Size-Dependent and Enables Limited Gene Delivery. *Mol. Pharm.* (2015).

156. Hoorn, E. J., Pisitkun, T., Yu, M.-J. & Knepper, M. A. Proteomic approaches for the study of cell signaling in the renal collecting duct. *Contrib. Nephrol.* **160,** 172–185 (2008).

157. Miranda, K. C. *et al.* Nucleic acids within urinary exosomes/microvesicles are potential biomarkers for renal disease. *Kidney Int.* **78,** 191–199 (2010).

158. Alvarez, M. L., Khosroheidari, M., Ravi, R. K. & DiStefano, J. K. Comparison of protein, microRNA, and mRNA yields using different methods of urinary exosome isolation for the discovery of kidney disease biomarkers. *Kidney Int.* **82,** 1024–1032 (2012).

159. Kozyraki, R. *et al.* The human intrinsic factor-vitamin B12 receptor, cubilin: molecular characterization and chromosomal mapping of the gene to 10p within the autosomal recessive megaloblastic anemia (MGA1) region. *Blood* **91,** 3593–3600 (1998).

160. De, S., Kuwahara, S. & Saito, A. The Endocytic Receptor Megalin and its Associated Proteins in Proximal Tubule Epithelial Cells. *Membranes* **4,** 333–355 (2014).

161. Corbetta, S. *et al.* Urinary exosomes in the diagnosis of Gitelman and Bartter syndromes. *Nephrol. Dial. Transplant. Off. Publ. Eur. Dial. Transpl. Assoc. - Eur. Ren. Assoc.* **30,** 621–630 (2015).

162. Sonoda, H. *et al.* Decreased abundance of urinary exosomal aquaporin-1 in renal ischemia-reperfusion injury. *Am. J. Physiol. - Ren. Physiol.* **297,** F1006–F1016 (2009).

163. Hoorn, E. J. *et al.* Prospects for urinary proteomics: Exosomes as a source of urinary biomarkers (Review Article). *Nephrology* **10,** 283–290 (2005).

164. Goodison, S., Rosser, C. J. & Urquidi, V. Bladder Cancer Detection and Monitoring: Assessment of Urine- and Blood-Based Marker Tests. *Mol. Diagn. Ther.* **17,** 71–84 (2013).

165. Gildea, J. J. *et al.* Exosomal transfer from human renal proximal tubule cells to distal tubule and collecting duct cells. *Clin. Biochem.* **47,** 89–94 (2014).

166. Van Koppen, A. *et al.* Human Embryonic Mesenchymal Stem Cell-Derived Conditioned Medium Rescues Kidney Function in Rats with Established Chronic Kidney Disease. *PLoS ONE* **7,** e38746 (2012).

167. Bruno, S. *et al.* Microvesicles Derived from Mesenchymal Stem Cells Enhance Survival in a Lethal Model of Acute Kidney Injury. *PLoS ONE* **7,** (2012).

168. Tomasoni, S. *et al.* Transfer of growth factor receptor mRNA via exosomes unravels the regenerative effect of mesenchymal stem cells. *Stem Cells Dev.* **22,** 772–780 (2013).

169. Burger, D. *et al.* Human endothelial colony-forming cells protect against acute kidney injury: role of exosomes. *Am. J. Pathol.* **185,** 2309–2323 (2015).

170. Borges, F. T. *et al.* TGF-β1–Containing Exosomes from Injured Epithelial Cells Activate Fibroblasts to Initiate Tissue Regenerative Responses and Fibrosis. *J. Am. Soc. Nephrol. JASN* **24,** 385–392 (2013).

171. Zhou, Y. *et al.* Exosomes released by human umbilical cord mesenchymal stem cells protect against cisplatin-induced renal oxidative stress and apoptosis in vivo and in vitro. *Stem Cell Res. Ther.* **4,** 34 (2013).

172. Zhang, L. *et al.* The 786-0 renal cancer cell-derived exosomes promote angiogenesis by downregulating the expression of hepatocyte cell adhesion molecule. *Mol. Med. Rep.* **8,** 272–276 (2013).

173. Yang, L., Wu, X., Wang, D., Luo, C. & Chen, L. Renal carcinoma cell-derived exosomes induce human immortalized line of Jurkat T lymphocyte apoptosis in vitro. *Urol. Int.* **91,** 363–369 (2013).

174. Mavani, G. P., DeVita, M. V. & Michelis, M. F. A Review of the Nonpressor and Nonantidiuretic Actions of the Hormone Vasopressin. *Front. Med.* **2,** (2015).

175. Knepper, M. A., Kwon, T.-H. & Nielsen, S. Molecular Physiology of Water Balance. *N. Engl. J. Med.* **372,** 1349–1358 (2015).

176. Vossenkämper, A. *et al.* Microtubules are needed for the perinuclear positioning of aquaporin-2 after its endocytic retrieval in renal principal cells. *Am. J. Physiol. Cell Physiol.* **293,** C1129–1138 (2007).

177. Kamsteeg, E.-J. *et al.* Short-chain ubiquitination mediates the regulated endocytosis of the aquaporin-2 water channel. *Proc. Natl. Acad. Sci. U. S. A.* **103,** 18344–18349 (2006).

178. Sandoval, P. C. *et al.* Proteome-Wide Measurement of Protein Half-Lives and Translation Rates in Vasopressin-Sensitive Collecting Duct Cells. *J. Am. Soc. Nephrol.* **24,** 1793–1805 (2013).

179. Ftouh, S. & Thomas, M. Acute kidney injury: summary of NICE guidance. *The BMJ* **347,** f4930 (2013).

180. Rahman, M., Shad, F. & Smith, M. C. Acute kidney injury: a guide to diagnosis and management. *Am. Fam. Physician* **86,** 631–639 (2012).

181. Solomon, R. & Dauerman, H. L. Contrast-Induced Acute Kidney Injury. *Circulation* **122,** 2451–2455 (2010).

182. Meinel, F. G., De Cecco, C. N., Schoepf, U. J. & Katzberg, R. Contrast-Induced Acute Kidney Injury: Definition, Epidemiology, and Outcome. *BioMed Res. Int.* **2014,** e859328 (2014).

183. Liu, Z. Z. *et al.* Iodinated contrast media cause direct tubular cell damage, leading to oxidative stress, low nitric oxide, and impairment of tubuloglomerular feedback. *Am. J. Physiol. Renal Physiol.* **306,** F864–872 (2014).

184. Seeliger, E., Sendeski, M., Rihal, C. S. & Persson, P. B. Contrast-induced kidney injury: mechanisms, risk factors, and prevention. *Eur. Heart J.* **33,** 2007–2015 (2012).

185. Doi, K. *et al.* Reduced Production of Creatinine Limits Its Use as Marker of Kidney Injury in Sepsis. *J. Am. Soc. Nephrol.* **20,** 1217–1221 (2009).

186. Edelstein, C. L. Biomarkers of Acute Kidney Injury. *Adv. Chronic Kidney Dis.* **15,** 222–234 (2008).

187. Mishra, J. *et al.* Identification of neutrophil gelatinase-associated lipocalin as a novel early urinary biomarker for ischemic renal injury. *J. Am. Soc. Nephrol. JASN* **14,** 2534–2543 (2003).

188. Devarajan, P. Neutrophil gelatinase-associated lipocalin (NGAL). *Scand. J. Clin. Lab. Investig. Suppl.* **241,** 89–94 (2008).

189. Hirsch, R. *et al.* NGAL is an early predictive biomarker of contrast-induced nephropathy in children. *Pediatr. Nephrol. Berl. Ger.* **22,** 2089–2095 (2007).

190. Vaidya, V. S., Ramirez, V., Ichimura, T., Bobadilla, N. A. & Bonventre, J. V. Urinary kidney injury molecule-1: a sensitive quantitative biomarker for early detection of kidney tubular injury. *Am. J. Physiol. Renal Physiol.* **290,** F517–529 (2006).

191. Han, W. K., Bailly, V., Abichandani, R., Thadhani, R. & Bonventre, J. V. Kidney Injury Molecule-1 (KIM-1): a novel biomarker for human renal proximal tubule injury. *Kidney Int.* **62,** 237–244 (2002).

192. Vaidya, V. S., Ferguson, M. A. & Bonventre, J. V. Biomarkers of Acute Kidney Injury. *Annu. Rev. Pharmacol. Toxicol.* **48,** 463–493 (2008).

193. Neal, C. S. *et al.* Circulating microRNA expression is reduced in chronic kidney disease. *Nephrol. Dial. Transplant.* **26,** 3794–3802 (2011).

194. Zhou, H. *et al.* Urinary exosomal transcription factors, a new class of biomarkers for renal disease. *Kidney Int.* **74,** 613–621 (2008).

195. Dear, J. W., Street, J. M. & Bailey, M. A. Urinary exosomes: A reservoir for biomarker discovery and potential mediators of intrarenal signalling. *PROTEOMICS* **13,** 1572–1580 (2013).

196. Stewart, G. D. *et al.* Carbonic Anhydrase 9 Expression Increases with Vascular Endothelial Growth Factor–Targeted Therapy and Is Predictive of Outcome in Metastatic Clear Cell Renal Cancer. *Eur. Urol.* **66,** 956–963 (2014).

197. Murakami, Y., Kanda, K., Tsuji, M., Kanayama, H. & Kagawa, S. MN/CA9 gene expression as a potential biomarker in renal cell carcinoma. *BJU Int.* **83,** 743–747 (1999).

198. Závada, J., Závadová, Z., Zat'ovičová, M., Hyršl, L. & Kawaciuk, I. Soluble form of carbonic anhydrase IX (CA IX) in the serum and urine of renal carcinoma patients. *Br. J. Cancer* **89,** 1067–1071 (2003).

199. Hosseini-Beheshti, E., Pham, S., Adomat, H., Li, N. & Guns, E. S. Exosomes as Biomarker Enriched Microvesicles: Characterization of Exosomal Proteins derived from a Panel of Prostate Cell Lines with distinct AR phenotypes. *Mol. Cell. Proteomics MCP* (2012).

200. Reed, G. F., Lynn, F. & Meade, B. D. Use of Coefficient of Variation in Assessing Variability of Quantitative Assays. *Clin. Diagn. Lab. Immunol.* **9,** 1235–1239 (2002).

201. Kanno, K. *et al.* Urinary Excretion of Aquaporin-2 in Patients with Diabetes Insipidus. *N. Engl. J. Med.* **332,** 1540–1545 (1995).

202. Zhou, H. *et al.* Collection, storage, preservation, and normalization of human urinary exosomes for biomarker discovery. *Kidney Int.* **69,** 1471–1476 (2006).

203. Tian, T. *et al.* Dynamics of exosome internalization and trafficking. *J. Cell. Physiol.* **228,** 1487–1495 (2013).

204. Collino, F. *et al.* AKI Recovery Induced by Mesenchymal Stromal Cell-Derived Extracellular Vesicles Carrying MicroRNAs. *J. Am. Soc. Nephrol. JASN* (2015).

205. Oosthuyzen, W. *et al.* Quantification of human urinary exosomes by nanoparticle tracking analysis. *J. Physiol.* **591,** 5833–5842 (2013).

206. Gupta, I. R. *et al.* Protein Kinase A Is a Negative Regulator of Renal Branching Morphogenesis and Modulates Inhibitory and Stimulatory Bone Morphogenetic Proteins. *J. Biol. Chem.* **274,** 26305–26314 (1999).

207. Kirchhausen, T., Macia, E. & Pelish, H. E. Use of dynasore, the small molecule inhibitor of dynamin, in the regulation of endocytosis. *Methods Enzymol.* **438,** 77–93 (2008).

208. Butterworth, M. B., Edinger, R. S., Johnson, J. P. & Frizzell, R. A. Acute ENaC Stimulation by cAMP in a Kidney Cell Line is Mediated by Exocytic Insertion from a Recycling Channel Pool. *J. Gen. Physiol.* **125,** 81–101 (2005).

209. Umenishi, F., Narikiyo, T., Vandewalle, A. & Schrier, R. W. cAMP regulates vasopressin-induced AQP2 expression via protein kinase A-independent pathway. *Biochim. Biophys. Acta BBA - Biomembr.* **1758,** 1100–1105 (2006).

210. Caporali, A. *et al.* Deregulation of microRNA-503 Contributes to Diabetes Mellitus–Induced Impairment of Endothelial Function and Reparative Angiogenesis After Limb Ischemia. *Circulation* **123,** 282–291 (2011).

211. Knepper, M. A. & Star, R. A. Vasopressin: friend or foe? *Nat. Med.* **14,** 14–16 (2008).

212. Kohan, D. E. Biology of endothelin receptors in the collecting duct. *Kidney Int.* **76,** 481–486 (2009).

213. Musch, M. W. *et al.* Cyclic AMP-mediated endocytosis of intestinal epithelial NHE3 requires binding to synaptotagmin 1. *Am. J. Physiol. Gastrointest. Liver Physiol.* **298,** G203–211 (2010).

214. Macia, E. *et al.* Dynasore, a cell-permeable inhibitor of dynamin. *Dev. Cell* **10,** 839–850 (2006).

215. Zhou, B. *et al.* MicroRNA-503 targets FGF2 and VEGFA and inhibits tumor angiogenesis and growth. *Cancer Lett.* **333,** 159–169 (2013).

216. Nawaz, M. *et al.* The emerging role of extracellular vesicles as biomarkers for urogenital cancers. *Nat. Rev. Urol.* **11,** 688–701 (2014).

217. Prunotto, M. *et al.* Proteomic analysis of podocyte exosome-enriched fraction from normal human urine. *J. Proteomics* **82,** 193–229 (2013).

218. Conde-Vancells, J. *et al.* Candidate biomarkers in exosome-like vesicles purified from rat and mouse urine samples. *PROTEOMICS – Clin. Appl.* **4,** 416–425 (2010).

219. Tian, T. *et al.* Exosome uptake through clathrin-mediated endocytosis and macropinocytosis and mediating miR-21 delivery. *J. Biol. Chem.* **289,** 22258–22267 (2014).

220. Charan, J. & Biswas, T. How to Calculate Sample Size for Different Study Designs in Medical Research? *Indian J. Psychol. Med.* **35,** 121–126 (2013).

221. Rieg, T., Richter, K., Osswald, H. & Vallon, V. Kidney function in mice: thiobutabarbital versus alpha-chloralose anesthesia. *Naunyn. Schmiedebergs Arch. Pharmacol.* **370,** 320–323 (2004).

222. Holstein-Rathlou, N. H., Christensen, P. & Leyssac, P. P. Effects of halothane-nitrous oxide inhalation anesthesia and Inactin on overall renal and tubular function in Sprague-Dawley and Wistar rats. *Acta Physiol. Scand.* **114,** 193–201 (1982).

223. Choi, H. S. *et al.* Renal Clearance of Nanoparticles. *Nat. Biotechnol.* **25,** 1165–1170 (2007).

224. Liu, J., Yu, M., Zhou, C. & Zheng, J. Renal clearable inorganic nanoparticles: a new frontier of bionanotechnology. *Mater. Today* **16,** 477–486 (2013).

225. El Andaloussi, S., Lakhal, S., Mäger, I. & Wood, M. J. A. Exosomes for targeted siRNA delivery across biological barriers. *Adv. Drug Deliv. Rev.* **65,** 391–397 (2013).

226. Devarajan, P. Biomarkers for the Early Detection of Acute Kidney Injury. *Curr. Opin. Pediatr.* **23,** 194–200 (2011).

227. Sandilands, E. A. *et al.* Mechanisms for an effect of acetylcysteine on renal function after exposure to radio-graphic contrast material: study protocol. *BMC Pharmacol. Toxicol.* **12,** 3 (2012).

228. Hiemstra, T. F. *et al.* Human Urinary Exosomes as Innate Immune Effectors. *J. Am. Soc. Nephrol.* **25,** 2017–2027 (2014).

229. Krawczeski, C. D. *et al.* Temporal relationship and predictive value of urinary acute kidney injury biomarkers after pediatric cardiopulmonary bypass. *J. Am. Coll. Cardiol.* **58,** 2301–2309 (2011).

230. Briguori, C. *et al.* Renal Insufficiency Following Contrast Media Administration Trial (REMEDIAL) A Randomized Comparison of 3 Preventive Strategies. *Circulation* **115,** 1211–1217 (2007).

231. Briguori, C., Quintavalle, C., Donnarumma, E. & Condorelli, G. Novel Biomarkers for Contrast-Induced Acute Kidney Injury. *BioMed Res. Int.* **2014,** (2014).

232. Matsui, K. *et al.* Clinical significance of tubular and podocyte biomarkers in acute kidney injury. *Clin. Exp. Nephrol.* **15,** 220–225 (2010).

233. Zeng, C. *et al.* Podocyte autophagic activity plays a protective role in renal injury and delays the progression of podocytopathies. *J. Pathol.* **234,** 203–213 (2014).

234. Sekulic, M. & Pichler Sekulic, S. A compendium of urinary biomarkers indicative of glomerular podocytopathy. *Pathol. Res. Int.* **2013,** 782395 (2013).

235. Larsson, A. *et al.* Validation of podocalyxin-like protein as a biomarker of poor prognosis in colorectal cancer. *BMC Cancer* **12,** 282 (2012).

236. Hara, M. *et al.* Urinary podocalyxin is an early marker for podocyte injury in patients with diabetes: establishment of a highly sensitive ELISA to detect urinary podocalyxin. *Diabetologia* **55,** 2913–2919 (2012).

237. Szymanski, C. J., Yi, H., Liu, J. L., Wright, E. R. & Payne, C. K. Imaging intracellular quantum dots: fluorescence microscopy and transmission electron microscopy. *Methods Mol. Biol. Clifton NJ* **1026,** 21–33 (2013).

238. Tang, K. W. A., Toh, Q. C. & Teo, B. W. Normalisation of urinary biomarkers to creatinine for clinical practice and research – when and why. *Singapore Med. J.* **56,** 7–10 (2015).

239. Wagner, B. D., Accurso, F. J. & Laguna, T. A. The applicability of urinary creatinine as a method of specimen normalization in the cystic fibrosis population. *J. Cyst. Fibros.* **9,** 212–216 (2010).

240. Preta, G., Cronin, J. G. & Sheldon, I. M. Dynasore - not just a dynamin inhibitor. *Cell Commun. Signal.* **13,** 24 (2015).

241. Ivanov, A. I. Pharmacological inhibition of endocytic pathways: is it specific enough to be useful? *Methods Mol. Biol. Clifton NJ* **440,** 15–33 (2008).

242. Chang, C.-C., Wu, M. & Yuan, F. Role of specific endocytic pathways in electrotransfection of cells. *Mol. Ther. — Methods Clin. Dev.* **1,** 14058 (2014).

243. Mulcahy, L. A., Pink, R. C. & Carter, D. R. F. Routes and mechanisms of extracellular vesicle uptake. *J. Extracell. Vesicles* **3,** (2014).

244. Christianson, H. C., Svensson, K. J., Kuppevelt, T. H. van, Li, J.-P. & Belting, M. Cancer cell exosomes depend on cell-surface heparan sulfate proteoglycans for their internalization and functional activity. *Proc. Natl. Acad. Sci.* **110,** 17380–17385 (2013).

245. Weisbord, S. D. & Palevsky, P. M. Radiocontrast-induced acute renal failure. *J. Intensive Care Med.* **20,** 63–75 (2005).